THE DAVID W. TAYLOR MODEL BASIN

UNITED STATES NAVY

CHARACTERISTICS OF THE NRL MARK 3 BOAT-TYPE BUOY AND DETERMINATION OF MOORING-LINE SIZES

BY ENSIGN P. EISENBERG, USNR

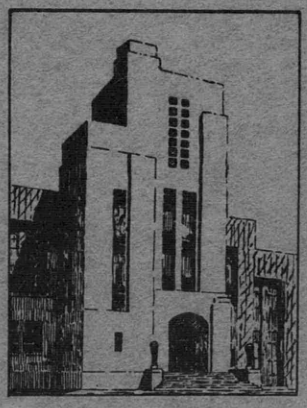

CONFIDENTIAL

37

SEPTEMBER 1945

REPORT 550

NAVY DEPARTMENT
DAVID TAYLOR MODEL BASIN
WASHINGTON, D.C.

RESTRICTED

The contents of this report are not to be divulged or referred to in any publication. In the event information derived from this report is passed on to officer or civilian personnel, the source should not be revealed.

CONFIDENTIAL

REPORT 550

CHARACTERISTICS OF THE NRL MARK 3 BOAT-TYPE BUOY AND DETERMINATION OF MOORING-LINE SIZES

BY ENSIGN P. EISENBERG, USNR

SEPTEMBER 1945

PERSONNEL

The project was carried out under the management of Ens. P. Eisenberg, USNR. R. Ebner, C Sp(X) USNR, assisted in the model basin tests and in the reduction of experimental data. The method of determining anchor-line sizes was suggested by L. Landweber and extended by Ensign Eisenberg. The analysis of Appendix 2 was contributed by L. Landweber.

The report was written by Ensign Eisenberg and checked by Mr. Landweber.

TABLE OF CONTENTS

page

CHARACTERISTICS OF THE NRL MARK 3 BOAT-TYPE BUOY AND DETERMINATION OF MOORING-LINE SIZES

ABSTRACT

Two 1/5-scale models of buoys designed as housings for sono-radio equipment to be anchored in strong currents and in deep water were tested at the David Taylor Model Basin. The tests were made to determine the characteristics of the buoys under loads such as those imposed by the fluid forces on a mooring line. The load-carrying capacity of each buoy when on the water surface was evaluated from surface towing tests in which observations were made of the drag and general behavior under various loads. To permit the designing of the mooring line for conditions under which the buoy may become submerged owing to fouling of the mooring line or a rough sea, tests were also conducted to determine the characteristics of the buoys when completely submerged. To facilitate transport of the buoys to an anchoring station, the best point of tow on the bow of each buoy and the horsepower required for towing astern of a vessel were determined. A final series of tests was also made to evaluate the drag coefficients of commercial straight-link chain which was being considered for use as a mooring line in conjunction with wire rope.

A graphical method is developed and employed for determining suitable sizes of mooring lines and maximum anchoring currents for each buoy. On the basis of this analysis of the two buoy designs submitted for test, the one permitting the widest range of operation is determined. Proper sizes of chain and wire rope are selected for various anchoring conditions of current velocity and water depth. The weights of concrete blocks to be used as anchors are also recommended.

INTRODUCTION

The Mark 3 Boat-Type Buoy was designed at the Naval Research Laboratory as a housing for sono-radio equipment to be anchored in strong currents and in deep water. The general design is based on that of a buoy developed by the U.S. Coast and Geodetic Survey (1)* for the observation of tidal currents. Although the latter buoy was reported to give satisfactory results in field trials, it was necessary to modify the design to accommodate much heavier equipment. For this reason, the Naval Research Laboratory (2) requested that model tests of two tentative designs of the Mark 3 buoy be made at the David Taylor Model Basin to determine the characteristics of each.

---

* Numbers in parentheses indicate references on page 46 of this report.

The following specific problems were outlined by the Naval Research Laboratory:

1. Determine the practicability of anchoring the buoy in 1200 feet of water, assuming a maximum current of 4 knots.

   a. If anchoring is practicable, recommend the size and type of anchor cable, the length of the anchor cable, and the weight of a concrete-block anchor.

   b. If anchoring in this depth of water and current is not practicable, recommend the maximum depth of water, the size and type of anchor cable, the length of the anchor cable, and the weight of the anchor, which are practicable in a current of 4 knots.

2. Determine the maximum safe current in which the buoy can be anchored, assuming a water depth of 600 feet.

   a. Recommend the size and type of chain, the length of the chain, and the weight of anchor, assuming only chain is used.

   b. Recommend the size and type of chain and wire rope, when used in combination, assuming the chain end to be fastened to the anchor.

3. Determine the maximum safe current in which the buoy can be anchored, assuming a water depth of 100 feet.

   a. Recommend the size and type of chain, the length of the chain, and the weight of anchor, assuming only chain is used.

4. Recommend a procedure for towing up to 3 buoys at one time. Recommend the size or horespower of the vessel required and the method of rigging, assuming a towing speed of 8 knots.

To obtain answers to the foregoing problems, it is necessary to know the forces acting on the buoy and on the anchoring cable. When an anchoring line of a certain length is to be used in water of a given depth and current velocity, the size of the line is governed by two requirements:

1. The size of the buoy must be sufficiently large compared with the size of the anchoring line so that the downward component of the fluid forces on the line and the weight of the line will not cause the total load on the buoy to exceed the maximum load it can carry without submergence.

2. The anchor line must be sufficiently strong compared with the maximum upward pull of the buoy so that the tension in the cable does not exceed the safe working load.

To determine the load-carrying characteristics of the buoys when on the surface, tests were made on the models under various loading conditions. Since, in actual operation, the buoys may at times become completely submerged, owing to the fouling of the anchor or to a heavy sea, the characteristics of the buoys were also determined when the buoys were running below the water surface. These tests, as well as the tests to determine horsepower requirements when towing the buoys, are reported in Part 1 of the report.

A graphical method for determining the optimum anchor-line sizes for use with a buoy of known characteristics is developed in Part 2. A problem somewhat similar to the present one is discussed in TMB Report 540 (3), in which a method of obtaining proper cable and buoy sizes is presented. Since the method described in that report is based on the special characteristics of the TMB planing float, it has been necessary to generalize the procedure, that is, to develop a method of obtaining limiting speeds and anchor-line sizes when the characteristics of a float and anchor line are given.

Using the characteristics of the Mark 3 buoy determined from experiments, the procedure outlined in Part 2 is used to select anchor-line sizes for the operating conditions outlined in the foregoing. The procedure followed when using two types of anchor line in combination is also given in Part 2 and the analysis for this condition is shown in Appendix 2. Since the hydrodynamic characteristics of a flexible cable in a stream are sufficiently well known (9), it was necessary only to determine the required drag coefficient for chain used as a mooring line. The results of the tests on chain of various sizes are reported in Appendix 1.

The anchor-line sizes recommended for use with the Mark 3 buoys are summarized in Part 3, and the working charts from which the sizes were selected are shown in Appendixes 3 and 4.

PART 1 - CHARACTERISTICS OF THE NRL MARK 3 BUOY

DESCRIPTION OF THE TWO NRL MARK 3 BUOYS

All buoy tests were conducted with 1/5-scale models of the Mark 3 buoy representing the two designs submitted by the Naval Research Laboratory. The models were constructed and furnished by the Naval Research Laboratory.

The NRL Mark 3 buoy designs, designated Buoy A and Buoy B, are similar in general shape but differ in total displacement. The buoys have the same dimensions in plan and have similar bow and keel shapes; however, Buoy A has a shallower draft than Buoy B. The dimensions of the actual models tested are shown in Figure 1. The principal features of the design are the ship-shaped bow, the 15-degree slope of the sides, the bottom in the form

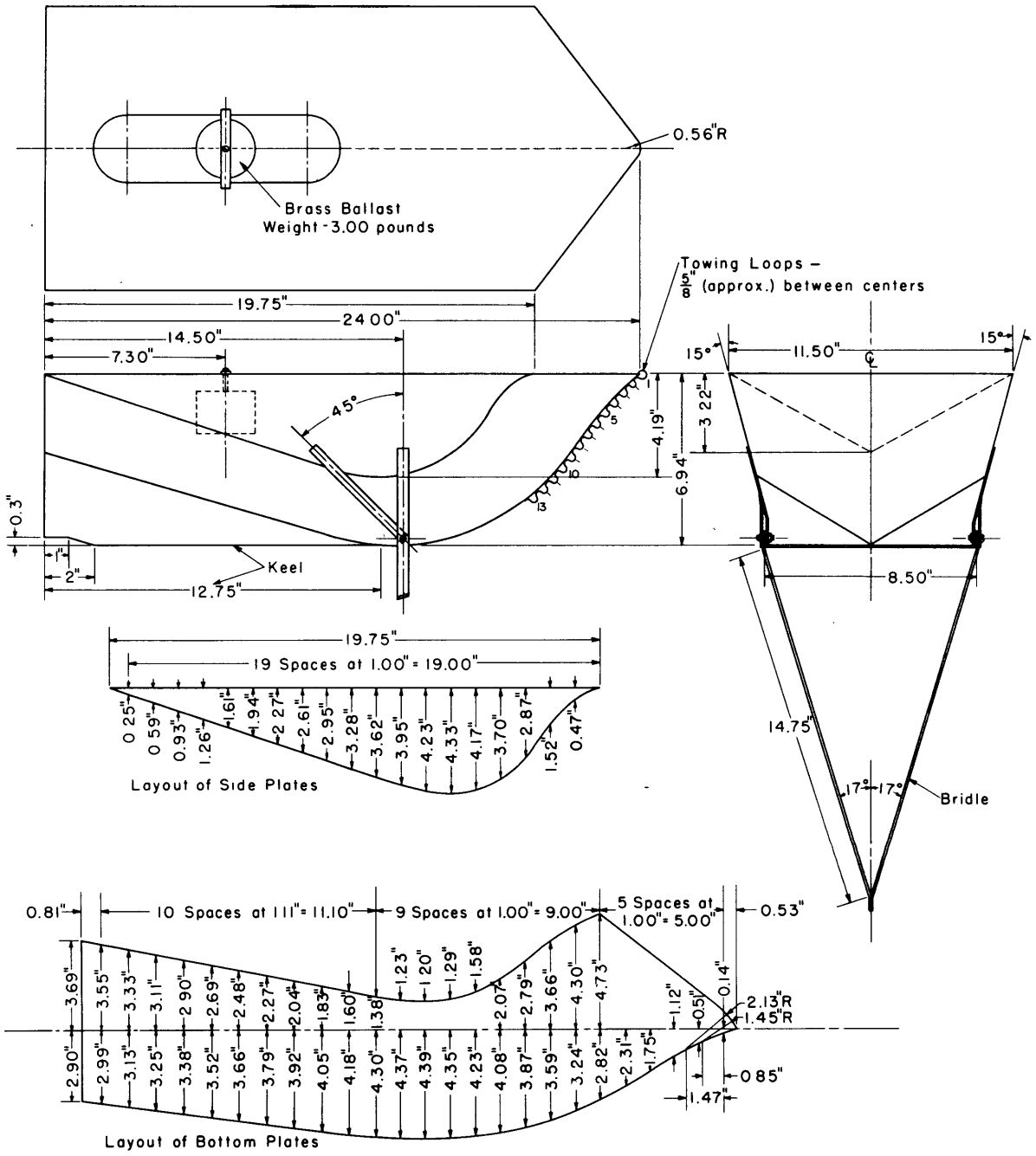

Figure 1a - Buoy A

of a planing surface of varying dead rise, and the transverse bridle in the shape of an isosceles triangle. The rate of change of curvature of the bottom surfaces of Buoy B is greater than that of Buoy A.

The buoy models are shown in simulated anchoring positions in Figures 2 and 3.

(Text continued on page 8)

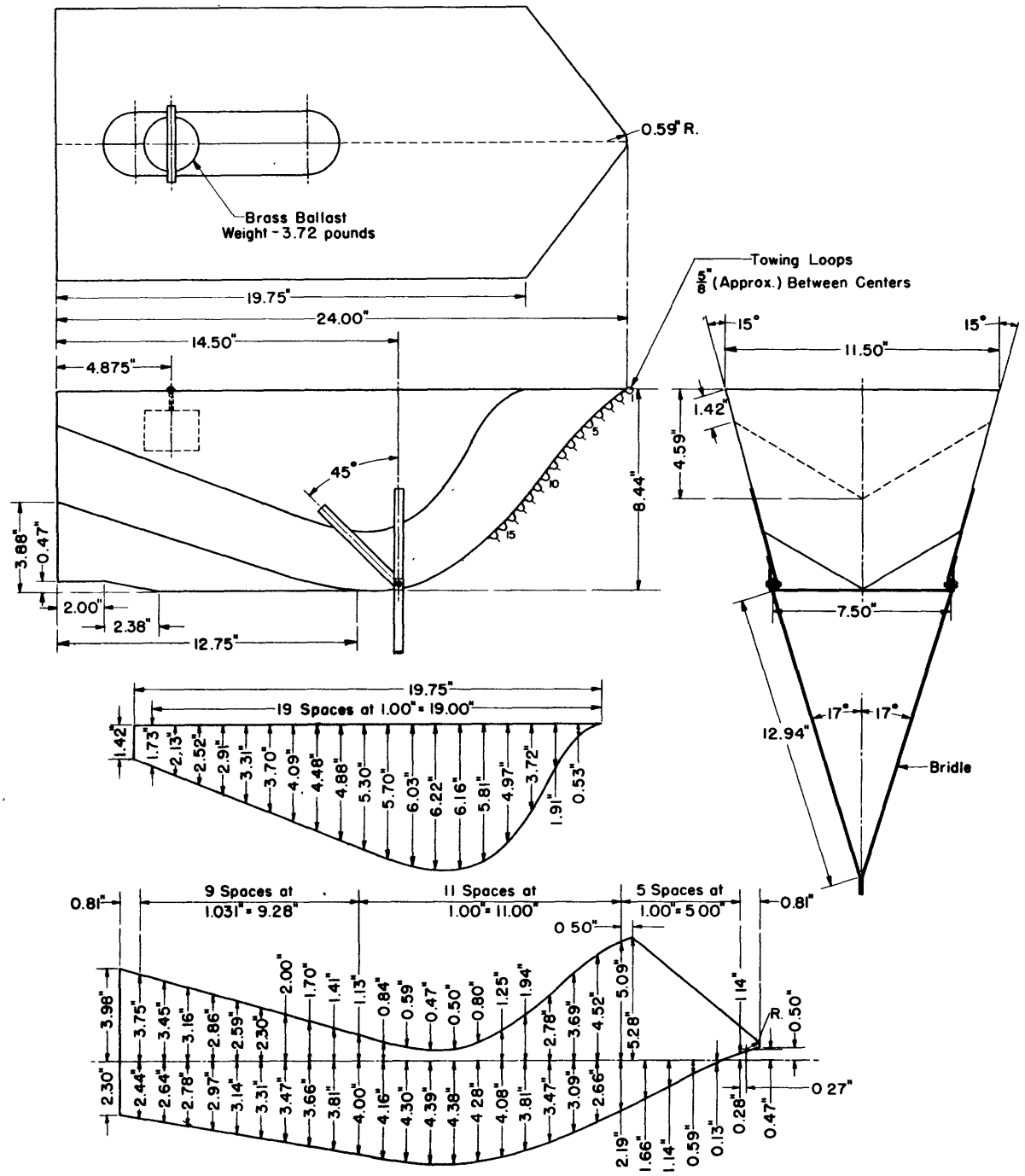

Figure 1b - Buoy B

Figure 1 - Dimensional Sketches of Test Models

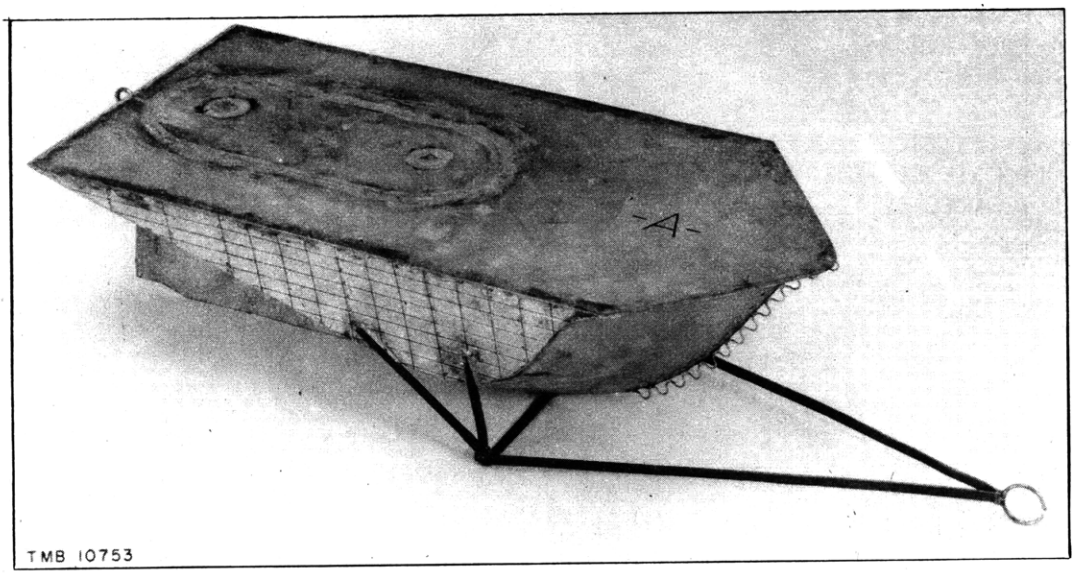

Figure 2a - View of Deck, Taken from the Starboard Bow

The hatch in the after portion of the deck is soldered into place after the weights, which simulate full-scale equipment and are shown in Figure 4, have been installed inside the body.

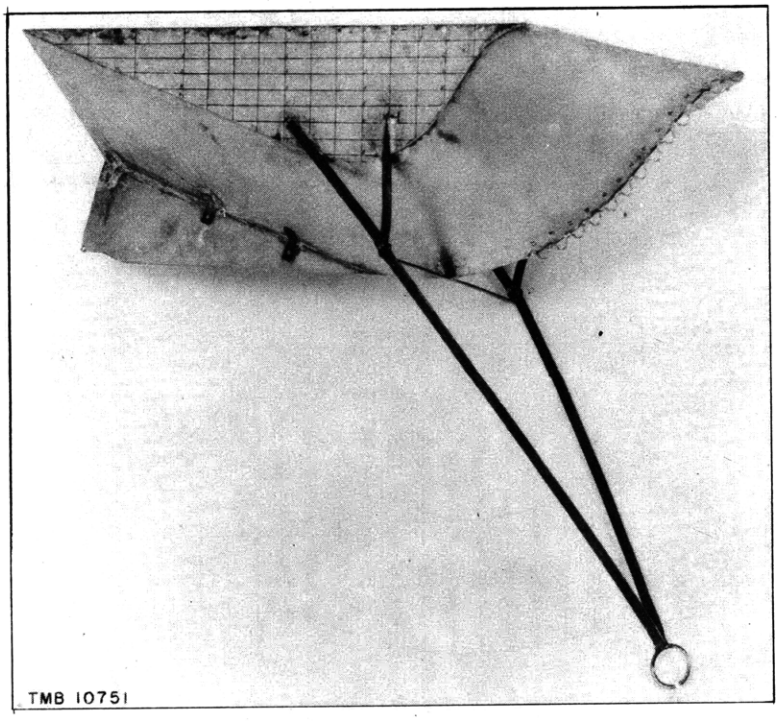

Figure 2b - View of Bottom, Taken from the Starboard Side, Showing the Model in Simulated Anchoring Position

Figure 2 - Photographs of 1/5-Scale Model of Buoy A

The model is built of sheet metal and is hollow. The wire loops along the stem were used to determine the most suitable point for securing a line to tow the model to its anchorage. The keel plate, which extends from the maximum section to the stern, is cut back near the stern to provide for nesting the bridle.

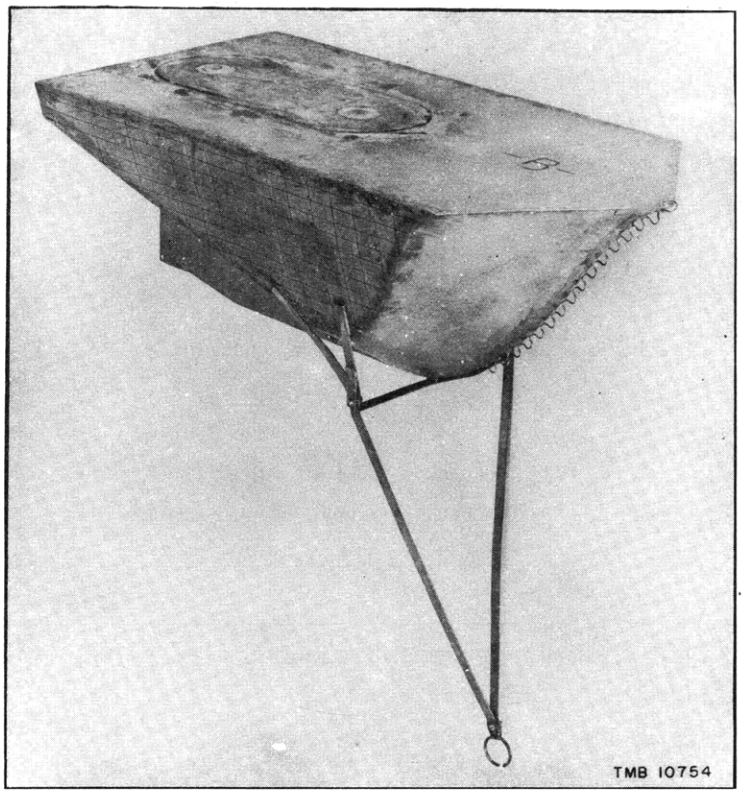

Figure 3a - View Taken from the Starboard Bow, Showing the Model in Simulated Anchoring Position

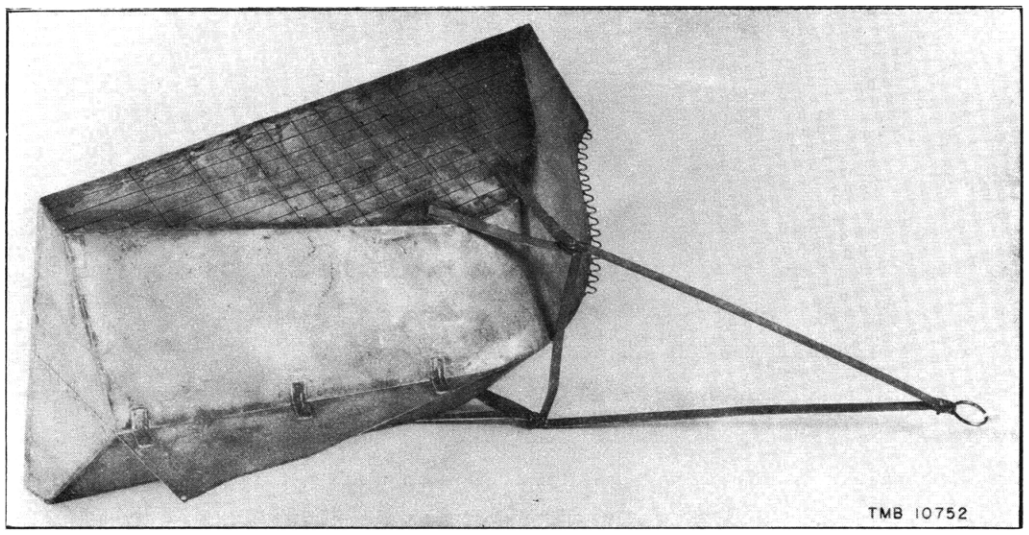

Figure 3b - View of Bottom, Taken from the Starboard Quarter

Figure 3 - Photographs of 1/5-Scale Model of Buoy B

The 1/5-scale model of Buoy B is similar to Buoy A in shape and plan dimensions. The chine line of the bottom surface intersects the stern below the deck, providing greater side area than that for Buoy A, in which the chine line intersects the stern at the deck. The altitude of the triangle formed by the bridle is somewhat shorter for Buoy B than for Buoy A.

The weight of the equipment to be installed in the full-scale buoys was simulated in the models by cylindrical brass weights in the positions shown in Figure 1. The method of installation of these weights in the buoys, and the internal construction of the models, are shown in Figure 4. The position of the center of gravity of the equipment was determined by the Naval Research Laboratory on the basis of initial trim tests and was standardized for each buoy.

The pertinent weight and buoyancy characteristics of the buoys are summarized in Table 1.

TABLE 1

Principal Buoy Characteristics

All values are full scale.

Item	Buoy A	Buoy B
Weight of buoy without equipment, pounds	1000	1200
Weight of equipment, pounds	375	465
Total weight of buoy plus equipment, pounds	1375	1665
Total available buoyancy, pounds	3750	4700
Reserve buoyancy without equipment, pounds	2750	3500
Reserve buoyancy with equipment, pounds	2375	3035
Position of center of gravity of equipment, inches from stern	36 1/2	24 3/8
Initial trim by the stern, degrees	8.7	13.9

BUOY TEST METHODS

To determine all of the characteristics of the buoys, two independent types of test were made. A first series of tests was conducted to determine the drag of each buoy under various loads at different speeds. From these tests, the maximum load at each speed to which a buoy can be subjected before submergence was also determined. The second series of tests was made to determine the characteristics of the buoys when completely submerged.

In actual operation, the load on the buoy is applied at the bridle apex and increases with increasing current speed, owing to the fluid forces on the anchoring line. To simulate these conditions the model test loads were applied by a model of the TMB fending kite (4) used as a depressor. This test arrangement is illustrated in Figure 5. The depressor towline and the line used for towing the system were both secured to the apex of the buoy

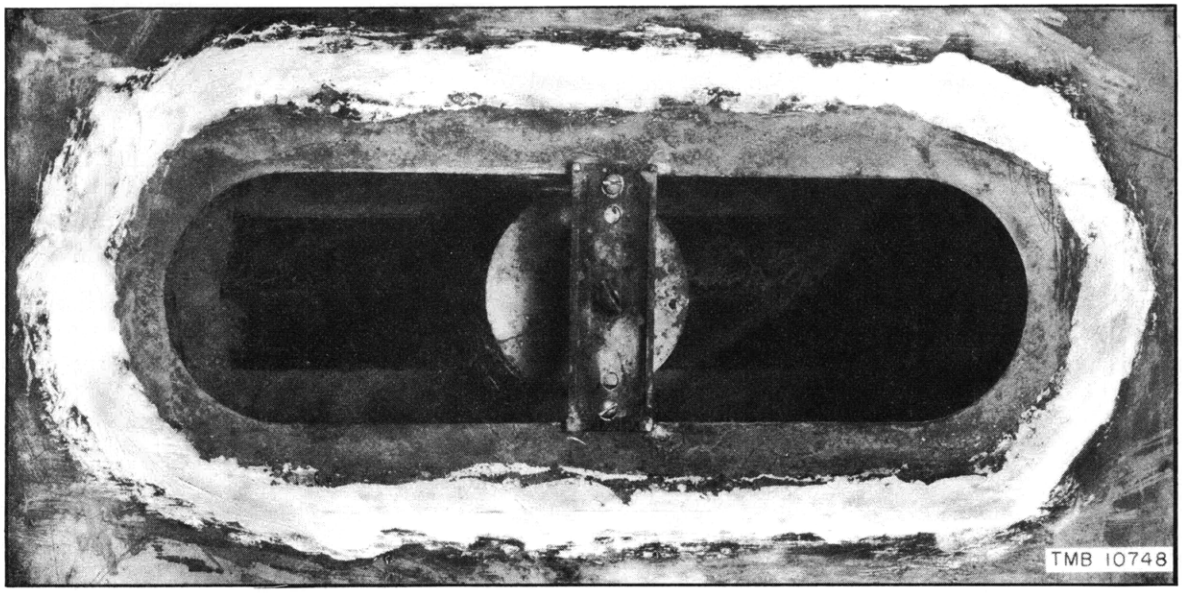

Figure 4a - Buoy A

The watertight hatch has been removed to show the position of the cylindrical brass weight used to simulate the equipment installed in the buoy. This weight corresponds to a prototype weight of 375 pounds with center of gravity at 36 1/2 inches from the stern. The keel stiffener can be seen below the weight.

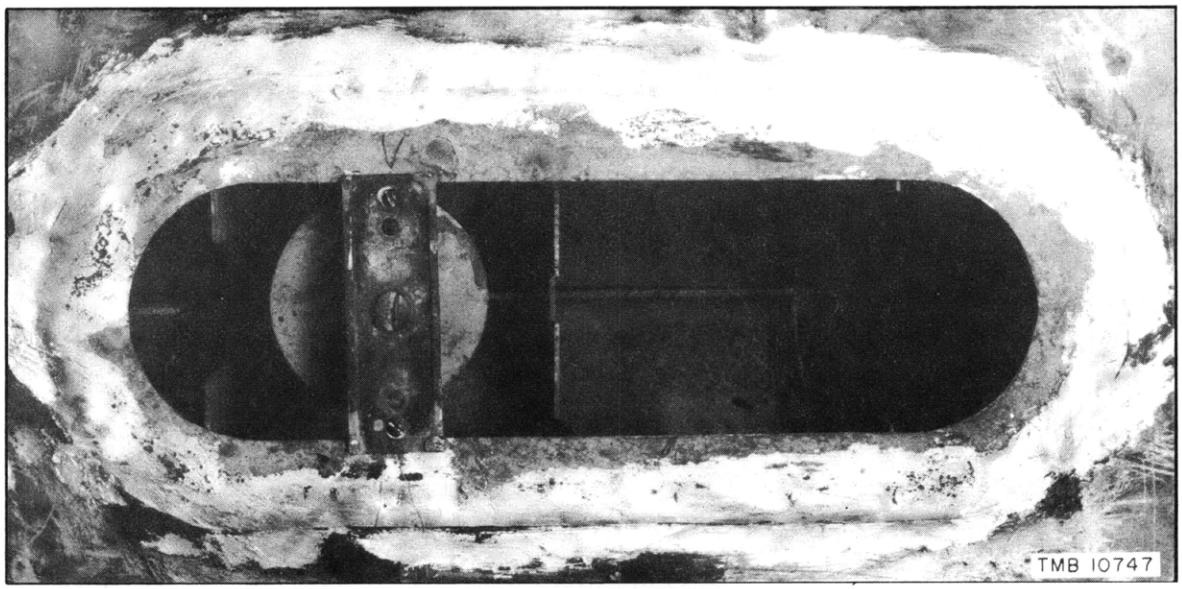

Figure 4b - Buoy B

The cylindrical brass weight corresponds to full-scale equipment weighing 465 pounds with center of gravity at 24 3/8 inches from the stern. The type of bulkhead reinforcement used is shown in the interior of the buoy.

Figure 4 - Position of Weights Simulating Equipment in the Model

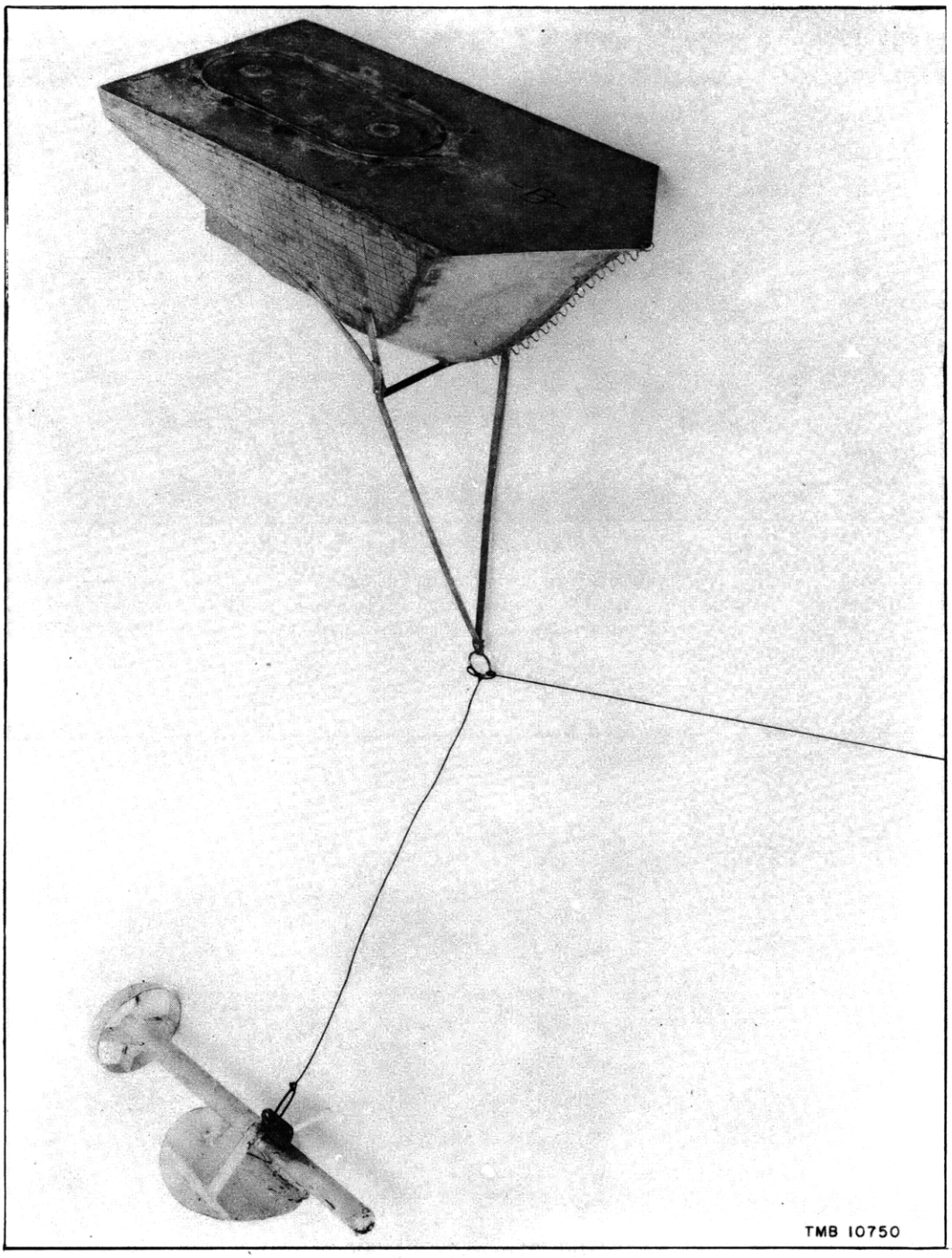

Figure 5 - Method of Load Application in Model Tests of NRL Mark 3 Buoy

Buoy B is shown in simulated towing position for model tests. The load on the buoy is applied by the downward component of the lift developed by the circular-wing depressor. Four depressor towpoints were used to obtain a series of loading conditions for the buoy tests. The system was towed by the line from the bridle apex which was secured to the floating beam of the towing-carriage dynamometer.

bridle. A watertight hatch was used to prevent flooding of the buoy when it became submerged during testing.

The depressor was first carefully calibrated by towing it at the end of a line which was adjusted during the test to maintain a constant length from the point of tow on the depressor to the water surface throughout the speed range. Towlines of the same length and size were subsequently used in the buoy tests. Four depressor towpoints were used to obtain a series of loading curves for the buoy tests. The method of calibrating the depressor is illustrated in Figure 6. The towline was led through a pulley at the center of a protractor and secured to the drag dynamometer on the towing carriage. The drag of the depressor with its towline, and the angle of the towline at the surface, were measured over a range of speeds for each depressor towpoint. From these measurements, the lift L_0 of the depressor was computed from the equation

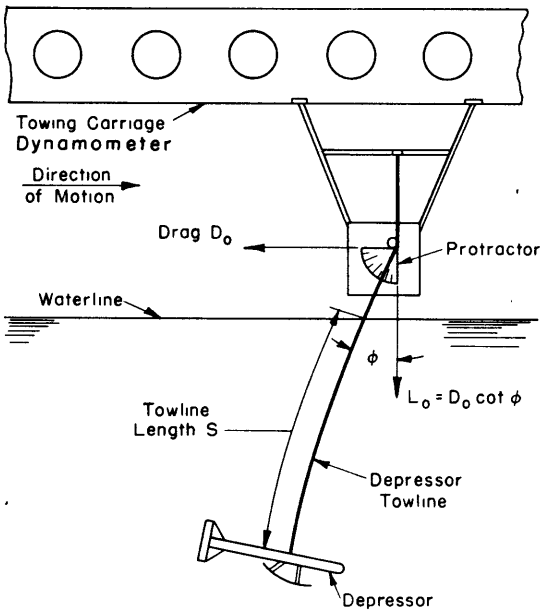

Figure 6 - Test Method for Calibration of Depressor

$$L_0 = D_0 \cot \phi \qquad [1]$$

where D_0 is the drag of the depressor and towline, and ϕ is the angle of the towline with the vertical at the water surface.

The characteristics of each buoy were obtained in the manner illustrated in Figure 7. The line used for towing the system was secured to the towing-carriage dynamometer at the center of a protractor. The drag of the system and the angle of the towing line at the protractor were measured over a range of speeds and at the various depressor settings. Since the shape of the depressor towline remains the same for a given length and size of line, the depressor calibration was used directly at each speed. The drag D of the buoy, then, is the difference between the measured drag F of the system and the drag D_0 of the depressor and its towline, or

$$D = F - D_0 \qquad [2]$$

Since a long line was used for towing the system, the angles of the line at the protractor were of the order of 5 degrees from the horizontal. As a

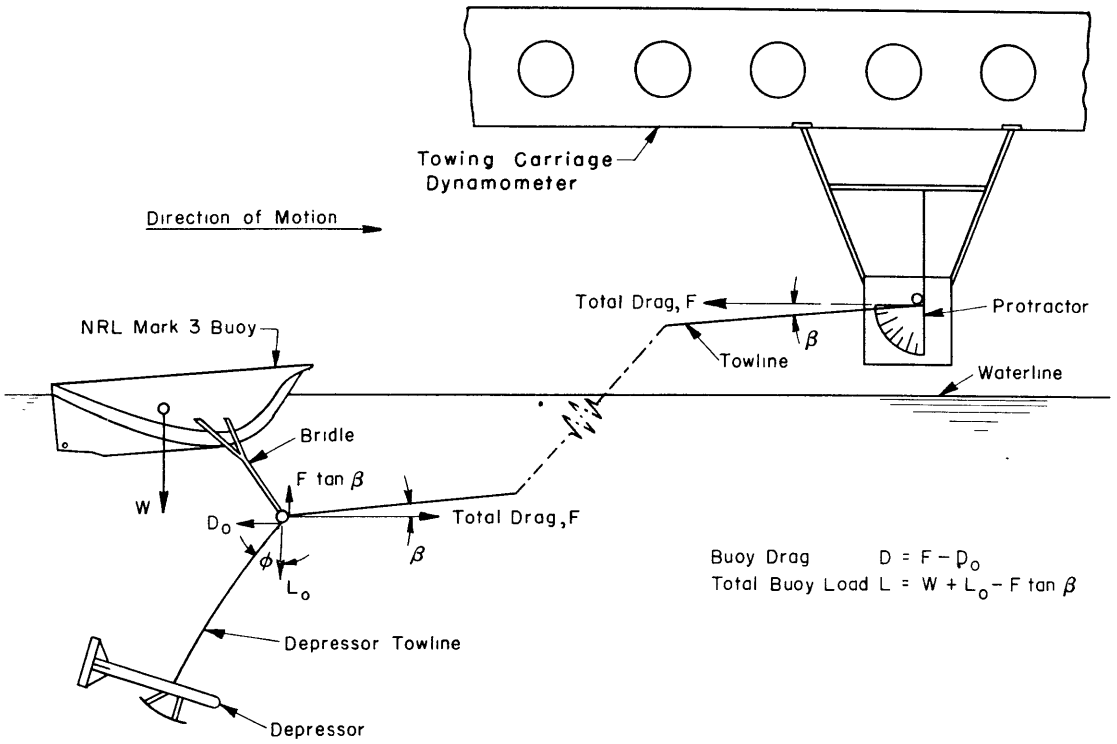

Figure 7 - Test Method for Determination of Characteristics of NRL Mark 3 Buoy

result, the fluid force on the cable was primarily tangential drag. Since the cable diameter was small, this force and the curvature of this cable were neglected in the analysis of the data.

The load on the buoy consists of its own weight, the weight of the equipment installed, and the algebraic sum of the vertical components of the tensions in the depressor and forward towlines, i.e.,

$$L = W + L_0 - F \tan\beta \qquad [3]$$

where L is the total load on the buoy,

W is the total weight of the buoy including the installed equipment,

β is the angle of the towing line with the horizontal, and

F and L_0 are as previously defined.

Here again the fluid forces on the line for towing the system were neglected.

The limiting loads to which a buoy can be subjected without submergence were determined by observation of its position in the water at every half knot of model speed. A buoy was considered overloaded when water just began overflowing the bow. When the deck of the buoy was clean of any overflow, it was considered capable of carrying the load regardless of the amount

of freeboard.* The conditions are illustrated in the photographs of Figure 8 taken during an actual test. The model of Buoy B is shown during a test with a single depressor setting. At the lower speed, Figure 8a, the water is just flowing over the top or deck and the buoy is considered overloaded. At the higher speed, Figure 8b, although the downward lift of the depressor has increased, the buoy has developed sufficient upward lifting capacity for this load; the bow spray is thrown forward and the top of the buoy is clean. In this latter condition, although the buoy has very little freeboard, it is considered not overloaded.

The characteristics of the buoys when completely submerged were determined by measuring the resultant force and the lift-drag ratio of the buoy when in that condition. This test was accomplished by towing the buoys with the towline in a horizontal plane in the same manner as paravanes are towed. The buoy was held in position by completely flooding the hull and then balancing the negative buoyancy by a vertical line secured to the buoy at the starboard bridle pivot. This line was oriented during a run to remain

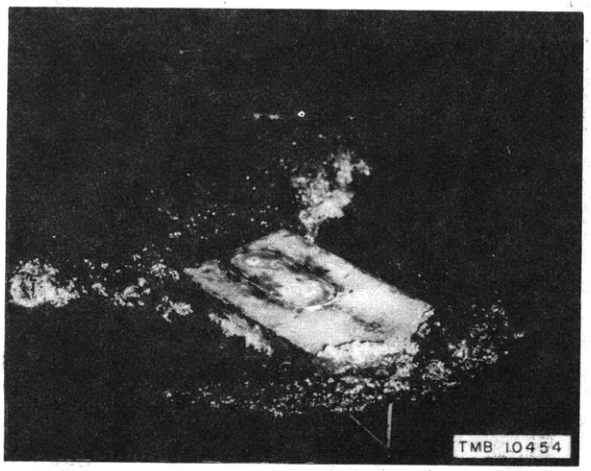

Figure 8a - Buoy B Towed at a Speed Corresponding to 5.59 Knots Full Scale

The total load on the buoy corresponds to a prototype load of 3030 pounds. Water is just flowing over the top or deck surface, and the buoy is considered overloaded.

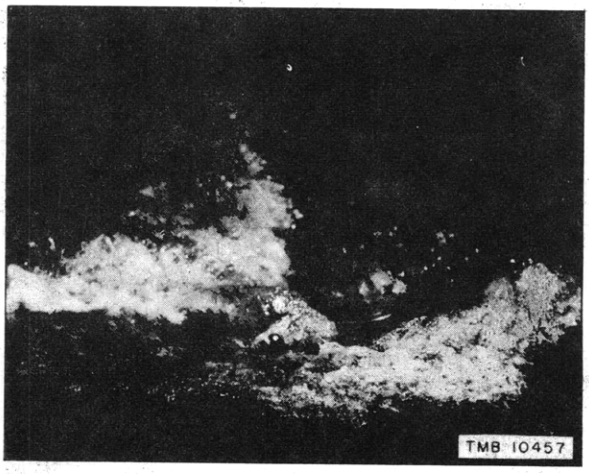

Figure 8b - Buoy B Towed at a Speed Corresponding to 7.83 Knots Full Scale

The total load on the buoy corresponds to a prototype load of 3740 pounds. Although the buoy is very low in the water with very little freeboard, the bow wave is thrown forward, and the deck is clean. The buoy is considered not overloaded in this condition.

Figure 8 - Determination of Maximum Buoy Loads

* Although this criterion may not be satisfactory for buoys having a shape different from that of the NRL Mark 3 buoys, the method proved very successful in the tests reported herein since the points of overload and the loads at which the buoys recovered were sharply defined. For other forms, a more general criterion would be to assume overload when the center of gravity of the buoy is submerged an arbitrary percentage of the initial draft.

vertical, thus eliminating any component in the plane of lift and drag due to angularity of the line. The method of conducting this test is illustrated in Figure 9. A buoy is shown completely submerged and towed with a line passing around a pulley free to swivel and then through a hollow tube to a spring dynamometer on which the towline tension was observed for a range of speeds. The angle of the bridle to a plane perpendicular to the direction of towing was determined by aligning one leg of a properly oriented protractor with the

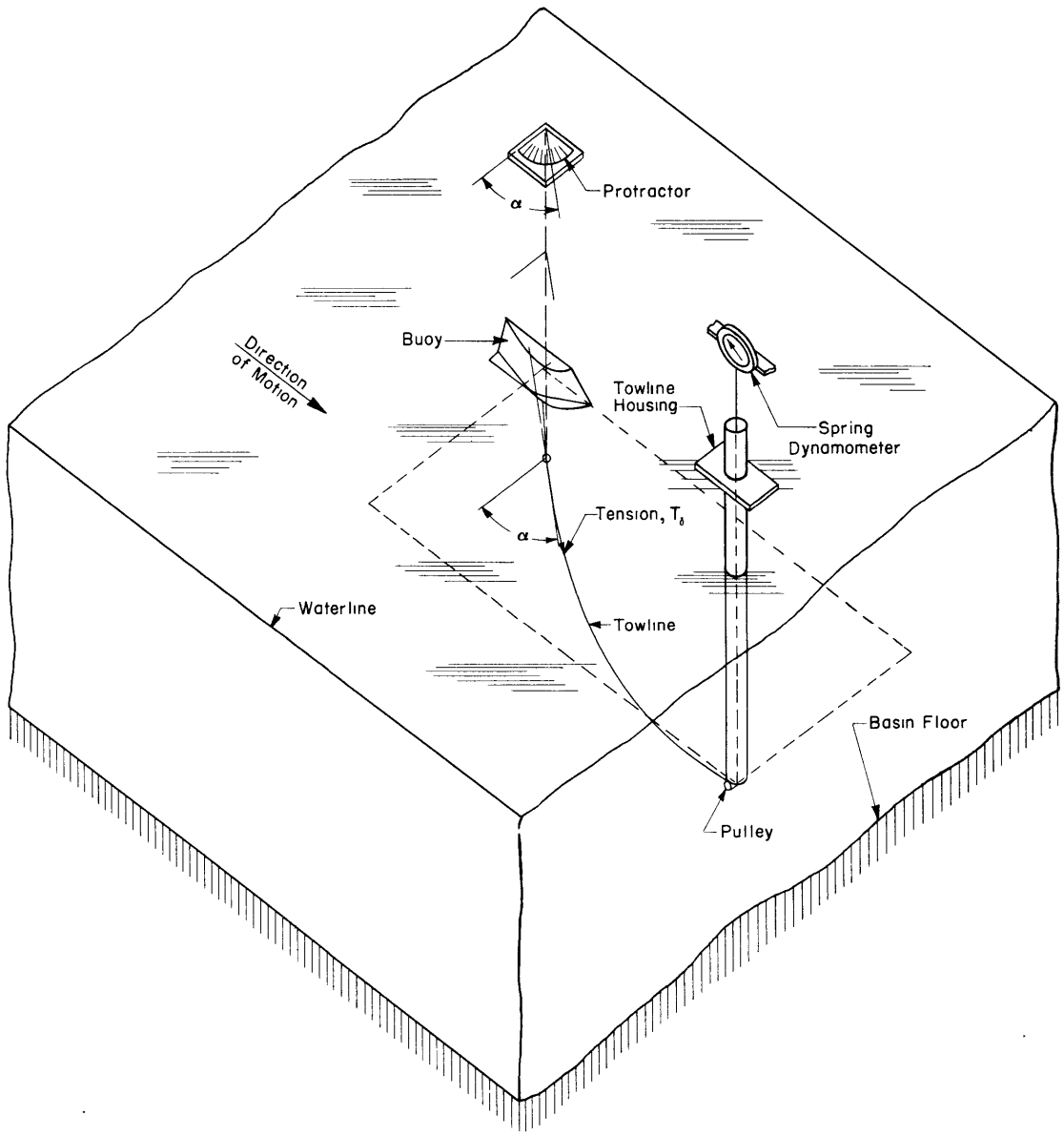

Figure 9 - Test Method for Obtaining Characteristics of NRL Mark 3 Buoy When Submerged

bridle. From these measurements the dynamic lift and the drag of the submerged buoy were evaluated by the equations

$$L_\delta = T_\delta \cos \alpha \qquad [4]$$

and

$$D_\delta = T_\delta \sin \alpha \qquad [5]$$

where L_δ is the dynamic lift of the submerged buoy,
D_δ is the drag of the submerged buoy,
T_δ is the tension in the towline, and
α is the angle of the towline at the body with a plane perpendicular to the direction of motion.

The total lift L developed by a submerged buoy, then, is the sum of the dynamic lift and its total buoyancy B, or

$$L = L_\delta + B \qquad [6]$$

BUOY TEST RESULTS

The loads under which each buoy was tested, stepped up to full scale, are shown by the curves marked "Imposed Load Curves" in Figures 10 and 11. The test data were analyzed by Equation [3]. Thus, although the shapes of the load curves are similar, the fact that the total loads are greater for Buoy B is due to the difference in total weight between the two buoys. The four loading conditions correspond to the four depressor settings used in the tests. The load under which the buoys became submerged and that at which they recovered while towing at a single depressor setting is indicated by the small arrows on each load curve. By joining these points, the curve of limiting loads at each speed is established. At the low speeds the curve was faired into the value of the total buoyancy of each buoy. This characteristic curve is marked "Limiting Loading Condition - Surface Buoy" on Figures 10 and 11. At each speed, then, the buoy can safely carry on the surface any load below this limiting value for that speed.

The drag characteristics of Buoy A and Buoy B under each condition of loading were evaluated by Equation [2] and are shown on Figures 10 and 11 by the curves marked "Drag - Surface Buoy." The drag of each buoy was also measured under the constant load of buoy weight only to establish the lower limit of drag of each speed. These data are also shown in Figures 10 and 11.

The maximum load to which the buoys can be subjected when submerged were evaluated from Equations [4], [5], and [6]. In this case the maximum lift of a buoy as a submerged hydrofoil was obtained directly, in contrast

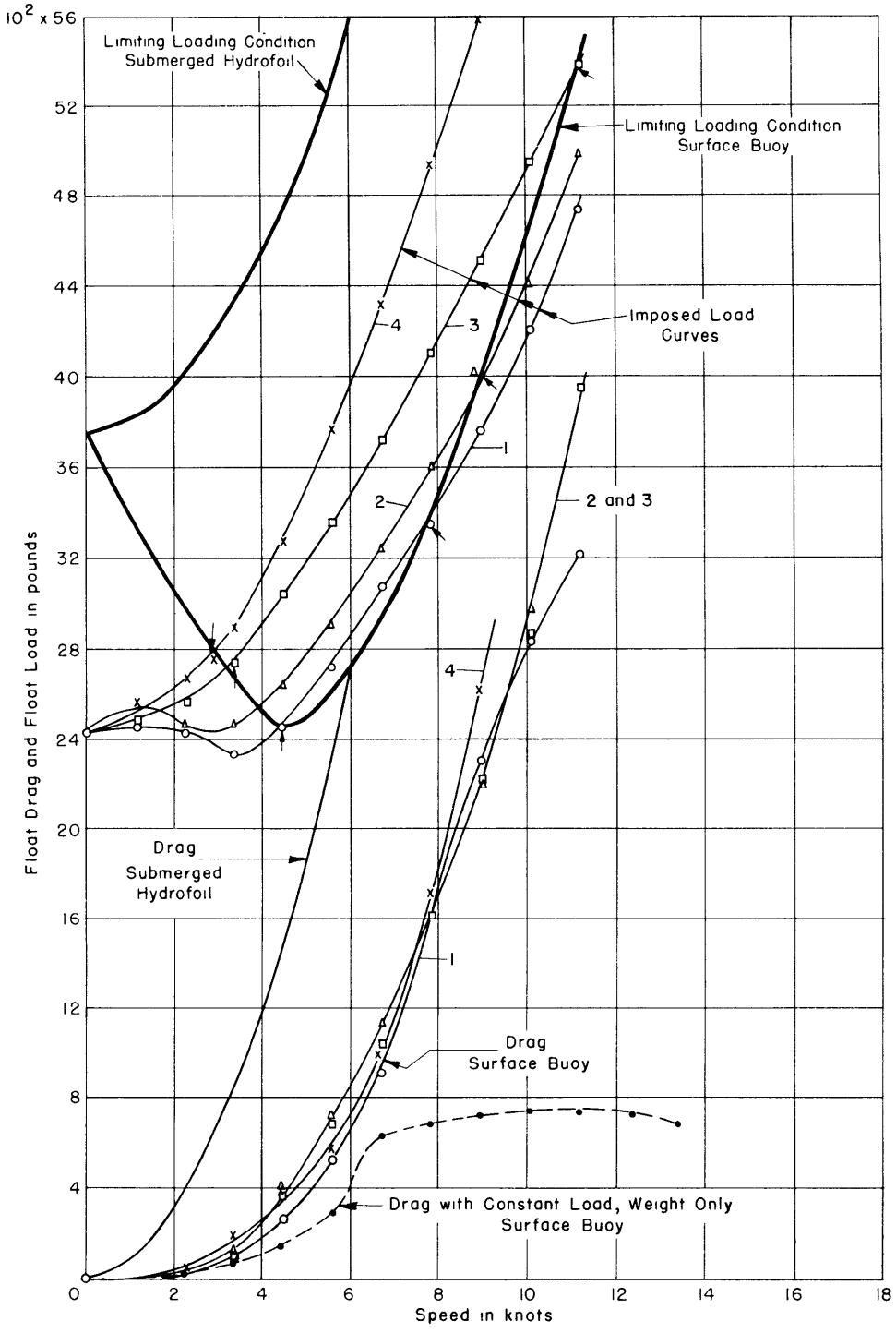

Figure 10 - Performance Characteristics of NRL Mark 3 Buoy A

All loads and speeds are for the full-scale buoy.

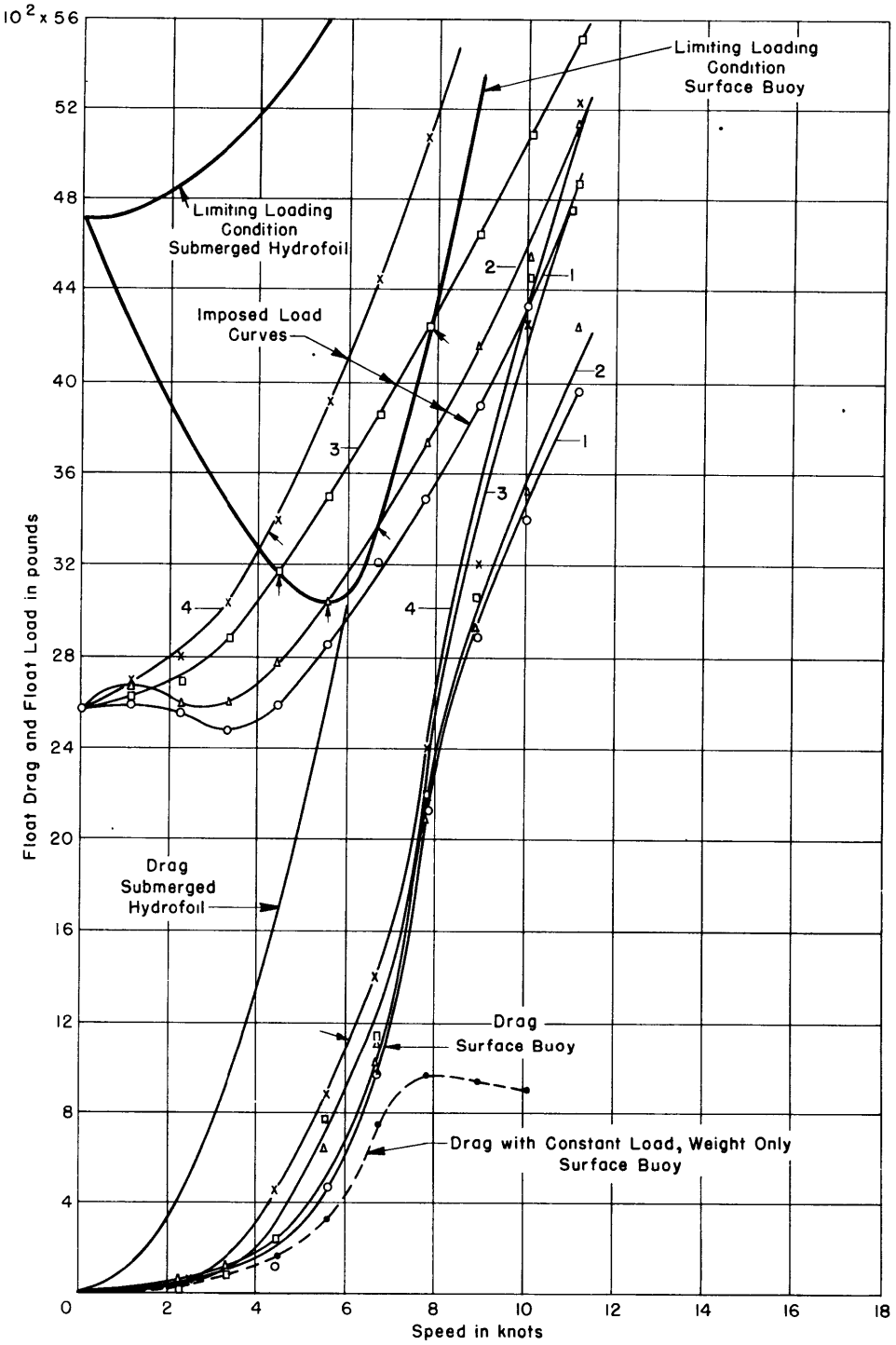

Figure 11 - Performance Characteristics of NRL Mark 3 Buoy B

All loads and speeds are for the full-scale buoy.

with the surface tests in which the behavior was observed under applied loads. The lift characteristics of the submerged buoys may be summarized by a single equation of the form

$$L = nqb^2 + B \qquad [7]$$

where L is the total lift of the submerged buoy in pounds,

n is the constant dimensionless dynamic lift coefficient for a particular design, equal to 0.812 for Buoy A and 0.458 for Buoy B,

$q = \frac{1}{2}\rho v^2$

ρ is the mass density of the fluid in slugs per cubic foot,

v is the speed in feet per second,

b is the beam of the buoy in feet, and

B is the total buoyancy in pounds.

The drag D of the submerged buoys may be written in the form

$$D = aqb^2 \qquad [8]$$

where a is a constant dimensionless drag coefficient equal to 1.184 for Buoy A and 1.318 for Buoy B.

The coefficients n and a were determined for each buoy from the submerged towing tests. For Buoy A, Equation [7] becomes

$$L = 0.812\, qb^2 + 3750 \text{ pounds} \qquad [7a]$$

and Equation [8] becomes

$$D = 1.184\, qb^2 \qquad [8a]$$

For Buoy B, Equation [7] becomes

$$L = 0.458\, qb^2 + 4700 \text{ pounds} \qquad [7b]$$

and Equation [8] becomes

$$D = 1.318\, qb^2 \qquad [8b]$$

Equations [7a], [8a], [7b], and [8b] are plotted in Figures 10 and 11 as the curves marked "Limiting Loading Condition - Submerged Hydrofoil" and "Drag - Submerged Hydrofoil."

DISCUSSION OF BUOY CHARACTERISTICS AND PERFORMANCE

In general behavior, Buoy A and Buoy B are quite similar. Both buoys exhibit a characteristic drop in load-carrying capacity on the surface at the lower speeds. The minimum surface capacity of Buoy A is reached at a full-scale speed of 4.5 knots while the capacity of Buoy B reaches a minimum

at about 5.5 knots. Although the rate of capacity drop for Buoy B is greater than that for Buoy A, the rate of increase of capacity beyond the minimum point is also greater for Buoy B than for Buoy A. The maximum drop in capacity below the value of the total buoyancy is approximately the same for each buoy, about 35 per cent of the total buoyancy.

Observations of the performance of the buoys during the towing tests suggest an explanation of the initial drop in the load-carrying capacity on the surface. When dead in the water, the models trimmed by the stern as listed in Table 1 on page 8. At the lower speeds, both models trimmed horizontally or with a slight negative or down-by-the-bow angle. As the speed corresponding to minimum capacity was reached, the trim angle became positive or down by the stern and increased in a positive direction with increasing speed and load. This behavior is illustrated in the photographs, Figures 12 to 19 inclusive, which were taken during the towing tests under the various loading conditions. The flow around the buoys at the lower speeds is primarily of the displacement type. The rapid change in curvature of the hull from bow to stern results in an increase of the relative velocity of the proximate fluid with a corresponding pressure drop. Furthermore, at these speeds, the dynamic reaction of the fluid forces producing lift on the bow surfaces is negligible, and, owing to the downward force produced by the pressure drop, an overall loss in the load-carrying capacity of each buoy develops.

The test results show that the difference in the capacities of Buoy A and Buoy B in the speed range below the speeds of minimum capacity is, in general, slightly less than the difference of the reserve buoyancies of the buoys when fully equipped; see Table 1, and Figures 10 and 11. Since the greater rate of change of curvature of the surfaces of Buoy B results in a larger pressure drop than for Buoy A, this result is not unexpected.

As the speed of the buoys is increased beyond the point of minimum capacity, the change to positive trim occurs simultaneously with the beginning of the increase in the loading characteristics. With the increase of the trim angle by the stern and the speed, the dynamic lift developed by the buoy becomes appreciable and the load-carrying capacity increases. Although the buoys were tested under much greater loads than are usually applied to planing surfaces, the development of the large dynamic lifts resembles the action of such surfaces. The planing action was more clearly demonstrated in the drag tests under the constant load of the weight of the buoy and equipment. In this case, the hump in the resistance curve, Figures 10 and 11, is characteristic of the resistance curves of planing surfaces under constant loading conditions (5).

(Text continued on page 28)

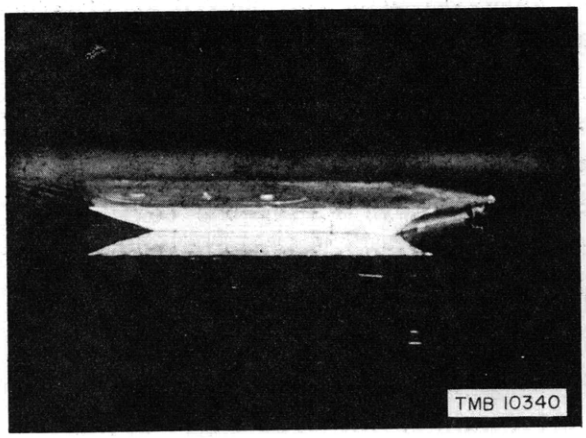

Speed, 1.12 Knot Load, 2450 Pounds

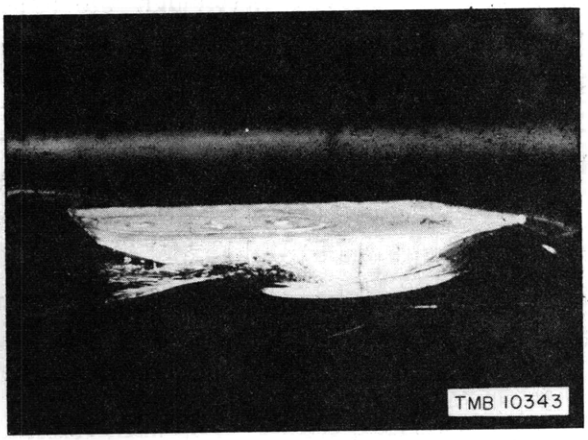

Speed, 3.35 Knots Load, 2340 Pounds

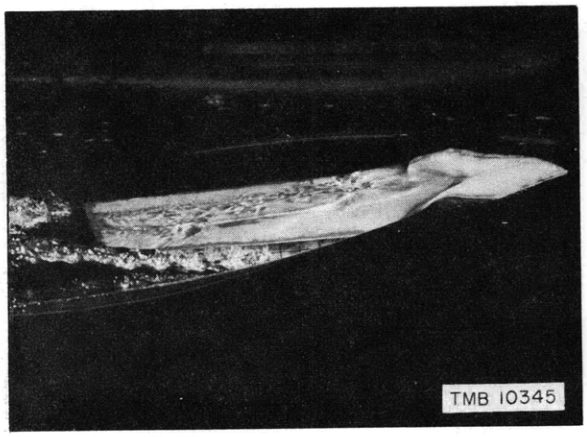

Speed, 5.59 Knots Load, 2750 Pounds

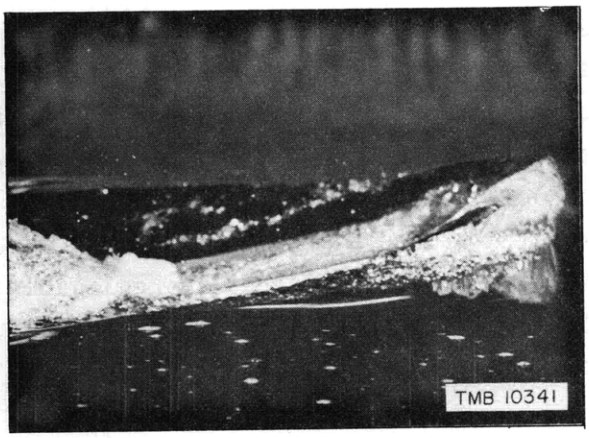

Speed, 6.70 Knots Load, 3070 Pounds

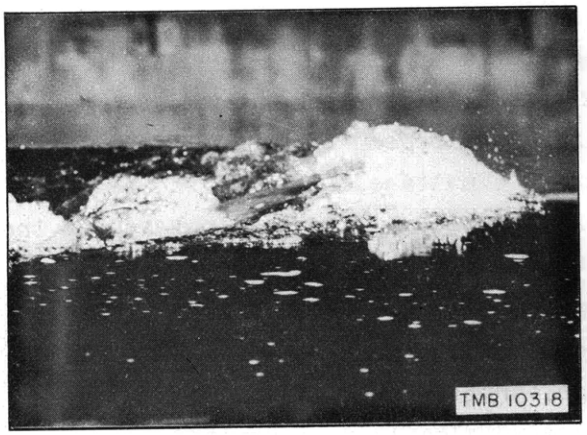

Speed, 7.82 Knots Load, 3370 Pounds

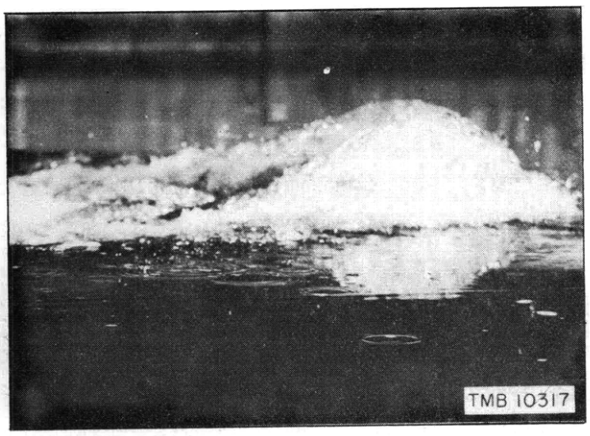

Speed, 10.08 Knots Load, 4210 Pounds

Figure 12 - Photographs of 1/5-Scale Model of NRL Mark 3 Buoy A Being Towed

These tests were made under conditions of the "Imposed Load Curve - 1" of Figure 10. All values are full scale. The buoy became submerged at a full-scale speed of 4.45 knots and recovered at 7.82 knots.

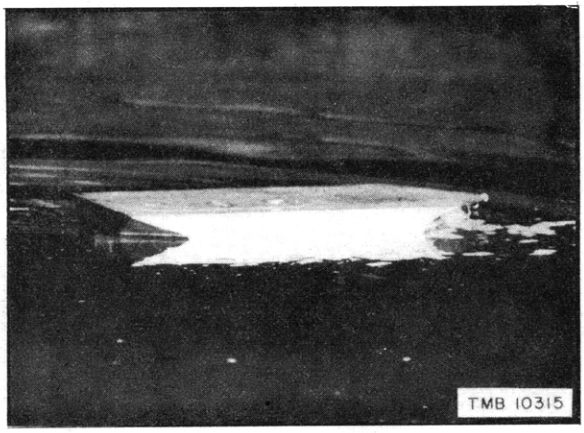

Speed, 1.10 Knot Load, 2540 Pounds

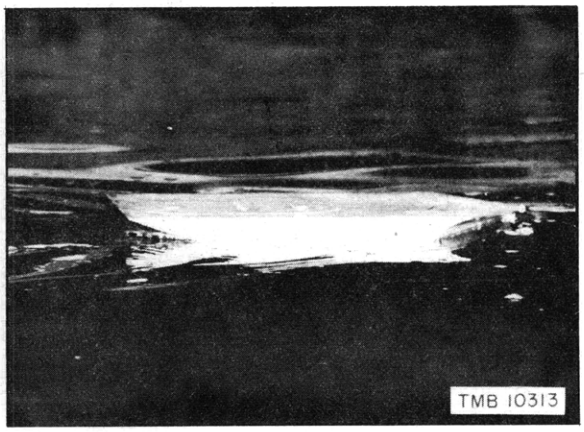

Speed, 2.26 Knots Load, 2460 Pounds

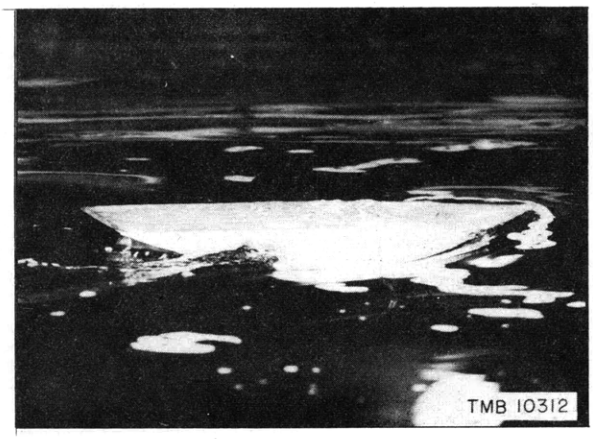

Speed, 3.35 Knots Load, 2460 Pounds

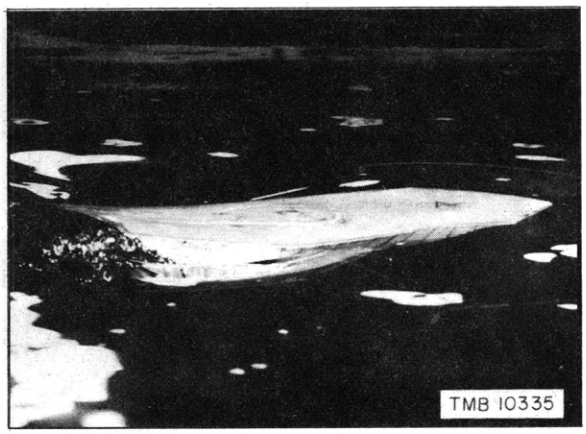

Speed, 4.45 Knots Load, 2640 Pounds

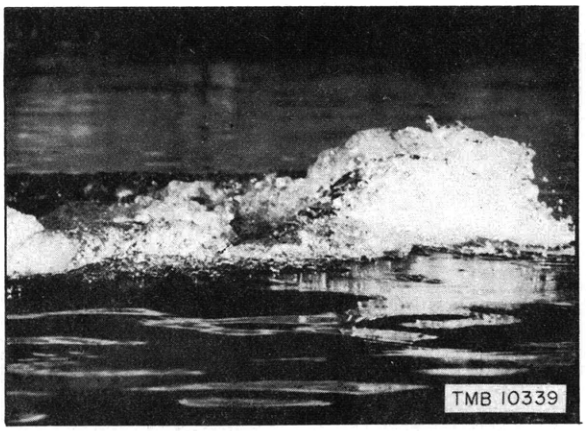

Speed, 8.94 Knots Load, 3990 Pounds

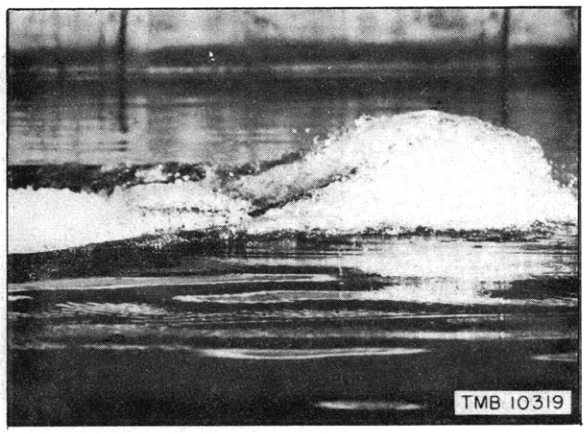

Speed, 10.06 Knots Load, 4430 Pounds

Figure 13 - Photographs of NRL Mark 3 Buoy A Being Towed

These tests were made under conditions of the "Imposed Load Curve - 2" of Figure 10. All values are full scale. The buoy was overloaded at a full-scale speed of 3.35 knots and recovered at 8.94 knots.

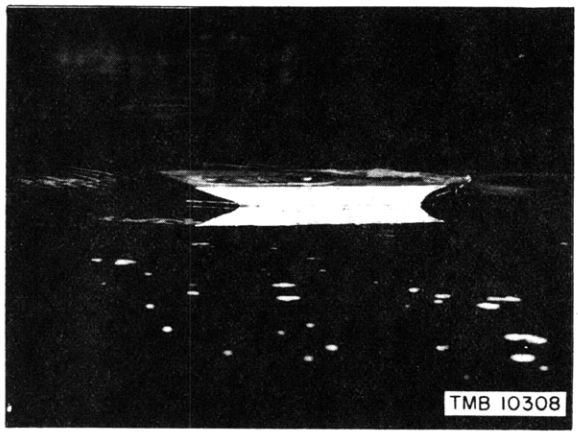

Speed, 1.16 Knot Load, 2490 Pounds

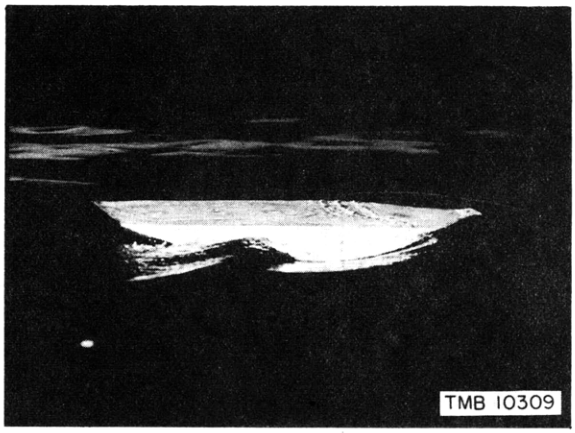

Speed, 3.35 Knots Load, 2750 Pounds

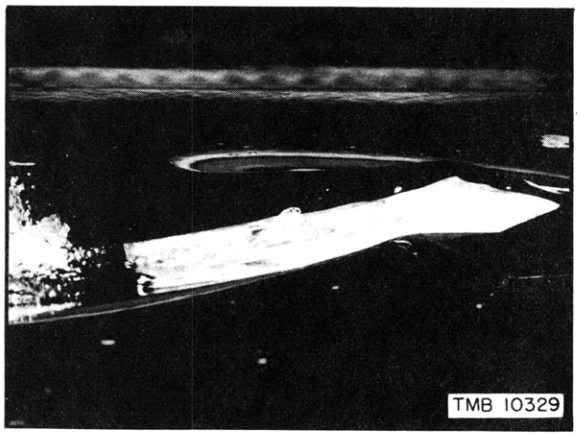

Speed, 6.73 Knots Load, 3730 Pounds

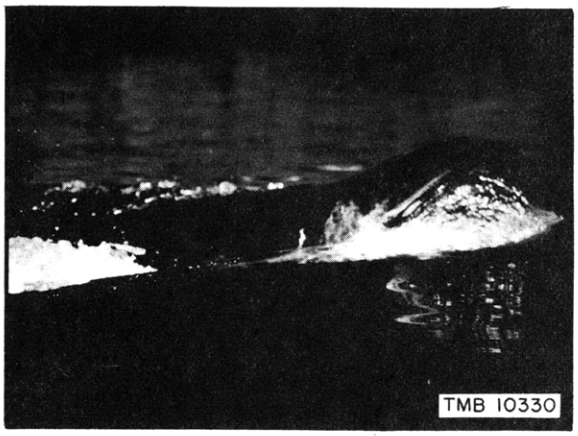

Speed, 8.94 Knots Load, 4520 Pounds

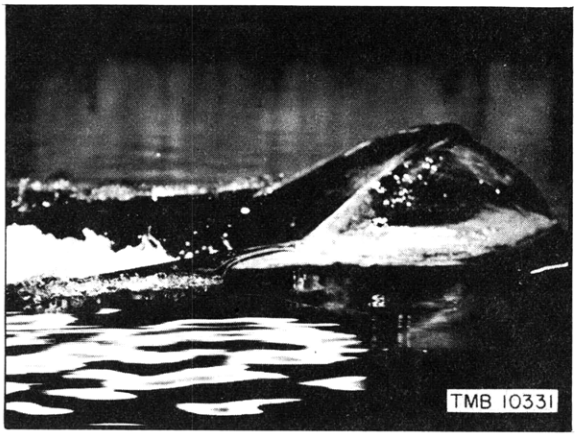

Speed, 10.08 Knots Load, 4950 Pounds

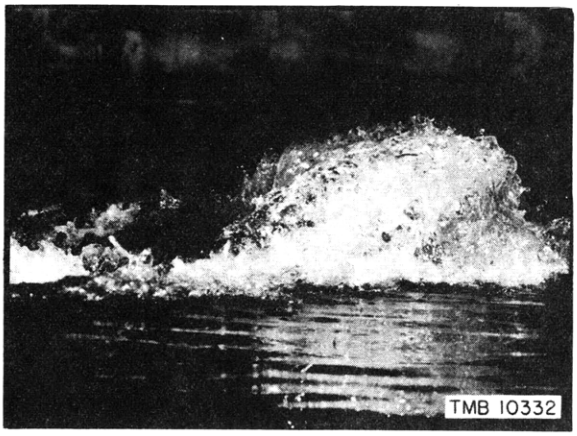

Speed, 11.18 Knots Load, 5390 Pounds

Figure 14 - Photographs of NRL Mark 3 Buoy A Being Towed

These tests were made under conditions of the "Imposed Load Curve - 3" of Figure 10. All values are full scale. The buoy became submerged at a full-scale speed of 3.35 knots and recovered at 11.18 knots.

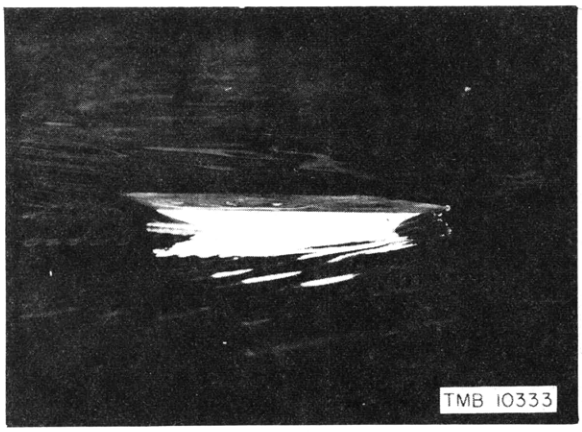

Speed, 1.16 Knot Load, 2520 Pounds

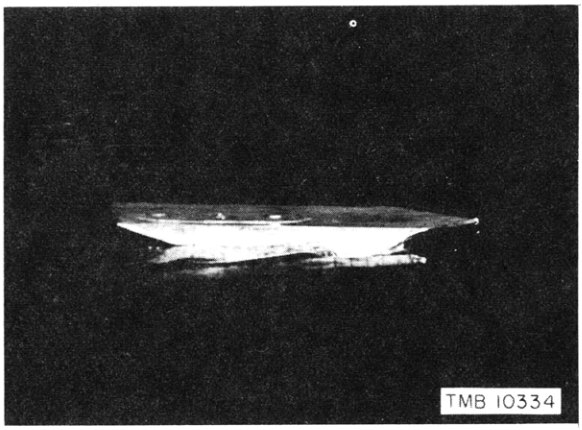

Speed, 2.26 Knots Load, 2670 Pounds

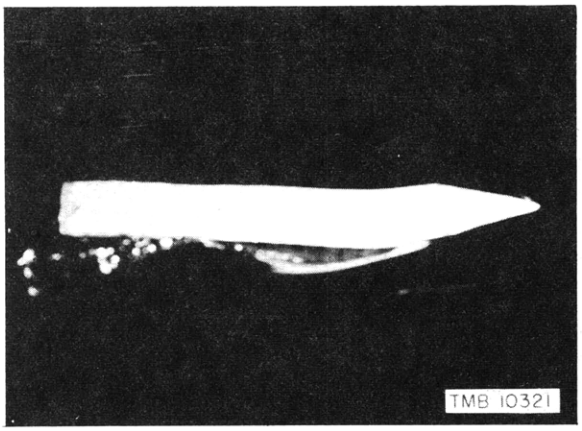

Speed, 3.35 Knots Load, 2900 Pounds

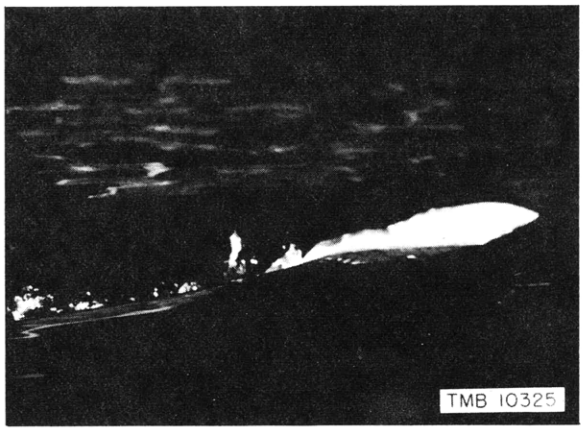

Speed, 7.82 Knots Load, 4930 Pounds

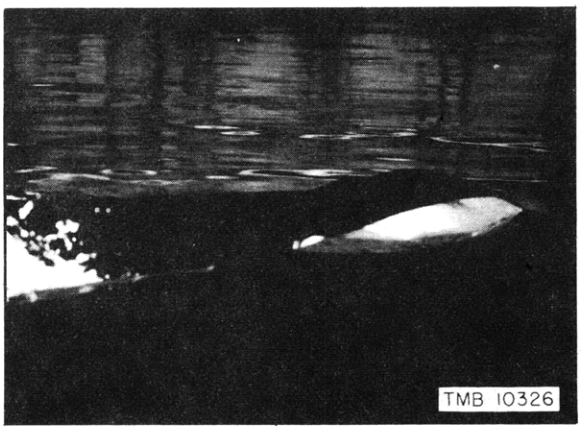

Speed, 8.94 Knots Load, 5590 Pounds

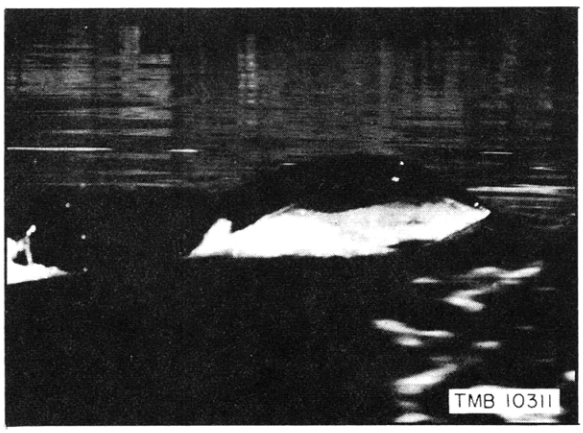

Speed, 10.06 Knots Load, 6430 Pounds

Figure 15 - Photographs of NRL Mark 3 Buoy A Being Towed

These tests were made under conditions of the "Imposed Load Curve - 4" of Figure 10. All values are full scale. The buoy became submerged at a full-scale speed just below 3.35 knots and did not recover throughout the range.

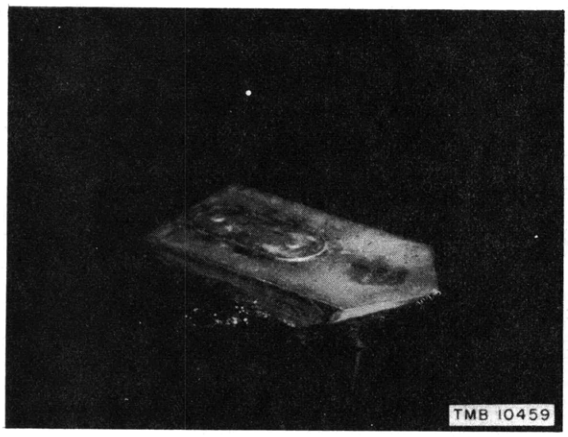

Speed, 3.35 Knots Load, 2470 Pounds

Speed, 6.71 Knots Load, 3180 Pounds

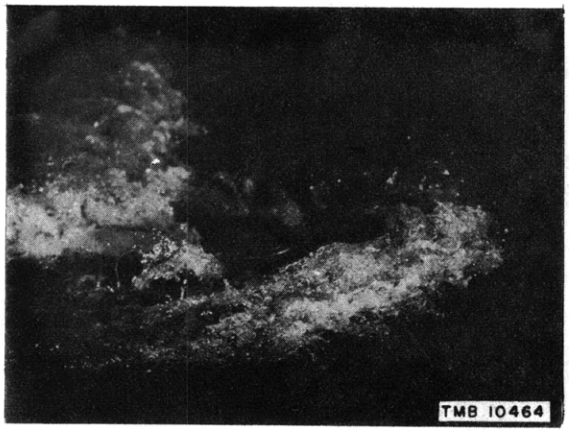

Speed, 7.82 Knots Load, 3510 Pounds

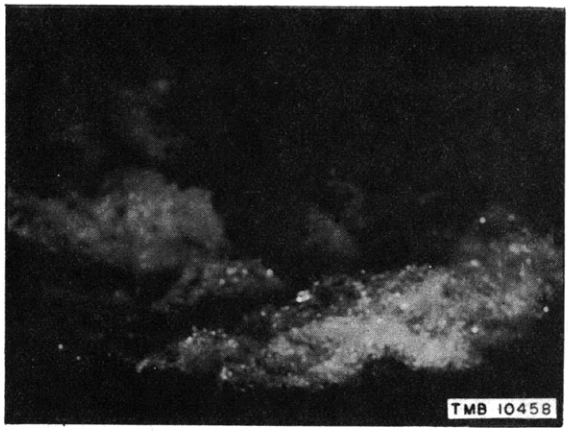

Speed, 8.94 Knots Load, 3900 Pounds

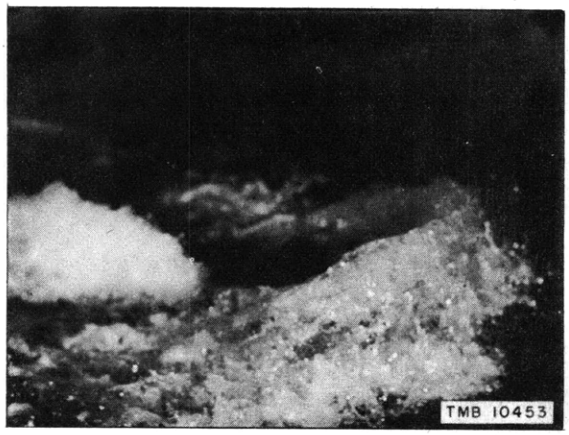

Speed, 11.18 Knots Load, 4870 Pounds

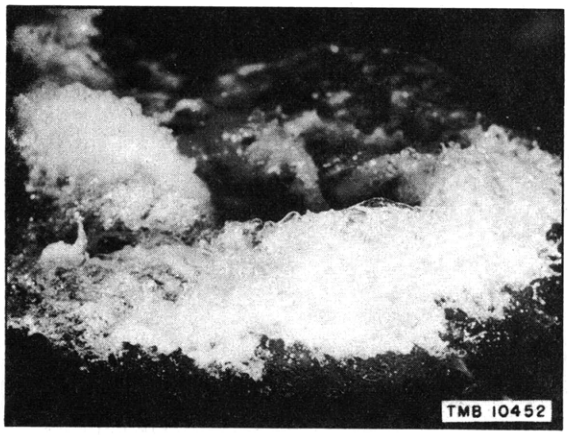

Speed, 12.29 Knots Load, 5350 Pounds

Figure 16 - Photographs of NRL Mark 3 Buoy B Being Towed

These tests were made under conditions of the "Imposed Load Curve - 1" of Figure 11. All values are full scale. The buoy carried the imposed load without submergence throughout the speed range.

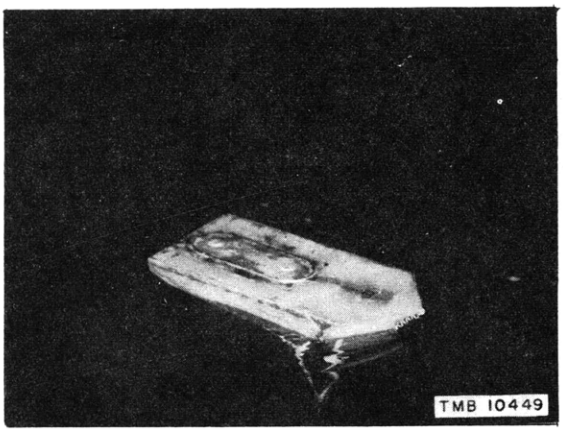

Speed, 1.12 Knot Load, 2670 Pounds

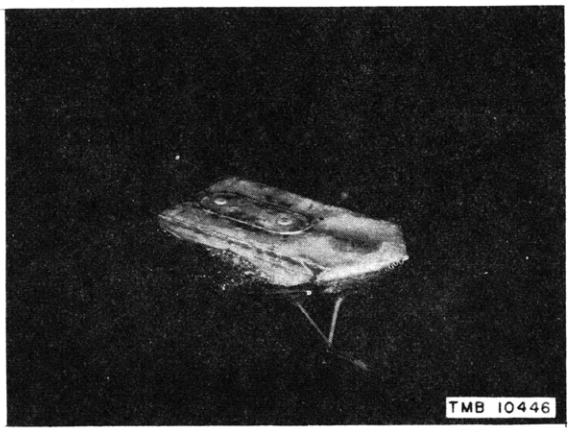

Speed, 3.35 Knots Load, 2600 Pounds

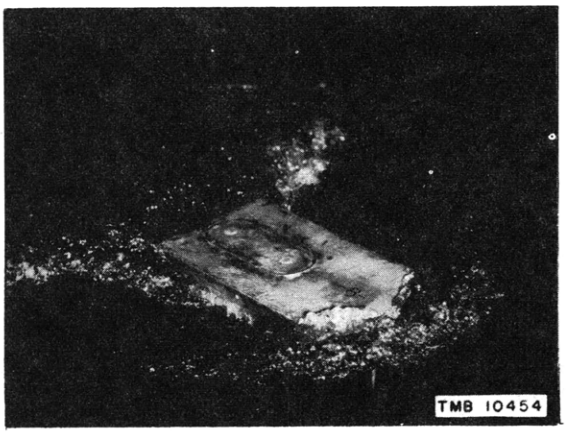

Speed, 5.59 Knots Load, 3030 Pounds

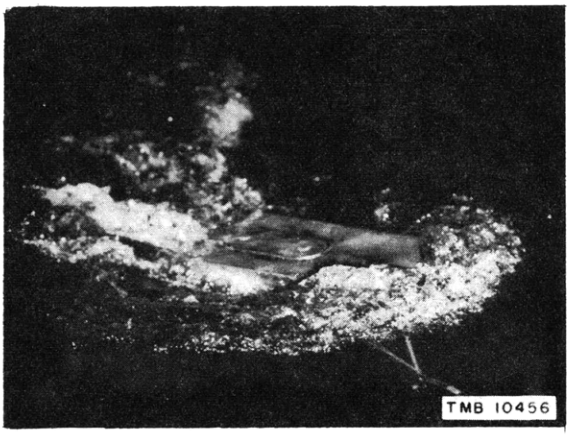

Speed, 6.71 Knots Load, 3370 Pounds

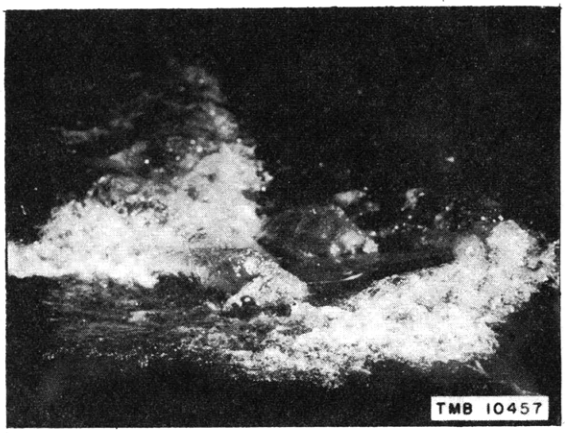

Speed, 7.82 Knots Load, 3740 Pounds

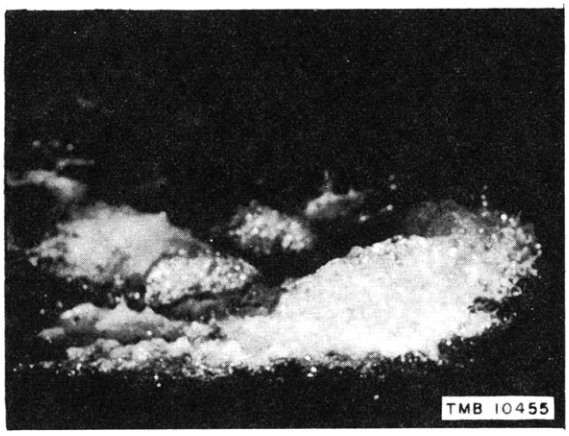

Speed, 10.06 Knots Load, 4630 Pounds

Figure 17 - Photographs of NRL Mark 3 Buoy B Being Towed

These tests were made under conditions of the "Imposed Load Curve - 2" of Figure 11. All values are full scale. The buoy became overloaded at a full-scale speed of 5.59 knots and recovered at 6.71 knots.

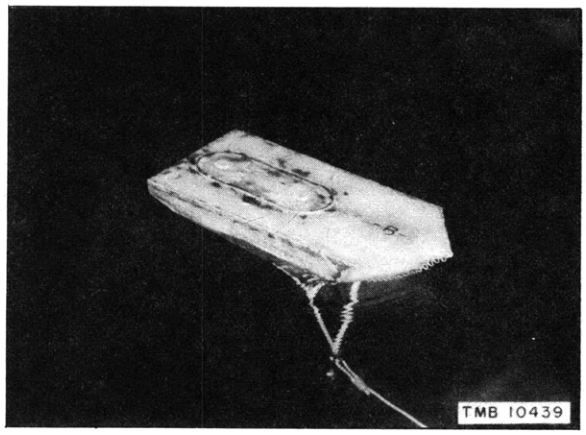

Speed, 1.12 Knot Load, 2620 Pounds

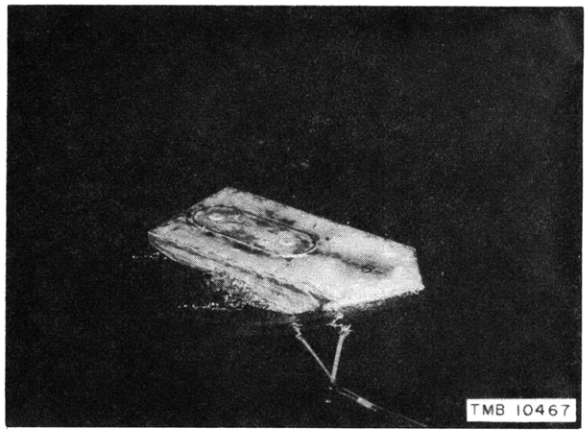

Speed, 3.35 Knots Load, 2870 Pounds

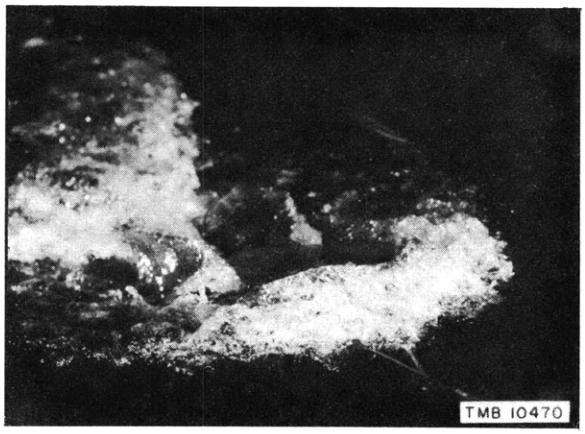

Speed, 6.71 Knots Load, 3860 Pounds

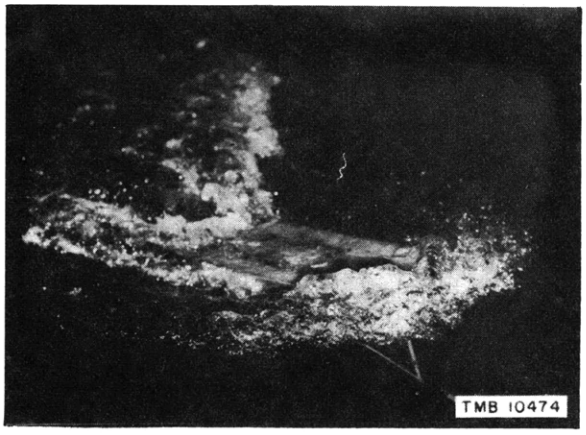

Speed, 7.82 Knots Load, 4240 Pounds

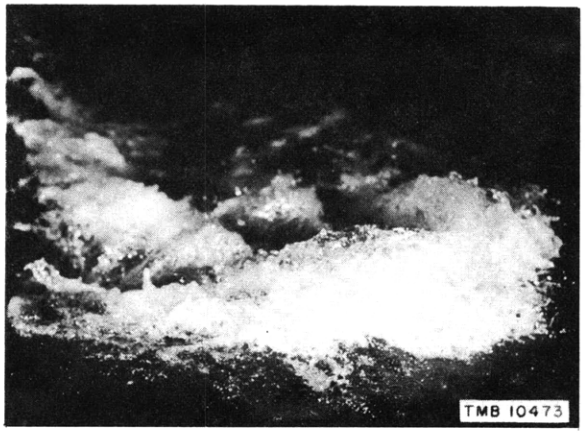

Speed, 8.94 Knots Load, 4660 Pounds

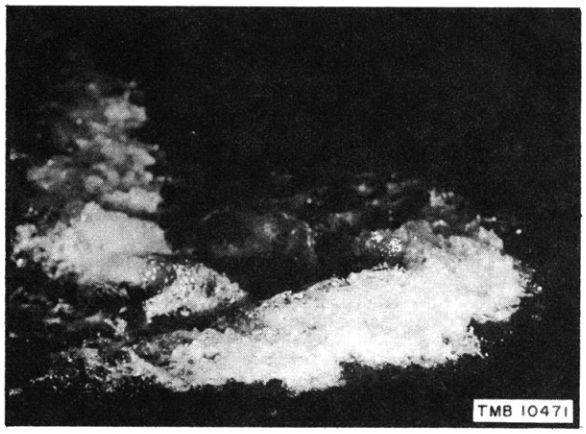

Speed 10.06 Knots Load 5080 Pounds

Figure 18 - Photographs of NRL Mark 3 Buoy B Being Towed

These tests were made under conditions of the "Imposed Load Curve - 3" of Figure 11. All values are full scale. The buoy became submerged at a full-scale speed of 4.42 knots and recovered at 7.82 knots.

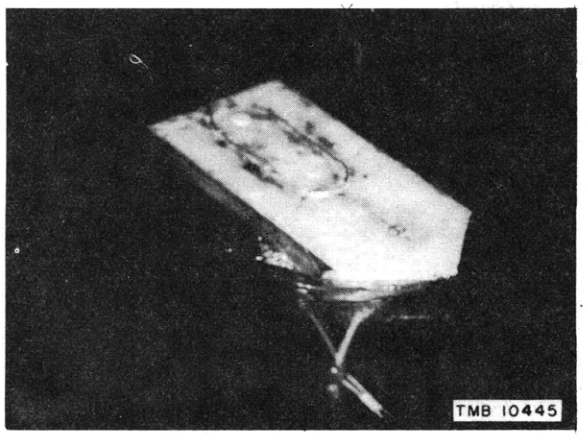

Speed, 2.23 Knots Load, 2830 Pounds

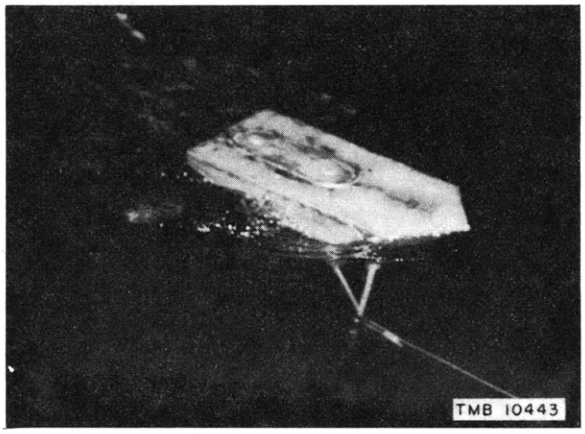

Speed, 3.35 Knots Load, 3040 Pounds

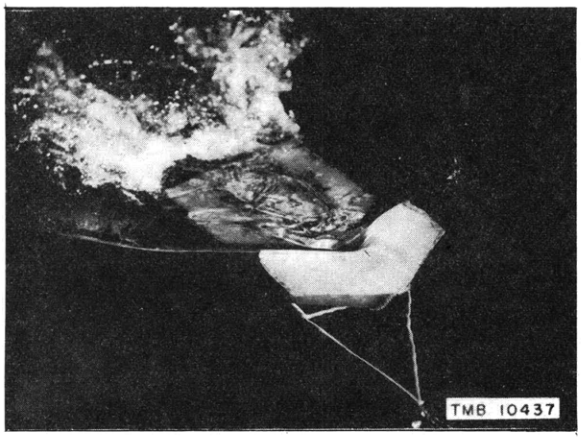

Speed, 6.71 Knots Load, 4450 Pounds

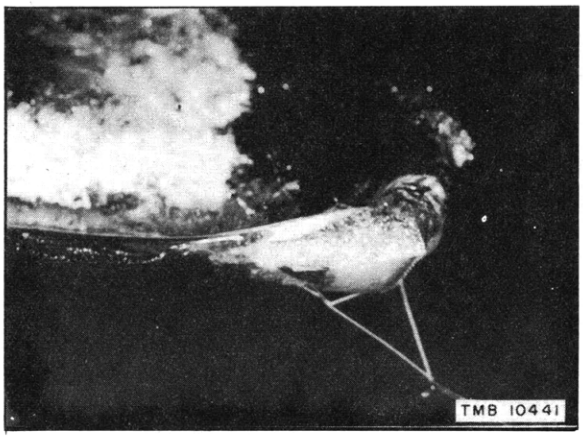

Speed, 7.82 Knots Load, 5060 Pounds

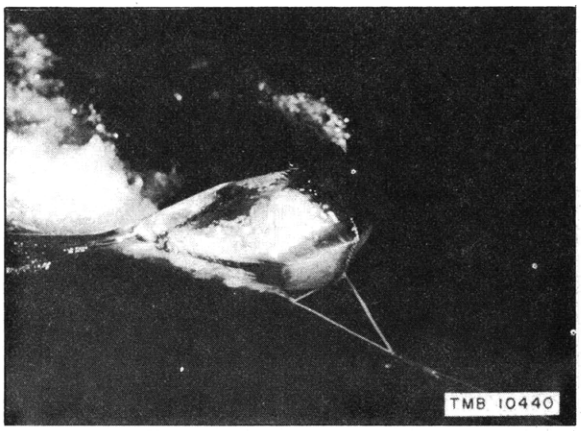

Speed, 10.06 Knots Load, 6680 Pounds

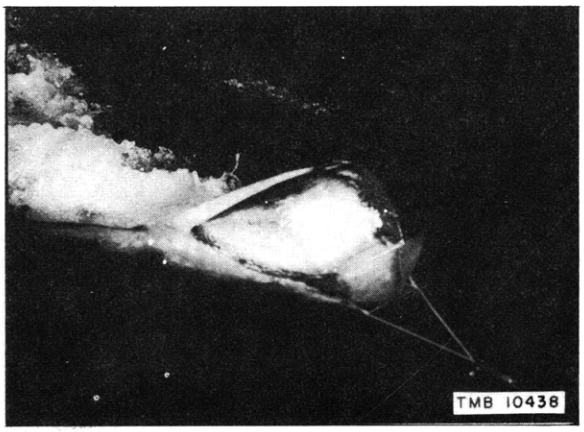

Speed, 11.18 Knots Load, 7650 Pounds

Figure 19 - Photographs of NRL Mark 3 Buoy B Being Towed

These tests were made under conditions of the "Imposed Load Curve - 4" of Figure 11. All values are full scale. The buoy became submerged at a full-scale speed of 4 knots and did not recover throughout the test range.

Both buoys exhibited very stable towing under all loading conditions. Directional stability as well as pitching and rolling characteristics were generally satisfactory.

In the submerged condition, the buoys may be considered as thick hydrofoils of low aspect ratio. The load-carrying capacity, composed of the dynamic lift developed by the buoys plus the total buoyancy, is considerably higher than for the surface condition. Beyond the point of minimum surface capacity, the load-carrying capacity in complete submergence is approximately double the capacity for surface loading. Systematic tests of various hydrofoils at several depths of submergence (6) (7) show an increase in lift characteristics at depths of 5 chord lengths from 25 to 100 per cent over the lift developed at depths of 1/2 chord length. The lift of a hydrofoil appears to approach a maximum limit at a depth of 5 chord lengths. On this basis, the load-carrying capacity of the buoys may be expected to reach a maximum at depths approaching 5 buoy lengths.

Throughout the tests for determining the surface characteristics, the applied loads never exceeded the maximum submerged capacity of the buoys. However, under overload with respect to the surface capacity, the buoys assumed a stable position of equilibrium below the water surface. These conditions are most clearly illustrated in Figures 15 and 19.

The angle of attack to the stream in the submerged tests was observed to be about 30 to 35 degrees bow up for each buoy. Despite this high angle, however, both buoys appeared to be well below the stall angle. The delay of the stall is an effect of the low aspect ratio of the buoys (8) and both buoys were stable throughout the test range. Although a delayed stalling angle allows the development of high lift coefficients for conventional shapes (8), the buoys are used as very inefficient lifting devices in the submerged condition, with resulting low dynamic lift and accompanying high drag. The total lift-drag ratios are high at the lower speeds where buoyancy is the major part of the lift, but rapidly decrease as the speed is increased and the dynamic lift becomes a large part of the total lift. Buoy A is the more efficient of the two buoys, with a dynamic lift coefficient of 0.812 as compared to 0.458 for Buoy B. However, over the speed range in which the buoy will be used, the greater buoyancy of Buoy B gives it a higher characteristic curve than Buoy A in the submerged condition as well as in the surface condition.

TOWING THE BUOYS ASTERN OF A VESSEL - HORSEPOWER REQUIRED

To determine the most practicable method for towing a number of the buoys astern of a vessel, each buoy was first tested singly. The buoys were

rigged only with the brass ballast weights and with the towline attached to the individual loops on the stem. These loops were equally spaced and were numbered consecutively from the deck in the manner illustrated in the sketches, Figures 1a and 1b on pages 4 and 5. The tests were conducted by securing the towline successively in the several positions and towing the buoy through the range of towing speeds. Observations were made of the stability of the model and the ease of towing, and preliminary drag measurements were made to permit selection of the optimum condition.

Representative photographs taken during the towing tests are shown in Figures 21, 22, and 23. On the basis of observations made during these tests, Towing Loop 4 was selected for both buoys, and more complete tests were made to evaluate the horsepower required and the towline tensions for this condition. The centerline of the selected loop is 7 1/2 inches from the deck on the full-scale buoys. The curves of horsepower required and the towline tension for a single towed buoy are shown in Figure 20. At the contemplated towing speed of 8 knots, the horsepower required is 22 for Buoy A and 30.5 for Buoy B.

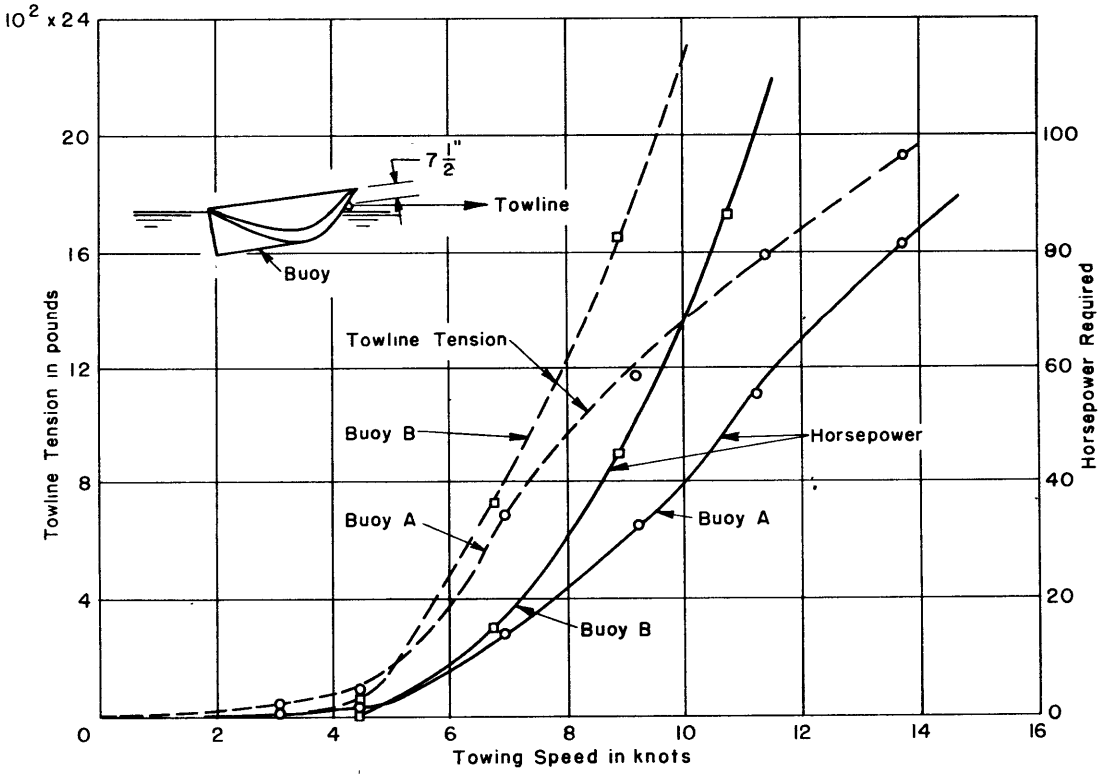

Figure 20 - Towline Tension and Horsepower Required for Towing NRL Mark 3 Buoy Astern of a Vessel

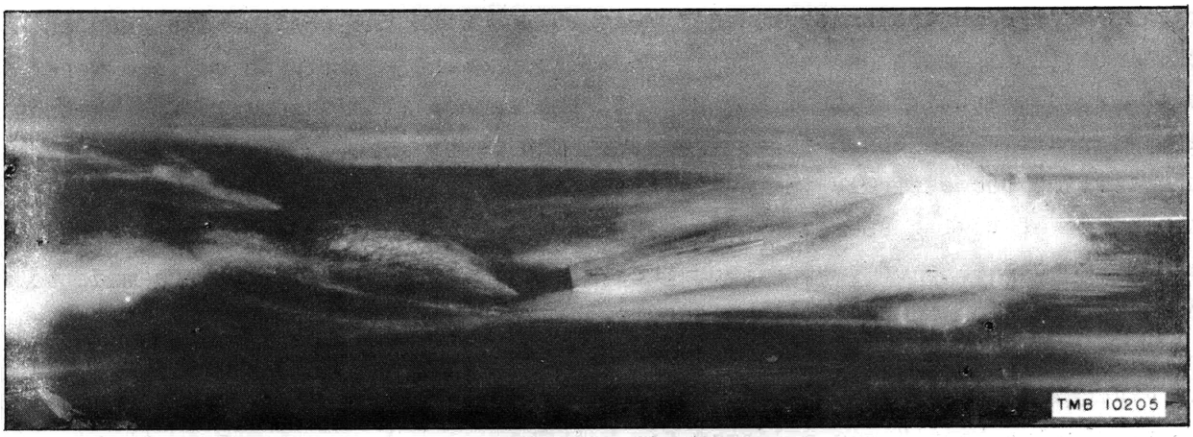

Figure 21a - Buoy A Towed from Loop 4 on Bow

The speed of towing corresponds to the full-scale value of 7.82 knots. This condition was finally chosen as the best on the basis of stability of the model, ease of towing, and horsepower required.

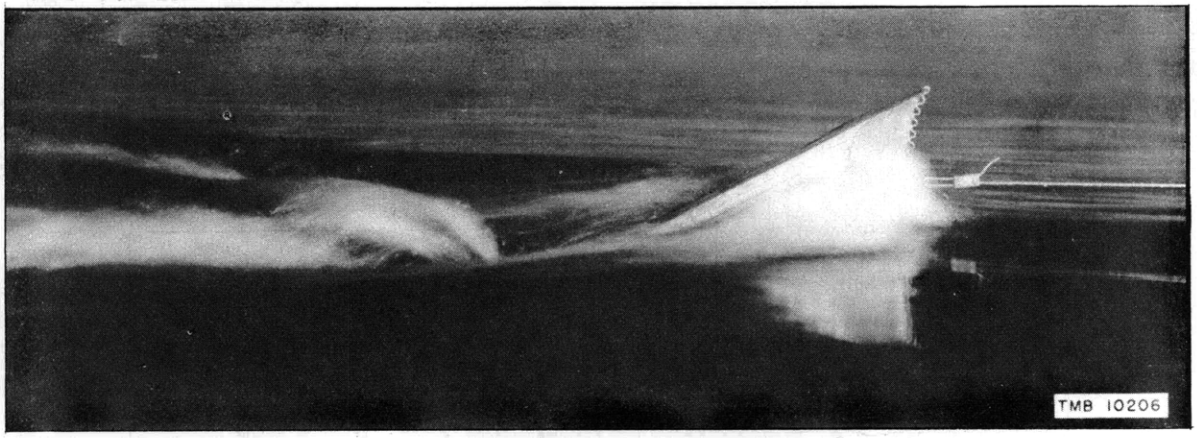

Figure 21b - Towing Loop 9; Speed, 7.82 Knots

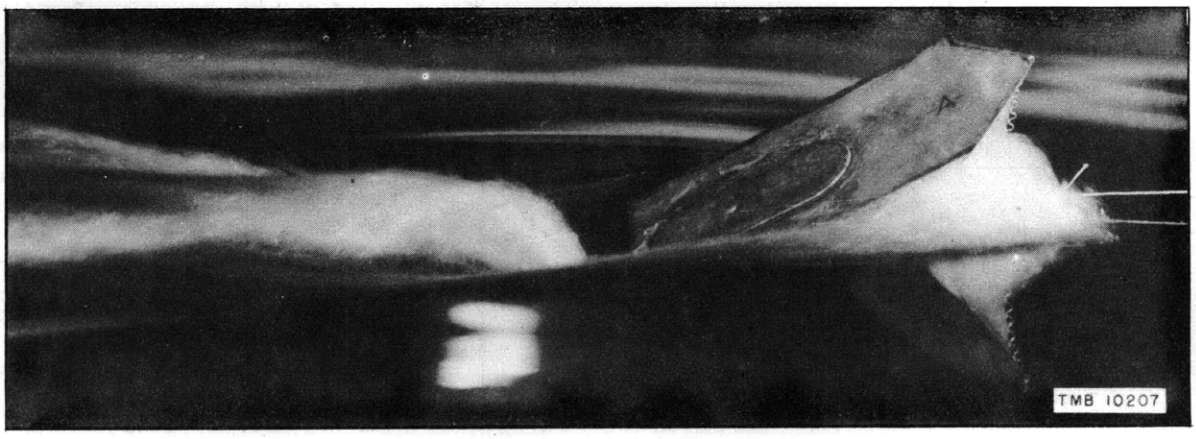

Figure 21c - Towing Loop 13; Speed, 7.82 Knots

Figure 21 - Photographs of NRL Mark 3 Buoy A Being Tested to Determine Method of Towing Astern of a Vessel

The indicated speeds are the full-scale values corresponding to the model tests.

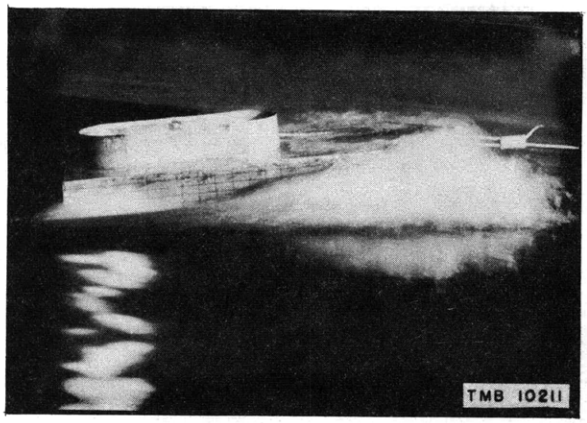

Figure 22a - Towing Loop 2; Speed, 7.82 Knots

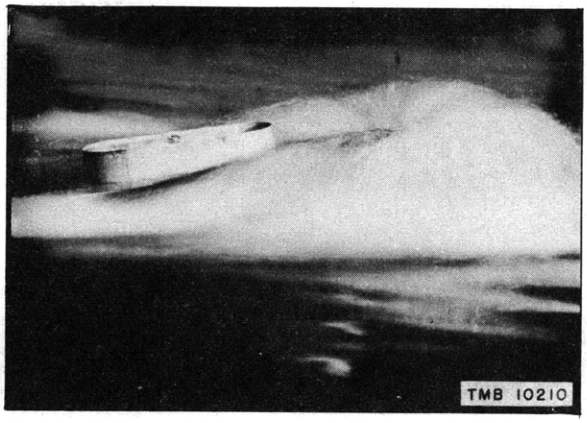

Figure 22b - Towing Loop 2; Speed, 9.61 Knots

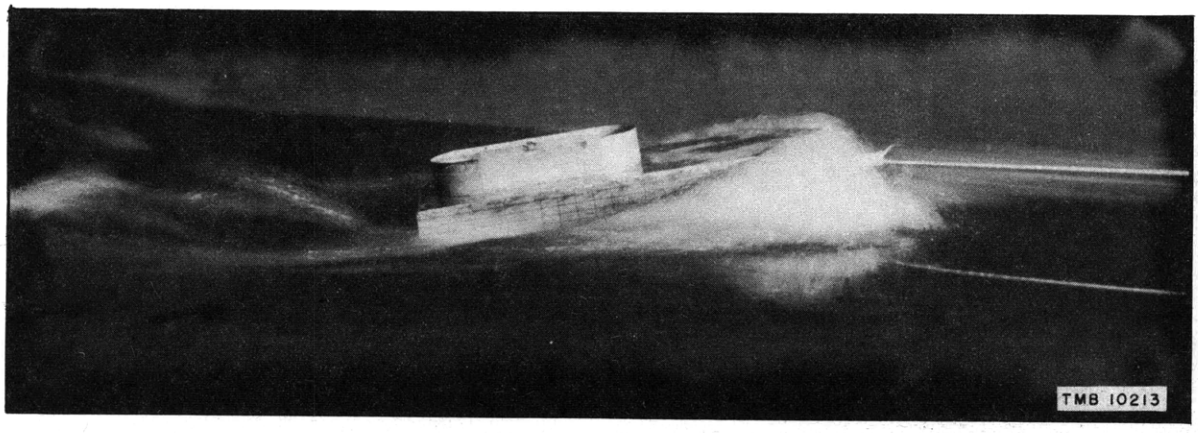

Figure 22c - Towing Loop 4; Speed, 7.82 Knots

This method of rigging was finally selected as the best on the basis of stability of the model, ease of towing, and horsepower required.

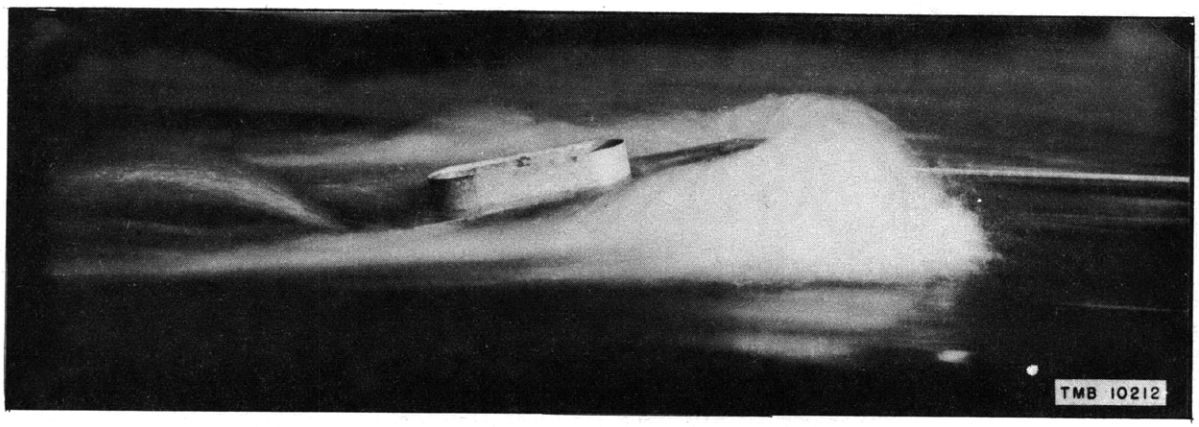

Figure 22d - Towing Loop 4; Speed, 9.61 Knots

Figure 22 - Photographs of NRL Mark 3 Buoy B Being Tested to Determine Method of Towing Astern of a Vessel

The indicated speeds are the full-scale values corresponding to the model tests. The coaming was added for this test to prevent flooding of the buoy since the hatch cover had already been removed.

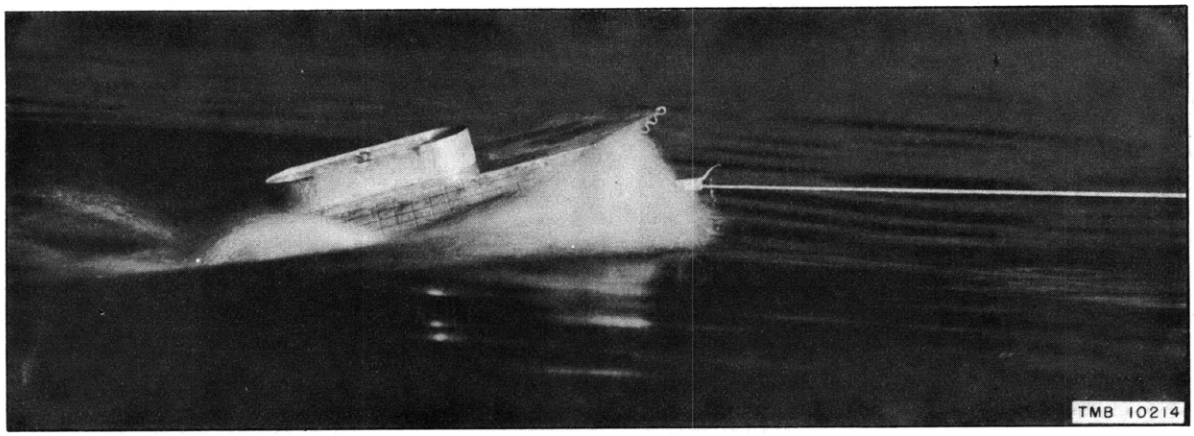

Figure 23a - Towing Loop 8; Speed, 7.82 Knots

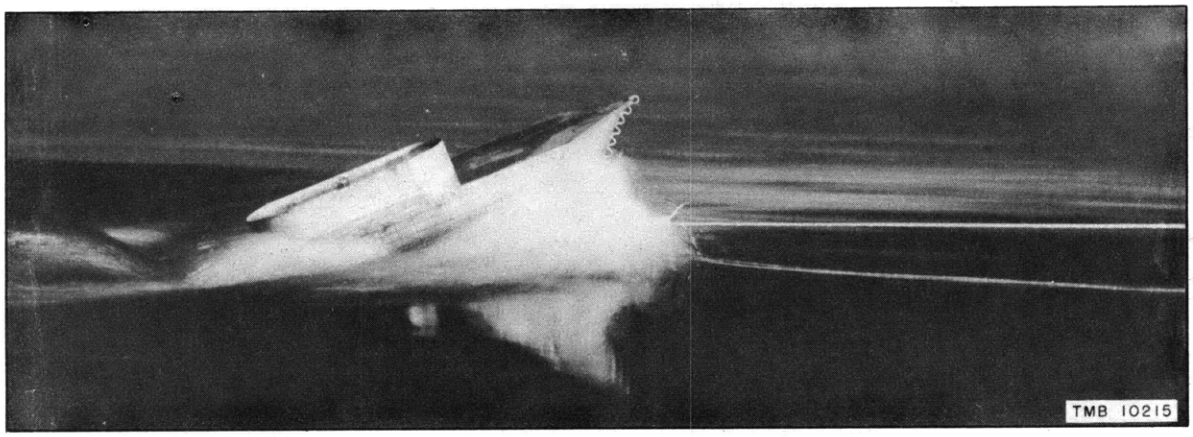

Figure 23b - Towing Loop 12; Speed, 7.82 Knots

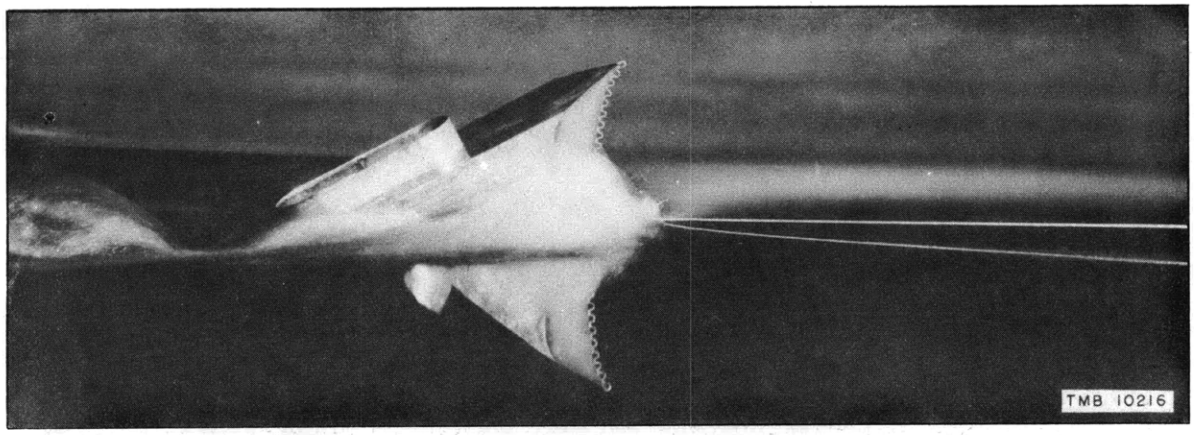

Figure 23c - Towing Loop 16; Speed, 7.82 Knots

Figure 23 - Photographs of NRL Mark 3 Buoy B Being Tested to Determine Method of Towing Astern of a Vessel

The indicated speeds are the full-scale values corresponding to the model tests.

DETERMINATION OF METHOD OF RIGGING FOR TOWING SEVERAL BUOYS ASTERN OF A VESSEL

Having determined the best point of tow on the stem of the buoys, this position, Towing Loop 4, was held constant, and tests were conducted to determine a suitable method for towing up to three buoys at one time. Since small vessels will probably be used, it was decided to concentrate on a tandem system of towing. The scheme finally selected is illustrated in Figure 24. A ring is welded directly to the stern plate on the longitudinal centerline of the buoy and tangent to the top or deck surface. The exact position of this ring is not critical, and the ring may be welded to the top surface at the stern. In any event, the centerline of the ring should be kept within one foot of the intersection of the deck and stern plates and on the longitudinal centerline of the buoy.

Two schemes for securing the bridle while towing a buoy to an anchoring station are suggested in Figure 24. Buoy A is shown with the towline passed between the legs of the bridle and secured to the stem. The

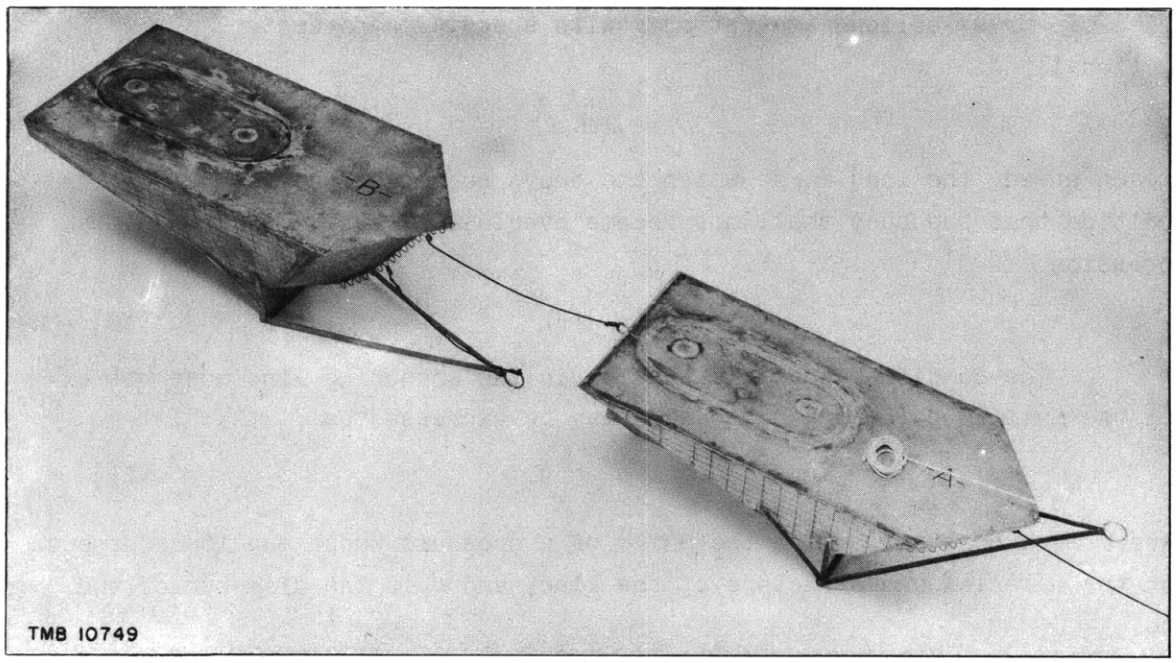

Figure 24 - Method of Rigging NRL Mark 3 Buoys for Towing Several Buoys Astern of a Vessel

The towlines to each buoy are secured in Towing Loop 4. The after buoy, Buoy B, is towed with a line from the lead buoy. This line is secured in a ring welded on the stern plate of the lead buoy just below the level of the deck and on the longitudinal centerline of the buoy.

Two methods for securing the bridle while underway are illustrated. Buoy A, the lead buoy, is shown with the towing line passed between the legs of the bridle and secured to the bow. The bridle is held up in an easily accessible position by the buoy anchoring line which is, in turn, secured on the deck of the buoy. The bridle on Buoy B, on the other hand, is secured by a lanyard to the stem of the buoy and may be retrieved by grappling the lanyard.

bridle is held up by the anchoring line which, in turn, is secured on deck. When the buoy is in anchoring position, the towline is cast loose and the anchor is secured to the anchoring line which is easily accessible in its position on the deck of the buoy. The method illustrated with Buoy B involves securing the bridle to a point on the stem with a lanyard which may be grappled by any suitable means so that the bridle may be lifted. It may be found desirable for accessibility in full-scale operation to secure the lanyard at the point used for towing.

If the towing vessel is sufficiently broad of beam, it may be found more convenient to simply tow one buoy off each after quarter with the third directly astern. For this method, the buoys could be towed in echelon formation to minimize possible damage due to collision.

PART 2 - DETERMINATION OF LINE SIZES FOR ANCHORING

LIMITING FLOAT AND CABLE CONDITIONS FOR THE SURFACE BUOY

From the tests of the buoys, it was found that the drag D is dependent upon the total load L and the speed v. The drag can be plotted as a series of curves of load against drag with speed as a parameter; or, written functionally

$$D = D(L,v) \qquad [9]$$

At each speed, the load L_M at which the buoys submerged was measured. The condition that the buoy shall not become overloaded, then, is given by the expression

$$L < L_M(v) \qquad [10]$$

The condition that the tension in the anchoring line must not exceed the maximum safe working tension may be expressed as

$$T < md^2 = T_M \qquad [11]$$

where m is a constant having the units of a pressure whose magnitude depends upon the material and structure of the line, and d is the diameter of the line.

MOORING-LINE RELATIONS

Referring to the force diagram of Figure 25, let L and D be the lift (dynamic plus buoyant) and drag of the buoy, W the weight of the buoy, and T the tension in the anchoring line which is at an angle ϕ_0 to the incident flow. Then, resolving forces,

$$T \cos\phi_0 = D \qquad [12]$$

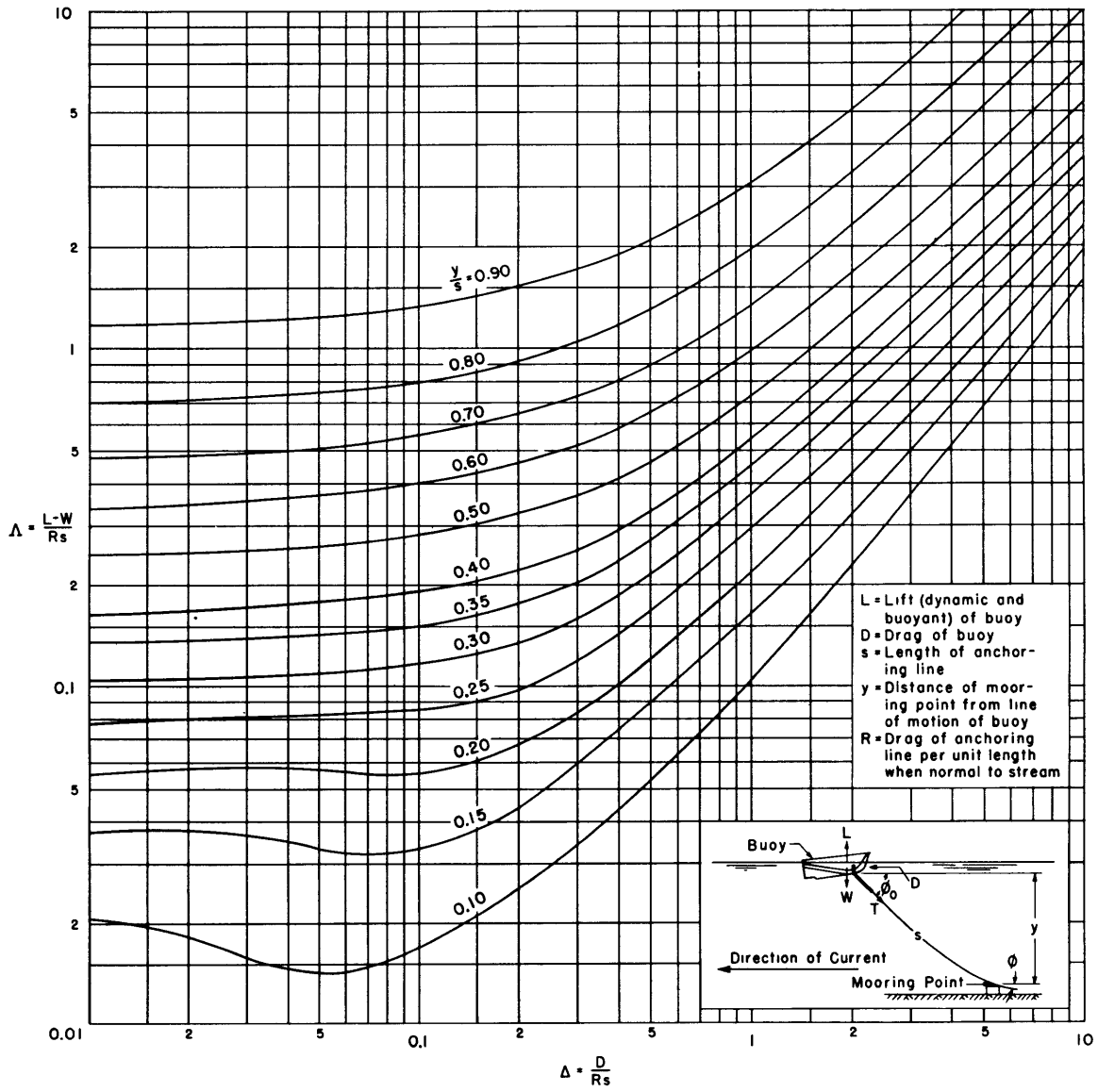

Figure 25 - Shape of and Forces on a Mooring Line

and

$$T \sin \phi_0 = L - W \qquad [13]$$

The load on the buoy and the tension in the anchor line depend both on the buoy characteristics, as given by Equations [9] and [10], and on the ralation between the shape of and forces on the anchor line. It is shown in Reference (9) that the latter relation for a light, flexible line is

$$\Lambda = \Lambda(\Delta, \eta) \qquad [14]$$

expressed as a chart of curves of Λ against Δ for various values of η, where

$$\Lambda = \frac{L - W}{Rs} \qquad [15]$$

$$\Delta = \frac{D}{Rs} \qquad [16]$$

$$\eta = \frac{y}{s} \qquad [17]$$

and also that

$$R = C_R q d \qquad [18]$$

where y is the depth of the mooring point below the buoy,
s is the length of anchor line,
R is the drag per unit length of line when normal to the stream,
C_R is a drag coefficient for the line, and
d is the diameter of the line.*

This chart is shown in Figure 25.

GRAPHICAL DETERMINATION OF SIZES OF MOORING LINE

The method used to determine mooring-line sizes is illustrated in Figures 26 to 28. A polar diagram, Figure 26a, of the drag D against load L - W is first plotted as curves of constant speed v, each curve terminating in the curve of maximum allowable load for a surface buoy. The maximum value of L - W represents the greatest load that may be imposed on the surface buoy over and above its own weight and ballast. Superposed on this diagram, the circles (center at origin, radius = T_M)

$$(L - W)^2 + D^2 = m^2 d^4 \ (= T_M^2) \qquad [19]$$

are plotted for various values of d. Finally, from the chart representing Equation [14], Figure 25, curves of L - W against D for a constant value of η are obtained and plotted for various values of Rs. The coordinates of a point on an Rs curve represent the downward component of the fluid forces on the line on the L - W scale and the drag component of the forces on the D scale for those sizes and lengths of line corresponding to the particular value of Rs. For each value of η a new chart should be plotted. This chart can then be applied for solving all of the problems previously outlined for the Mark 3 buoys in the surface condition.

---

* The results of drag tests on chain and the selection of coefficients for chain and wire rope are discussed in Appendix 1.

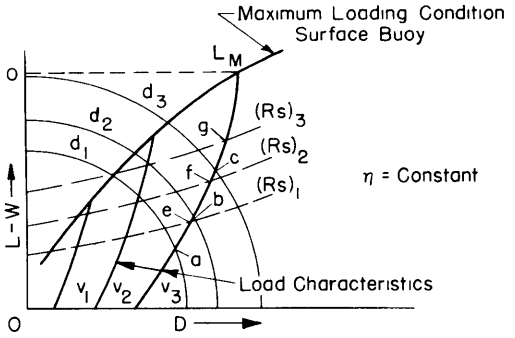

Figure 26a

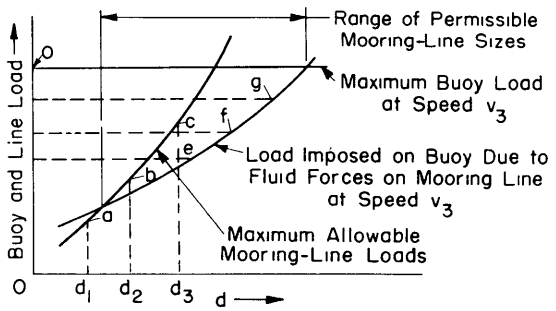

Figure 26b

Figure 26 - Determination of Permissible Anchoring-Line Sizes at a Given Speed and Constant Depth

The problem of selecting proper sizes of anchoring lines when it is desired to anchor in water of a given depth and current velocity with a prescribed length of line consists of finding a range of line sizes within the following limits:

1. The lower limit is determined by the minimum line size which is sufficiently strong compared with the maximum upward pull of the buoy so that the tension in the line does not exceed the safe working tension.

2. The upper limit is determined by the maximum line size that may be used so that the downward component of the fluid forces on the line does not cause the total load on the buoy to exceed the maximum load it can carry without submergence.

On Figure 26a, at each intersection of a characteristic curve of constant speed with a curve of constant Rs, the value of $L - W$ is noted. The diameter d corresponding to this value of $L - W$ is computed from the equation

$$d = \frac{Rs}{C_R q s} \qquad [18a]$$

The series of loads against diameters obtained at the speed in question is plotted as shown on Figure 26b as the imposed-load curve. At the terminal point of the characteristic curve in the maximum-loading curve, L_M, Figure 26a, the maximum permissible diameter is obtained from the value of Rs corresponding to that point. This point is defined on Figure 26b by the intersection of the maximum buoy-load ordinate and the curve of imposed loads, and defines the upper limit of sizes that may be used at that speed.

The lower limit of sizes is determined from a curve of maximum allowable loads for the mooring line, obtained in the following manner. Again working along the constant-speed curve in Figure 26a, the values of

maximum allowable load are noted for each diameter at the intersections with the circles of limiting tension for that diameter. The value of $L - W$ at an intersection is the maximum allowable for a given diameter and speed, since a point on the constant-speed curve with a larger value of $L - W$ is outside the permissible circle for the given diameter. The values of $L - W$ against d given by these intersections are plotted on Figure 26b as the curve "Maximum Allowable Mooring-Line Loads." Line sizes below and to the right of this curve are safe. As a result, the lower limit, based on safe working loads for the line, is established by the intersection of the imposed-load curve and the curve of safe line sizes.

Determination of the maximum current in which a buoy may be anchored with a predetermined type and length of line and a given depth of water follows directly from the problem of determining the range of permissible line sizes at a given speed. The process consists in determining the permissible range at several speeds. The maximum speed is determined when the lower and upper limits of the permissible line sizes coincide. The process is illustrated diagrammatically in Figure 27. In Figure 27a the permissible range of line sizes is determined for several speeds in the manner shown in Figure 26b. By replotting the intersections of the maximum buoy-load ordinates and the imposed-load curves at the various speeds, a curve of maximum safe line sizes against speed is obtained, as shown on Figure 27b. The minimum safe line sizes are obtained from the intersections of the imposed-load curves with the maximum allowable line-load curves of Figure 27a. The curve of minimum safe line sizes against speed is then also plotted on Figure 27b. The intersection of the two curves thus determines the maximum safe speed, since the safe line sizes must be below the curves of maximum sizes and above the curve of minimum sizes. The shaded area on Figure 27b defines the region from which line sizes may be selected. The vertical distance between the two curves

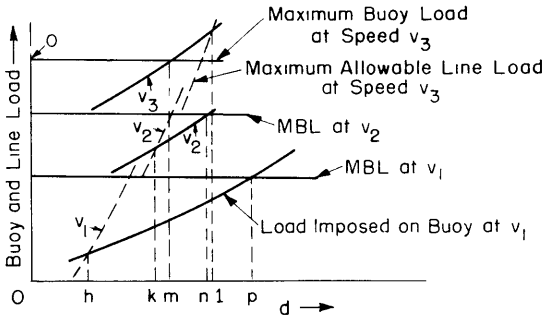

Figure 27a

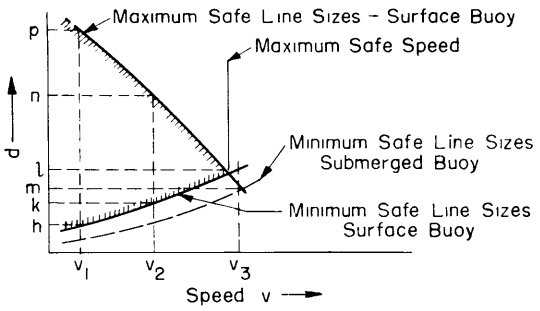

Figure 27b

Figure 27 - Determination of Maximum Safe Anchoring Current at Constant Depth

at any speed gives the permissible range of sizes that may be used at that speed.

The inverse problem of finding the maximum allowable anchoring depth at a given speed with a line of prescribed diameter may also be solved directly from Figure 26a. Since the diameter d and the speed v are given, the value of s corresponding to the intersection of the constant-speed curve with an Rs curve can be computed from Equation [18a]. The corresponding depth then is ηs. The intersection of the characteristic curve of constant speed with the curve of maximum allowable buoy load determines the maximum depth on the basis of buoy load. The intersection of the limiting tension circle for the given diameter with the characteristic curve of constant speed determines depth on the basis of maximum line load.

PROCEDURE IN USING TWO TYPES OF ANCHOR LINE IN COMBINATION

If it is desired to use two types of anchoring line in combination, such as wire rope and chain as sketched in Figure 28, it is shown in Appendix 2 that the chart of Figure 25 and hence the Rs curves in Figure 26a may be applied by using a mean value for R and taking the overall length as s in using the Rs contours, as in Equation [18a].

Let $R_1 s_1$ and $R_2 s_2$ be the values of Rs for the chain and cable parts of the anchoring line, as shown in Figure 28. Put $S = s_1 + s_2$ and define a mean value $\overline{R}$ by

$$\overline{R} = \frac{R_1 s_1 + R_2 s_2}{S} \qquad [20]$$

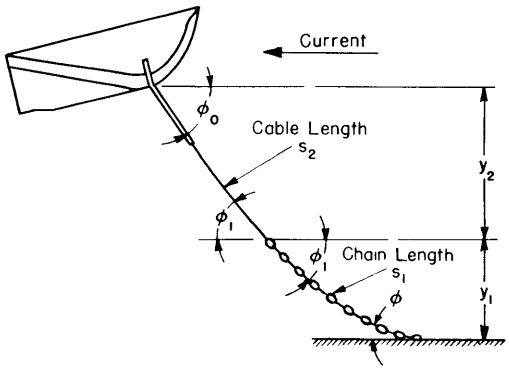

Figure 28 - Combination Chain and Cable Anchoring Line

By expressing the length and drag of the chain in terms of the cable diameter, Equation [20] can be put into more convenient form for application of Figure 26a. For maximum efficiency, it is desirable to use an anchoring line whose component parts are of equal strength, or

$$T_{ML} = T_{MC} \qquad [21]$$

where T_{ML} is the maximum working strength of chain and T_{MC} is the maximum working strength of cable. Thus, from Equation [11],

$$m_L d_L^2 = m_C d_C^2$$

and

$$d_L = d_C \sqrt{\frac{m_C}{m_L}} \qquad [22]$$

Writing Equation [20] in terms of the definition of R,

$$C_{RL} q d_L s_1 + C_{RC} q d_C s_2 = \bar{R}S$$

Let s_1 equal $k s_2$, and substitute for d_L in terms of d_C. Then

$$C_{RL} q d_C \sqrt{\frac{m_C}{m_L}}\, k s_2 + C_{RC} q d_C s_2 = \bar{R}S$$

or, combining terms,

$$\bar{R}S = q d_C s_2 \left(C_{RL} k \sqrt{\frac{m_C}{m_L}} + C_{RC} \right) \qquad [23]$$

Using this value of $\bar{R}S$, Figure 26a is entered and the solutions are obtained as before.

CORRECTION FOR WEIGHT OF ANCHORING LINE

The methods outlined in the foregoing for the solution of the various problems encountered in selecting proper sizes of anchoring line were derived on the assumption that the weight of the line could be neglected. For long lines and low speeds, however, the weight of the line contributes an appreciable part to the total tension in the line. In the case of the Mark 3 buoys anchored in deep water of low current velocities, an approximate correction for the weight of the cable was made in the total load imposed on the buoys.

In Reference (10), it is shown that the tension in a cable towing a body is increased by the magnitude of wy, where w is the unit weight of the cable and y is the vertical distance between the end points considered. The additional downward load imposed at the buoy, then, was assumed to be

$$L_w = wy \sin\phi_0 \qquad [24]$$

where L_w is a correction to the value $L - W$ of downward load obtained in using Figure 26a. The angle $\phi_0 = \tan^{-1} \frac{L - W}{D}$ is large under loading conditions at low speeds (see Figure 30, Appendix 3 and Figure 39, Appendix 4) and, since the sine of the larger angles changes slowly, no attempt was made to correct the angle of the anchoring line at the buoy.

CHECK ON LINE SIZES WHEN BUOY BECOMES SUBMERGED

The solutions obtained by the use of the chart derived in Figure 26a apply, in all cases, to the conditions for a surface buoy. In the event

that the buoy becomes submerged, however, due to fouling of the anchoring line or to heavy sea, the line must be strong enough to carry the total lift developed by the submerged buoy. As a result, the line sizes selected for use with the buoys must be checked for these conditions.

The tension in the anchoring line when the buoy becomes submerged is given by the expression

$$T_s = \sqrt{(nqb^2 + B - W)^2 + (aqb^2)^2} \qquad [25]$$

where W is the total weight of the buoy and installed equipment, and the other terms are defined as in Equations [7] and [8].

The proper diameter d_s of mooring line may be determined for each speed from the equation

$$d_s = \sqrt{\frac{T_s}{m}} \qquad [11a]$$

and plotted as a curve of minimum sizes for the submerged condition as in Figure 27b. The maximum safe speed for the submerged condition is then determined by the intersection of this curve with the curve of maximum allowable sizes. Maximum allowable currents are thus determined for both the surface condition and the submerged condition. The lower of these two currents fixes the maximum current in which the buoy may be anchored. In Figure 27b, the maximum safe current is controlled by the surface condition, and the current in which the buoy is anchored must be limited to this speed.

PART 3 - SELECTION OF ANCHORING LINES FOR THE MARK 3 BUOYS

In selecting wire rope and chain for use with the Mark 3 buoys, the cost and availability of materials were considered, as well as strength and durability. On this basis, plow steel cable,* "proof coil"* and a high carbon content "high test"* chain were investigated. For anchoring in a seaway, it will be necessary to coat this chain or cable with a suitable corrosion-resistant material.**

The best sizes of chain and cable were first determined for each specific condition under which the Mark 3 buoys will be anchored as outlined in the INTRODUCTION. From these data, Buoy B is shown to allow a wider range of operation than Buoy A. On this basis, then, the single chain size and cable size most closely meeting all conditions for Buoy B were selected to provide uniformity in the field.

---

* These are the manufactures' designations.

** If corrosion-resistant types of chain and cable are procurable, see Appendix 4 for the proper method of interpreting the data for use with types other than those considered herein.

A ratio of depth to anchor-line length of 0.5 has been used throughout the analysis as giving the best efficiency in the use of both the buoys and anchoring lines. A higher depth-length ratio would necessitate heavier line sizes owing to increased tensions with resulting buoy overload at lower speeds; while lower ratios result in uneconomical lengths of line.

The ranges of anchor-line sizes for the various conditions are shown graphically in detail in the Appendixes. From these charts the optimum sizes have been selected and summarized in Tables 2 and 3. The best sizes and the optimum speeds are enumerated as directly derived from the analysis. In the adjacent columns the commercial sizes most closely approximating these optimum sizes are listed. The maximum speeds when using the recommended sizes are also given.

The establishment of suitable safety factors in selecting chain and cable sizes was considered on the basis of shock forces encountered in rough seas, the higher tensions in the submerged conditions for the buoys, and possiblity of wear on the anchor lines in raising and lowering the anchor. The use of chain for the lower half of the anchoring line is to provide a better wearing material should the line drag on a hard sea bottom at

TABLE 2

Summary of Anchor-Line Sizes for Buoy A

Anchoring Depth feet	Type of Anchoring Line	Anchoring Line Length, feet		Maximum Current knots	Anchor Line Sizes at Maximum Current inches		Recommended Anchoring Line Sizes, inches			Maximum Current for Recommended Sizes, knots
		Cable	Chain		Cable Diameter	Chain (Bar Size)	Cable Diameter	Chain (Bar Diameter)		
								Actual	"Trade"	
1200	Plow-Steel Cable	2400		4.0	0.229					
600	High-Carbon High-Test Chain		1200	3.95		0.184		7/32	3/16	3.68
600	Proof-Coil Chain		1200	2.75		0.325		11/32	5/16	2.65
600	Plow-Steel Cable plus High-Carbon High-Test Chain	600	600	4.5	0.241	0.184	1/4	7/32	3/16	4.28
600	Plow-Steel Cable plus Proof-Coil Chain	600	600	4.05	0.215	0.270	1/4	9/32	1/4	3.94
100	High-Carbon High-Test Chain		200	>9.0				11/32	5/16	>9.0
100	Proof-Coil Chain		200	7.55		0.432		13/32	3/8	7.30

TABLE 3

Summary of Anchor-Line Sizes for Buoy B

Anchoring Depth feet	Type of Anchoring Line	Anchoring Line Length, feet		Maximum Current knots	Anchor Line Sizes at Maximum Current inches		Recommended Anchoring Line Sizes, inches			Maximum Current for Recommended Sizes, knots
		Cable	Chain		Cable Diameter	Chain (Bar Size)	Cable Diameter	Chain (Bar Diameter)		
								Actual	"Trade"	
1200	Plow-Steel Cable	2400		4.0	0.226-0.368		1/4			4.25
600	High-Carbon High-Test Chain		1200	4.62		0.212		7/32	3/16	4.55
600	Proof-Coil Chain		1200	3.06		0.397		13/32	3/8	3.0
600	Plow-Steel Cable plus High-Carbon High-Test Chain	600	600	5.33	0.271	0.205	1/4	7/32	3/16	5.12
600	Plow-Steel Cable plus Proof-Coil Chain	600	600	4.48	0.281	0.352	5/16	11/32	5/16	4.35
100	High-Carbon High-Test Chain		200	>9.0				15/32	7/16	>9.0
100	Proof-Coil Chain		200	8.18		0.582		17/32	1/2	7.90

low current speeds. For all surface conditions, a safety factor of 4 is used for the plow-steel cable and the proof-coil chain, while a factor of 3 is used for the high-test chain.* Since the tensions in the surface condition are much higher than in the submerged condition, a safety factor of 1 is used in the latter case. Had a higher factor of safety been selected on the basis of the submerged requirements, a practicable size of anchoring line which would not overload the buoy on the surface could not have been obtained. The lines are strong enough to take the shock loads encountered in rough seas. If the buoys become submerged in waves, the large change in lift will enable rapid recovery, thus overloading the anchoring line for only very short periods. The most serious case in which the buoys will be submerged will be the result of fouling of the anchoring line either because of improper anchoring or entanglement on the sea floor. In this case, the anchoring line will be overloaded only if the buoy remains submerged and is in the maximum allowable current for that anchoring line. In currents below the maxima listed in Tables 2 and 3 for the recommended sizes, the anchoring line will not be

* These safety factors are in agreement with manufacturer's minimum recommendations as well as previous experience of the Taylor Model Basin in work of this type.

overloaded. In any event, proper care exercised in launching and anchoring should forestall these exigencies.

STANDARD CHAIN AND CABLE SIZES FOR FIELD INSTALLATION OF BUOY B

On the basis of the chain and cable sizes shown in Tables 2 and 3, Buoy B was recommended for field installations. Several sizes and combinations of anchoring lines were investigated to determine the single size and type of chain and cable permitting the widest range of operation at all speeds; see Figure 48, Appendix 4. As a result of this investigation, plow-steel cable, 3/8-inch in diameter, and "high-test" chain, 9/32-inch (1/4-inch "trade" size) bar diameter, were selected. For full-scale installations, these sizes can be standardized and issued to the various field stations with the instructions of Table 4.

Table 4 has been prepared for ready reference in the field for the selection of proper lengths and combinations of chain and wire rope. For example, for an anchoring depth of 600 feet with a current of 4.0 knots, chain and cable should be used in combination, in lengths which are indicated in Table 4. If the current exceeds 4 knots, wire rope only should be used. If the current is above 5.2 knots, the buoy cannot be anchored with this size cable. In the latter condition, which will seldom be encountered in this depth of water, reference should be made to Figure 48, Appendix 4, and at 600 feet a new size should be selected. In this case, a cable 5/16 inch in diameter is found to be satisfactory in currents up to 5.9 knots.

The weight of a cubical concrete block used as an anchor is also shown in Table 4 for each current speed. The controlling basis for the weight is the upward or lifting component of the anchor-line tension. Based on sliding friction only, much lighter weights would be adequate.

CONCLUSIONS AND RECOMMENDATIONS

In general, Buoy B has a greater load-carrying capacity than Buoy A and is therefore recommended for field installations.

Both buoys possess very stable characteristics in roll and pitch, as well as directional stability under all loading conditions.

The large drop in loading capacity at the lower speeds can probably be reduced by decreasing the rapid change in curvature of the bottom surfaces. Since this would require major changes in the design of the buoys, and since the reserve buoyancy of the buoys is large, this change is not recommended for the present design.

TABLE 4

Anchor-Line Sizes and Combinations for Various Anchoring Depths and Currents for NRL Mark 3 Buoy B

Anchor Line:
3/8-inch Diameter Plow-Steel Cable
9/32 (1/4)-inch High-Carbon High-Test Steel Chain

Anchor Line Length = 2 x Anchoring Depth

For Combination Chain and Cable Anchor Line:
Chain Length = Cable Length

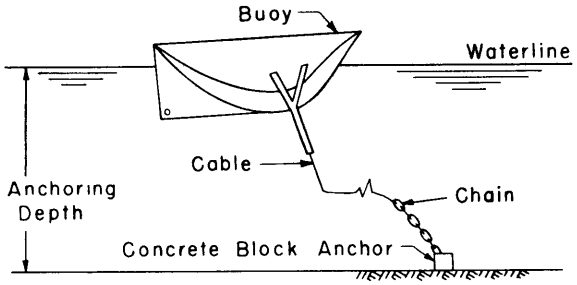

Anchor Depth, feet		100	200	300	400	600	900	1200
Maximum Current knots	Anchor Weight pounds	Recommended Anchor Line						
1.0	1500	Chain and Cable	Chain and Cable	Chain and Cable	Chain and Cable	Chain and Cable	Chain and Cable	Chain and Cable
2.0	1600	Chain and Cable	Chain and Cable	Chain and Cable	Chain and Cable	Chain and Cable	Chain and Cable	Chain and Cable
3.0	1700	Chain and Cable	Chain and Cable	Chain and Cable	Chain and Cable	Chain and Cable	Chain and Cable	Cable
4.0	1900	Chain and Cable	Chain and Cable	Chain and Cable	Chain and Cable	Chain and Cable	Cable	Maximum Current 3.96 knots
5.0	2200	Chain and Cable	Chain and Cable	Chain and Cable	Chain and Cable	Cable	Maximum Current 4.55 knots	
6.0	2500	Chain and Cable	Chain and Cable	Chain and Cable	Cable	Maximum Current 5.2 knots		
7.0	3000	Chain and Cable	Chain and Cable	Chain and Cable	Maximum Current 6.9 knots			
8.0	3700	Maximum Current 7.9 knots	Maximum Current 7.7 knots	Maximum Current 7.25 knots				

Although the buoy shapes are very inefficient for lifting when submerged, the large amount of reserve buoyancy results in high total lift-drag ratios throughout the operating speed range.

Anchoring-line sizes recommended in Tables 2, 3, and 4 should be used in the field installations.

For towing behind a ship, the towline should be secured to the stem of the buoy at a point 7 1/2 inches from the deck.

The buoys may be successfully towed in tandem as shown in Figure 24.

REFERENCES

(1) "Current Survey of Puget Sound and Development of the Radio Current Method," by E.B. Roberts, U.S. Coast and Geodetic Survey Season's Report CS-273, 1943.

(2) BuShips CONFIDENTIAL letter (945), Serial 945-936 of 18 November 1943 to TMB, copies to NRL, CNO. TMB file C-S65-5.

(3) "Design and Performance of the TMB Planing Float as a Towed Position Indicator," by L. Landweber and Ensign P. Eisenberg, USNR, TMB Report 540, March 1945.

(4) TMB CONFIDENTIAL letter C-L5-2(154) of 8 May 1943 to BuShips.

(5) "Tank Tests of Flat and V-Bottom Planing Surfaces," by J.M. Shoemaker, NACA Technical Note 509, November 1934.

(6) "Preliminary Tests in the NACA Tank to Investigate the Fundamental Characteristics of Hydrofoils," by Kenneth E. Ward and Norman S. Land, NACA ACR, September 1940.

(7) "Characteristics of an NACA 66, S-209 Section Hydrofoil at Several Depths," by Norman S. Land, NACA CONFIDENTIAL Bulletin 3E27, May 1943.

(8) "Characteristics of Clark Y Airfoils of Small Aspect Ratios," by C.H. Zimmerman, NACA Report 431, May 5, 1932.

(9) "The Shape and Tension of a Light, Flexible Cable in a Uniform Current," by L. Landweber and M.H. Protter, TMB Report 533, October 1944.

(10) "On the Resistance of a Heavy Flexible Cable for Towing a Surface Float behind a Ship," by J.G. Thews and L. Landweber, TMB Report 418, March 1936.

(11) "Notes on the Resistance of Rods, Cables, and Ropes in Water," TMB Report R-31, December 1940.

(12) "The Tension in a Loop of Cable Towed through a Fluid," by J.G. Thews and L. Landweber, TMB Report 422, June 1936.

(13) "Principles of Naval Architecture," edited by H.E. Rossell and L.B. Chapmann, Vol. 2, 1939, p. 114.

This project carries Bureau of Ships Research Symbol S66. All correspondence on it will be found on TMB CONFIDENTIAL file C-S65-5.

APPENDIX 1

DRAG TESTS OF COMMERCIAL STRAIGHT-LINK CHAIN

To evaluate the forces on a buoy due to the fluid forces on the anchoring line, the coefficients of drag for the line must first be known. In general, the drag coefficients for ordinary commercial wire rope may be taken as the coefficients for long circular cylinders (11). In the range of Reynolds numbers in which the buoys will be operating, the coefficient is usually taken as a constant value of 1.20. Recent tests* at the Taylor Model Basin, however, indicate slightly higher values for stranded wire rope depending on variations in size and vibration characteristics of the cable. Based on these tests, a coefficient of 1.5 is used for diameters of 1/2 inch or less in determining anchor-line sizes when wire rope is used.

Since the drag characteristics of chain were not known, a series of drag tests were conducted to determine the coefficients for commercial straight-link chain. The tests, though not exhaustive, cover the range of Reynolds numbers anticipated in full-scale operation.

The manner in which the tests were conducted is illustrated diagrammatically in Figure 29. The chain under test was secured to the drag dynamometer of the towing carriage and passed around a pulley at the center point of a protractor. The chain was adjusted during the tests to maintain a constant length in the water throughout the speed range. Three sizes, comprising two types of chain were tested. The average dimensions of the "machine" chain and "proof-coil" chain links are shown in Figure 29. The degree of geometrical similarity is indicated on the basis of the ratio of length of link to overall width of link and bar stock diameter to overall width of link.

Drag and angle of the chain were measured at several speeds, and the data were analyzed on the basis of the forces assumed to be acting on the chain and shown in Figure 29. As verified in Reference (12), the normal force per unit length of chain is given by $R \sin^2\theta$, where R is the force per unit length of chain when normal to the stream, and θ is the angle that the chain makes with the direction of motion.

If W is the total chain weight and s is the chain length, then, resolving forces normal to the chain

$$R \sin^2\theta = \frac{W}{s} \cos\theta \qquad [26]$$

---

* These tests have not as yet been reported.

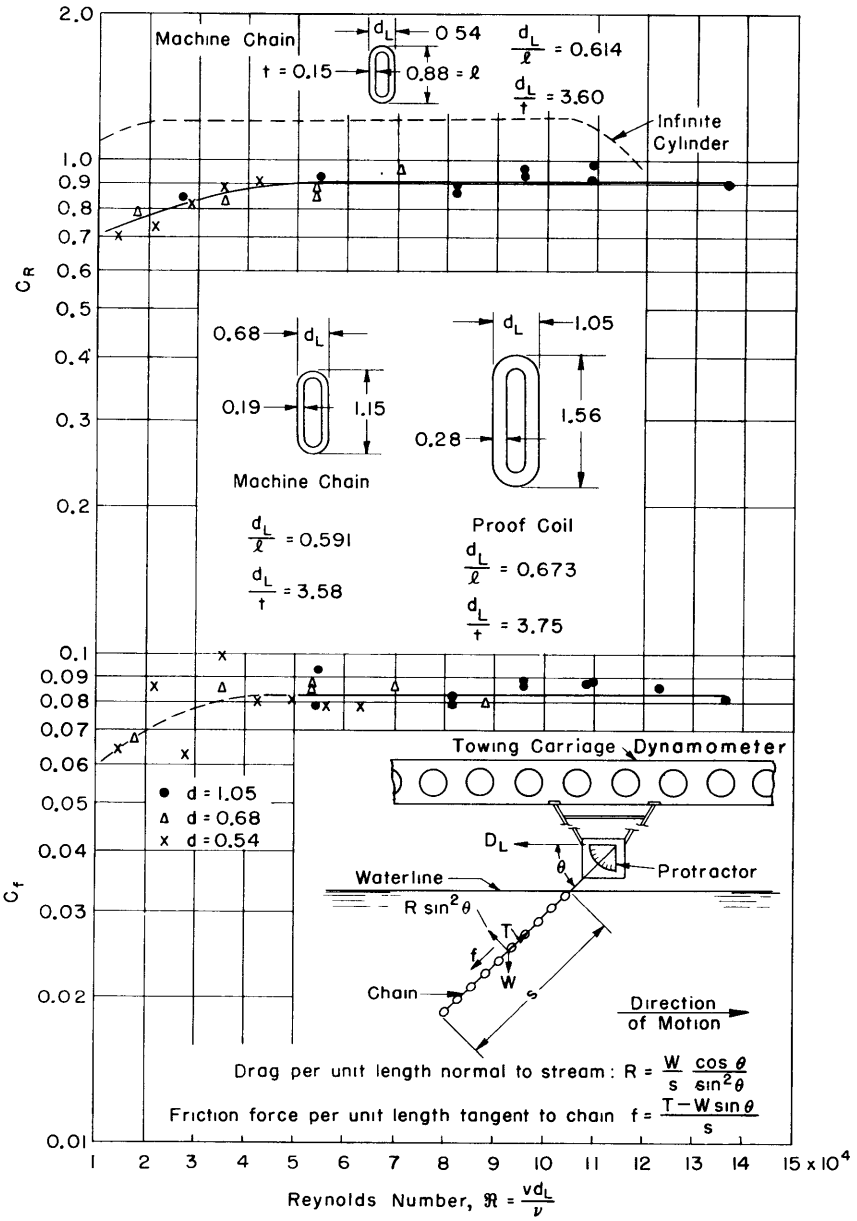

Figure 29 - Drag Coefficients for Commercial Straight-Link Chain

and

$$R = \frac{W}{s}\,\frac{\cos\theta}{\sin^2\theta} \qquad [26a]$$

The tension in the chain is given by

$$T = D_L \sec\theta \qquad [27]$$

where T is the tension and D_L is the measured drag. But

$$D_L \sec\theta = fs + W\sin\theta \qquad [28]$$

where f is the frictional drag per unit length tangent to the chain.

From Equations [27] and [28], then,

$$f = \frac{1}{s}(T - W\sin\theta) \qquad [29]$$

The data are plotted in Figure 29 as coefficients of normal and tangential drag against Reynolds number. The normal drag coefficient as defined by Equation [18] is

$$C_R = \frac{R}{qd_L} \qquad [18b]$$

where C_R is a dimensionless coefficient,

R is the drag per foot of chain when normal to the stream, in pounds,

d_L is the overall width of the chain link, in feet, and

q is as defined previously.

The tangential drag coefficient is defined by

$$C_f = \frac{f}{qd_L} \qquad [30]$$

where C_f is a dimensionless coefficient, and f is the tangential drag per foot of chain in pounds. The Reynolds number is written

$$\Re = \frac{Vd_L}{\nu} \qquad [31]$$

where V is the speed in feet per second and ν is the kinematic viscosity in square feet per second (13).

The overall width d_L of the chain link was chosen as the length parameter in writing the coefficients and Reynolds numbers in order to make a comparison with circular-cylinder data. In this way, the efficiency of chain for towing or mooring, as compared to wire rope of equivalent strength, can be determined. Furthermore, when using this parameter, the coefficients for all three sizes of chain lie on a single curve, whereas, if the length of link or the bar-stock size were used, a relatively larger scatter of the data would result. This indicates that for straight-link chain, whether geometrically similar or not, the same normal drag coefficients based on the link width may be used, at least in the range of Reynolds number of the present tests.

In the range of Reynolds numbers in which the buoys will be used, the normal drag coefficients for chain may be taken as a constant value of 0.91. In this same range, the coefficient for an infinite cylinder (Figure 29) is 1.20, and the coefficient for wire rope, as used in this report, is

1.50. Thus the coefficient of drag for wire rope is about 65 per cent greater than the coefficient for chain. However, if the wire rope and chain are made of the same material and, assuming that the chain and the wire rope develop the same percentage of the aggregate strength of two single bars or of all the wires, the overall width of the chain link based on the dimensions of "proof-coil" chain must equal about 2.65 wire-rope diameters for equivalent strength. On this basis, the actual drag of chain is about 60 per cent greater than the drag of wire rope of equivalent strength. As a result, it appears that wire rope is, in general, more efficient for towing or anchoring bodies where speeds are appreciable and drag is an important factor.

The coefficient of frictional drag of chain, while showing a greater scatter of the test results, may be taken as 0.085 in the range of operation of the Mark 3 buoy.

APPENDIX 2

ANALYSIS WHEN TWO TYPES OF ANCHOR LINE ARE USED IN SERIES

It is intended to show that Figures 25 and 26a, on pages 35 and 37, based on the analysis of a single uniform line, apply for a cable consisting of two lines of different characteristics in series.

Figure 25 expresses $(T \sin \phi_0)/Rs$ against $(T \cos \phi_0)/Rs$ for various values of y/s for a single uniform cable. As shown in Reference (9) the chart was computed from equations of the form

$$\frac{Rs}{T} = F_1(\phi) - F_1(\phi_0) \qquad [32]$$

and

$$\frac{Ry}{T} = F_2(\phi) - F_2(\phi_0) \qquad [33]$$

Hence

$$\frac{y}{s} = \frac{F_2(\phi) - F_2(\phi_0)}{F_1(\phi) - F_1(\phi_0)} = \eta \qquad [34]$$

Eliminating ϕ between Equations [32] and [34], Rs/T is obtained as a function of η and ϕ_0. Since Rs/T and ϕ_0 give corresponding values of $(T \sin \phi_0)/Rs$ and $(T \cos \phi_0)/Rs$, this gives the relations from which Figure 25 was constructed.

Now consider two cables in series as in Figure 28. Let ϕ_1 be the angle at the junction of the two sections of cable, ϕ_0 and ϕ the angles at the float and anchor as usual. Let s_1 and R_1 be the length and specific drag of the lower section, s_2 and R_2 the corresponding values for the upper section.

Applying Equation [32] to each of the cable sections,

$$\frac{R_1 s_1}{T} = F_1(\phi) - F_1(\phi_1)$$

$$\frac{R_2 s_2}{T} = F_1(\phi_1) - F_1(\phi_0)$$

Hence, adding

$$\frac{R_1 s_1 + R_2 s_2}{T} = F_1(\phi) - F_1(\phi_0) \quad [35]$$

Similarly

$$\frac{R_1 y_1 + R_2 y_2}{T} = F_2(\phi) - F_2(\phi_0) \quad [36]$$

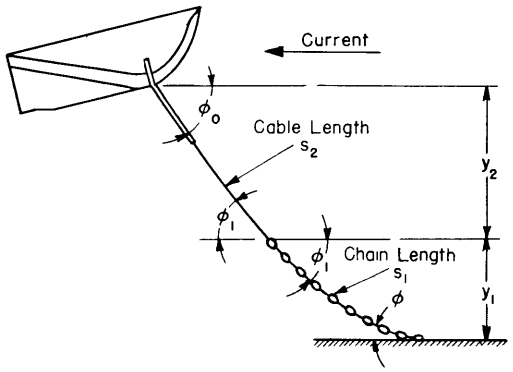

Figure 28 - Combination Chain and Cable Anchoring Line

Putting $S = s_1 + s_2$ and $Y = y_1 + y_2$, mean values of the specific drag can be defined by

$$\bar{R} = \frac{R_1 s_1 + R_2 s_2}{S} \quad [37a]$$

and

$$\bar{R}' = \frac{R_1 y_1 + R_2 y_2}{Y} \quad [37b]$$

Hence, from Equations [39] and [40],

$$\frac{\bar{R} S}{T} = F_1(\phi) - F_1(\phi_0) \quad [35a]$$

$$\frac{\bar{R}' Y}{T} = F_2(\phi) - F_2(\phi_0) \quad [36a]$$

$$\frac{\bar{R}' Y}{\bar{R} S} = \frac{F_2(\phi) - F_2(\phi_0)}{F_1(\phi) - F_1(\phi_0)} = \eta \quad [38]$$

Equations [35a] and [38] for the combination cable are identical in form with Equations [32] and [34] for a single uniform cable. Hence Figure 25, which is derived from these equations, applies also for a combination cable, with $\bar{R}$ as the specific drag and the parameter η which is held constant along the curves given by $\eta = \bar{R}'Y/\bar{R}S$.

It will now be proved, by a purely mathematical argument, that if $R_1 > R_2$ then $\bar{R}' < \bar{R}$. Suppose, on the contrary, that $\bar{R}' \geq \bar{R}$. Then, from [37a] and [37b],

$$\frac{R_1 y_1 + R_2 y_2}{y_1 + y_2} \geqq \frac{R_1 s_1 + R_2 s_2}{s_1 + s_2}$$

or

$$R_2 + \frac{y_1(R_1 - R_2)}{y_1 + y_2} \geqq R_2 + \frac{s_1(R_1 - R_2)}{s_1 + s_2}$$

Hence, since $R_1 - R_2 > 0$,

$$\frac{y_1}{y_1 + y_2} \geqq \frac{s_1}{s_1 + s_2}$$

or, inverting and simplifying,

$$\frac{y_2}{y_1} \leqq \frac{s_2}{s_1} \qquad [39]$$

From Figure 28, the shape of the cable is concave upwards; that is, the angle ϕ increases in passing up along the cable so that ϕ_1 is the largest angle of the lower segment and the smallest of the upper segment. Hence

$$y_1 = \int_0^{s_1} \sin\phi \, ds < \int_0^{s_1} \sin\phi_1 \, ds = s_1 \sin\phi_1$$

and similarly

$$y_2 = \int_0^{s_2} \sin\phi \, ds > s_2 \sin\phi_1$$

Consequently

$$\frac{y_2}{y_1} > \frac{s_2 \sin\phi_1}{s_1 \sin\phi_1} = \frac{s_2}{s_1} \qquad [40]$$

which contradicts [39]. Hence the inequality $\overline{R}' < \overline{R}$ is established.

In actual case $\overline{R}$ will be given but $\overline{R}'$ can be determined only by a detailed analysis. Since, as will be shown by an example, the ratio $\overline{R}'/\overline{R}$ differs little from unity, the difference will be neglected in the applications. From Equation [38] this is equivalent to taking $\eta = Y/S$ for a combination cable, as is the case for a single uniform cable.

This analysis may be summed up as follows:

To a close approximation, a combination cable is equivalent to a single uniform cable of the same overall length and having the specific drag $\overline{R}$. The equivalent cable will give a value for Y/S that is small by the ratio of $\overline{R}'/\overline{R}$.

EXAMPLE

Assume Buoy B anchored completely submerged in a 4-knot current with 1200 feet of anchor line. The anchor line is composed of 600 feet of 3/8-inch wire rope and 600 feet of 9/32-inch chain. From Figure 11, or

Equations [7b] and [8b], the total lift L_T developed by the buoy at 4 knots is 5170 pounds, and the drag D_s of the submerged buoy is 1335 pounds. The tension in the mooring line, by Equation [25], is

$$\sqrt{(L_T - W)^2 + D_s^2} = 3750 \text{ pounds}$$

The drag per foot of wire rope when normal to the stream is

$$R_C = C_{RC} q d_C = 1.5 \times \frac{1.99}{2} \times 2.85 \times 16 \times \frac{3}{8} \times \frac{1}{12} = 2.13 \text{ pounds per foot}$$

For the chain

$$R_L = C_{RL} q d_L = 0.91 \times \frac{1.99}{2} \times 2.85 \times 16 \times \frac{9}{32} \times 3.75 \times \frac{1}{12} = 3.63 \text{ pounds per foot}$$

Neglecting frictional forces on the mooring line, the shape of the part composed of the wire rope is given by, Reference (11),

$$\frac{R_C s_2}{T} = \cot\phi_1 - \cot\phi_0 \qquad [41]$$

where ϕ_0 is defined by

$$\tan^{-1} \frac{L_T - W}{D_s} = \tan^{-1} 2.626 = 69.15 \text{ degrees}$$

Then,

$$\cot\phi_1 = \frac{2.13 \times 600}{3750} + 0.381 = 0.341 + 0.381 = 0.722$$

and

$$\phi_1 = 54.18 \text{ degrees}$$

The equation for y_2 is given by, Reference (11),

$$\frac{R_C y_2}{T} = \log \cot \frac{\phi_1}{2} - \log \cot \frac{\phi_0}{2} \qquad [42]$$

and

$$\frac{2.13\, y_2}{3750} = 0.670 - 0.372 = 0.298$$

$$y_2 = 524.5 \text{ feet}$$

For the part composed entirely of chain, the slope at the point of attachment to the wire rope is $\phi_1 = 54.18$ degrees. The angle at the mooring point is

$$\cot\phi = \frac{R_L s_1}{T} + \cot\phi_1$$

and

$$\cot\phi = \frac{3.63 \times 600}{3750} + 0.722 = 1.303$$

$$\phi = 37.5 \text{ degrees}$$

The equation for y_1 is

$$\frac{R_L y_1}{T} = \log \cot \frac{\phi}{2} - \log \cot \frac{\phi_1}{2} \qquad [42a]$$

and

$$y_1 = \frac{3750}{3.63}(1.080 - 0.670) = 423.5 \text{ feet}$$

The vertical distance from the mooring point to the line of motion of the buoy, then, is

$$Y = y_1 + y_2 = 524.5 + 423.5 = 948 \text{ feet}$$

The ratio

$$\frac{Y}{S} = \frac{948}{1200} = 0.79$$

Solving for the vertical distance from the mooring point to the line of motion of the buoy by the approximate method, the mean value $\overline{R}$ for the mooring line, as given by Equation [20], is

$$\overline{R} = \frac{3.63 \times 600 + 2.13 \times 600}{1200} = 2.88$$

Solving directly for ϕ,

$$\cot\phi = \frac{2.88 \times 1200}{3750} + 0.381 = 1.303$$

and

$$\phi = 37.5 \text{ degrees}$$

The vertical distance, then, is

$$Y' = \frac{3750}{2.89}(1.083 - 0.372) = 922 \text{ feet}$$

The ratio

$$\frac{Y'}{S} = \frac{922}{1200} = 0.768$$

The per cent error in using the approximate method in this case is therefore only 2.8 per cent.

APPENDIX 3

DETERMINATION OF ANCHOR-LINE SIZES FOR BUOY A

POLAR DIAGRAM OF BUOY CHARACTERISTICS

The polar diagram of the characteristics of the buoy when on the surface is shown in Figures 30, 31, and 32. The limiting loading curve is plotted directly from the characteristic curves of Figure 10 on page 16. The characteristic curves of drag against load for constant speeds were derived from the drag and imposed-load curves of Figure 10. The values of $L - W$ were obtained by plotting the difference of the total load capacity and the dead load of buoy weight and installed equipment. Although the weight of buoy and equipment as shown in Table 1 is 1375 pounds, a weight of 1575 pounds was used, including a 200-pound margin of safety for such eventualities as additional equipment, change in plating sizes for the prototype, and the possibility of ice formation in some areas.

DERIVATION OF THE Rs CURVES

The family of Rs curves in Figures 30, 31, and 32 were derived from Equations [15] and [16] for the curve of $\eta = y/s = 0.5$ of Figure 25. From the coordinates Λ and Δ of this curve, the values of $L - W$ and D were derived for a constant value of Rs; hence

$$L - W = \Lambda(Rs) \qquad [15a]$$

and

$$D = \Delta(Rs) \qquad [16a]$$

CURVES OF CHAIN AND CABLE STRENGTH

The concentric circles of strength of plow-steel cable, Figure 30, are plotted from the equation

$$T_M = 18250\ d_C^2 \qquad [11a]$$

where the coefficient includes a safety factor of 4 on the breaking strength, and d_C is the cable diameter in inches.

The strength of proof-coil chain as shown in Figure 31 does not vary exactly as the square of the bar size, but, for the range of sizes investigated, the breaking strength may be taken as

$$T_B = 46000\ d_t^2 \qquad [11b]$$

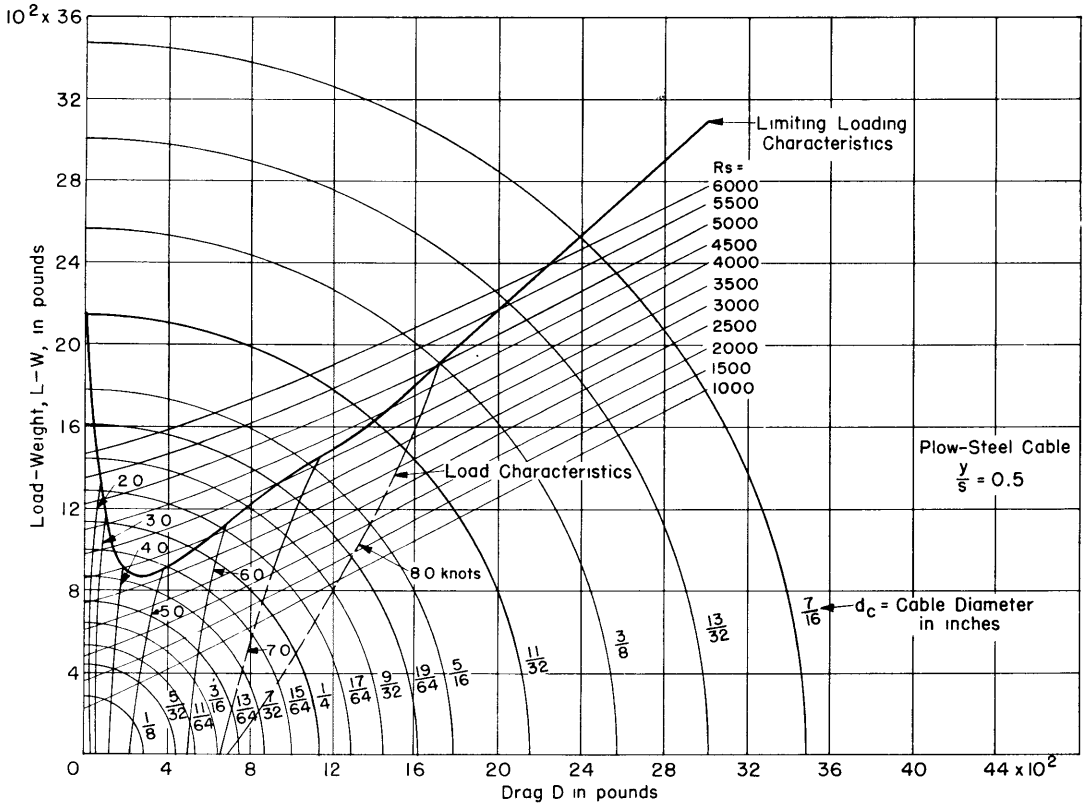

Figure 30 - Determination of Cable Sizes for Buoy A

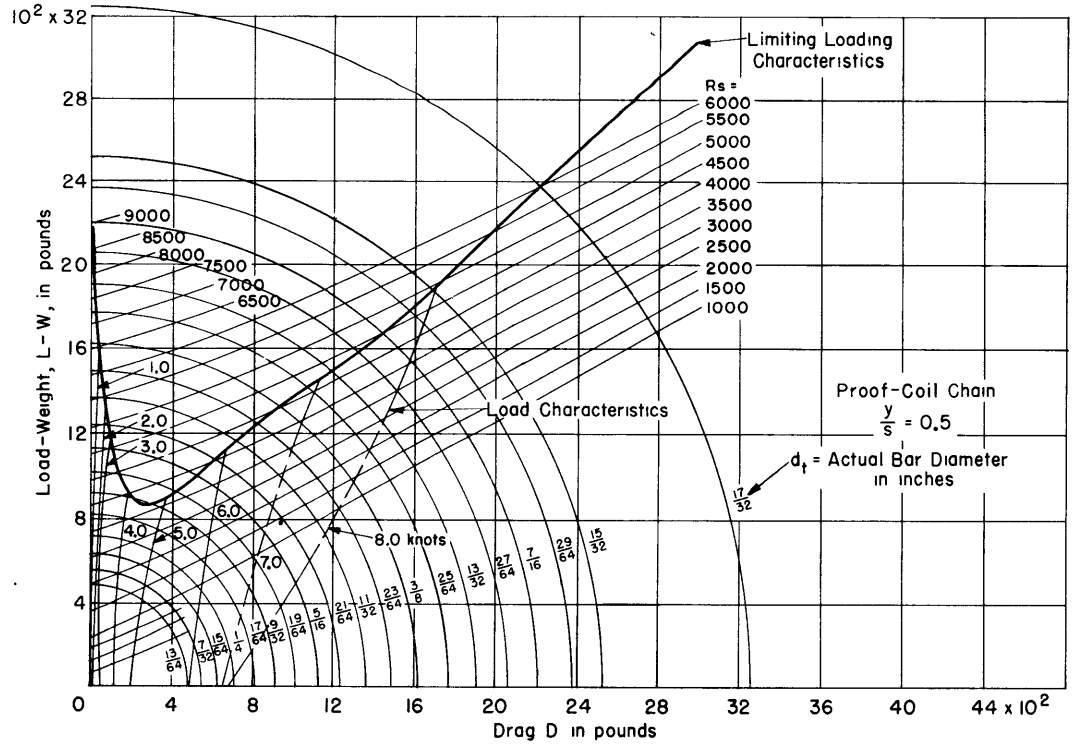

Figure 31 - Determination of Sizes of Proof-Coil Chain for Buoy A

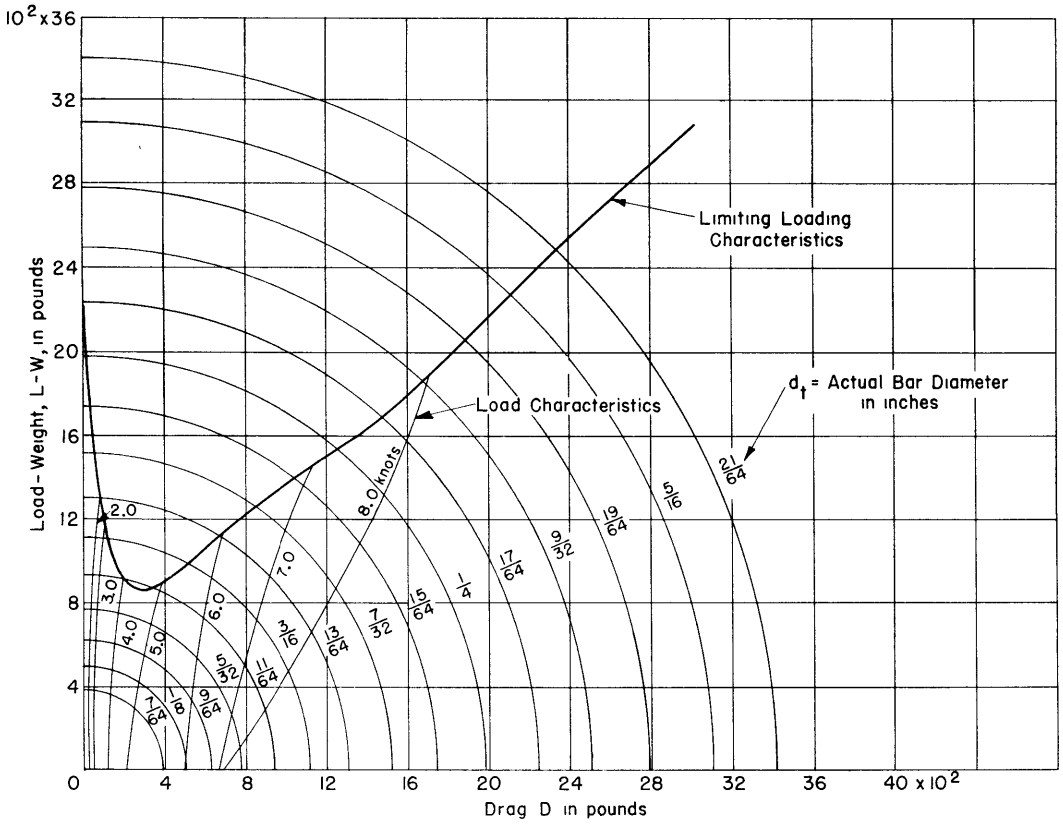

Figure 32 - Determination or Sizes of High-Carbon High-Test Chain for Buoy A

where d_t is the diameter of a single bar. Using a safety factor of 4, this becomes

$$T_M = 11500\ d_t^2 \qquad [11c]$$

and, on the basis of link width,

$$T_M = \frac{11500}{3.75^2}\ d_L^2 = 820\ d_L^2 \qquad [11d]$$

For high-carbon high-test chain, Figure 32. the working strength, including a safety factor of 3, is

$$T_M = 31600\ d_t^2 \qquad [11e]$$

based on bar size, and, on the basis of link width,

$$T_M = 2250\ d_L^2 \qquad [11f]$$

PROBLEM 1: CABLE SIZES FOR ANCHORING IN 1200 FEET OF WATER AT A MAXIMUM CURRENT OF 4 KNOTS

The determination of permissible cable sizes for this condition is shown in Figure 33 which was derived, using Figure 30, in the manner explained in Figure 26. For the surface condition, the permissible diameters, using 2400 feet of cable, vary from 0.225 to 0.229. The absolute minimum size is 0.211 on the basis of the submerged condition. Since there is no commercial size which falls in the permissible range, anchoring the buoy with plow-steel cable is not practicable, with 2400 feet of cable. By paying out more cable the range may be extended to include a diameter of 1/4 inch as a practical solution.

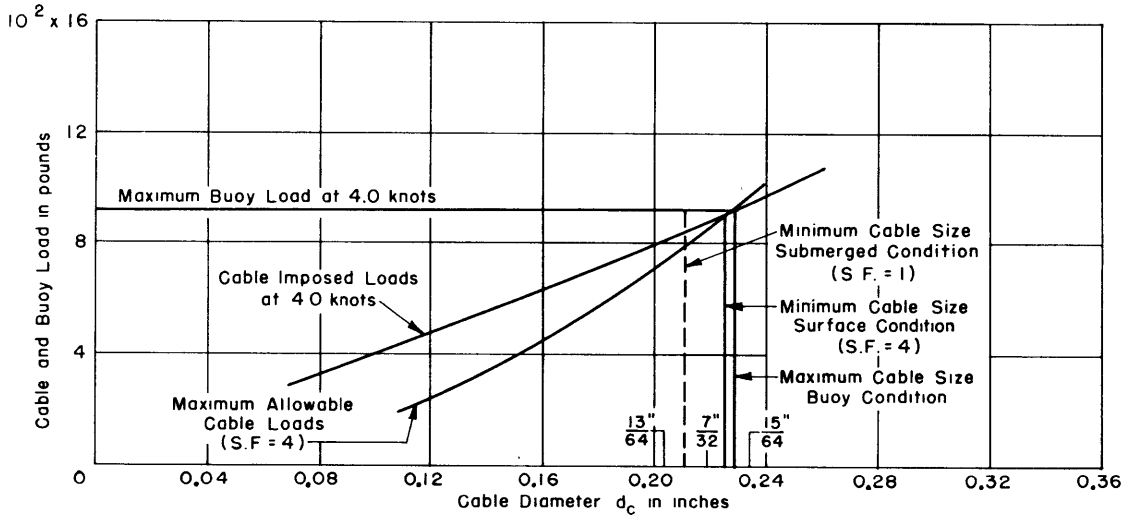

Figure 33 - Determination of Permissible Cable Sizes for Plow-Steel Cable

The anchoring depth is 1200 feet, cable length is 2400 feet and current speed is 4 knots.

PROBLEM 2a: MAXIMUM SAFE CURRENT FOR ANCHORING IN 600 FEET OF WATER WITH CHAIN ONLY

Figures 34a, 34b, and 34c show the steps in the determination of the maximum safe current and the chain sizes for this condition. These charts are derived from Figures 31 and 32 in the manner explained in Figure 27. For the curves of maximum allowable chain load, Figure 34a, single curves were plotted, since the angle of the anchor line at the buoy varies only slightly over the speed range considered, and the vertical component is taken as independent of speed. The dashed line in Figure 34a defines the maximum safe line sizes on the basis of buoy overload and is replotted on Figures 34b and 34c as the upper limit of permissible sizes.

Figure 34b, which corresponds to Figure 27b, for high-test chain, shows that the minimum sizes in this case are controlled by the tensions

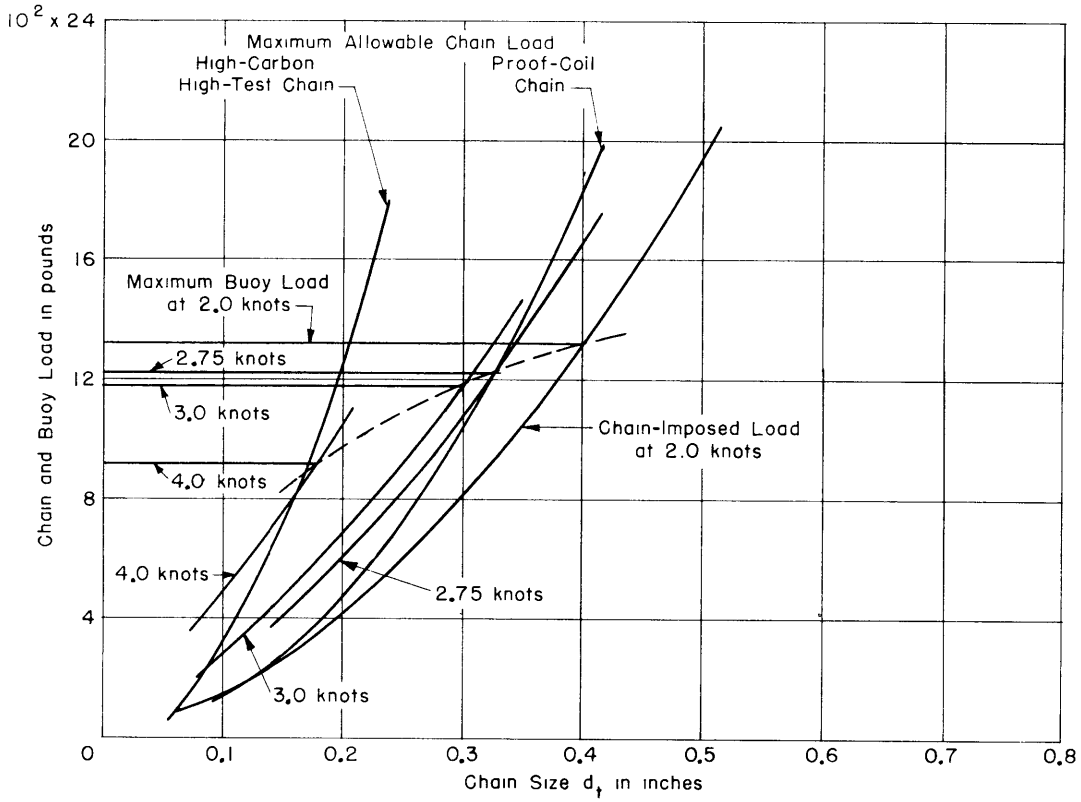

Figure 34a

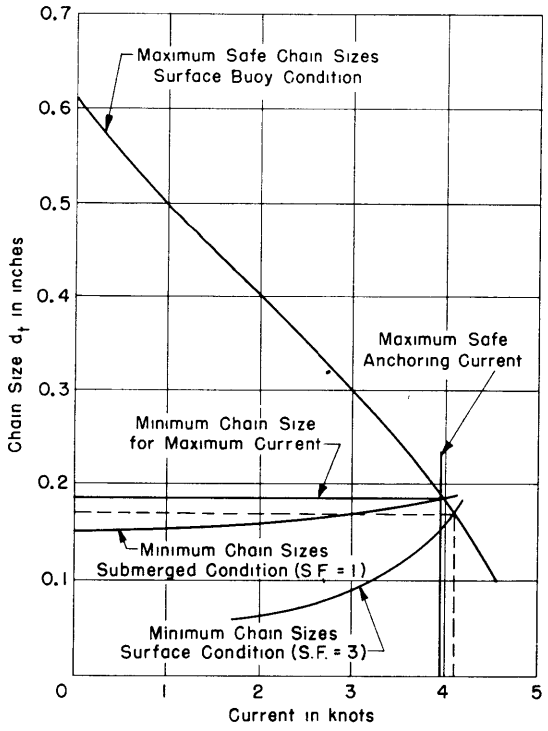

Figure 34b - High-Carbon High-Test Chain

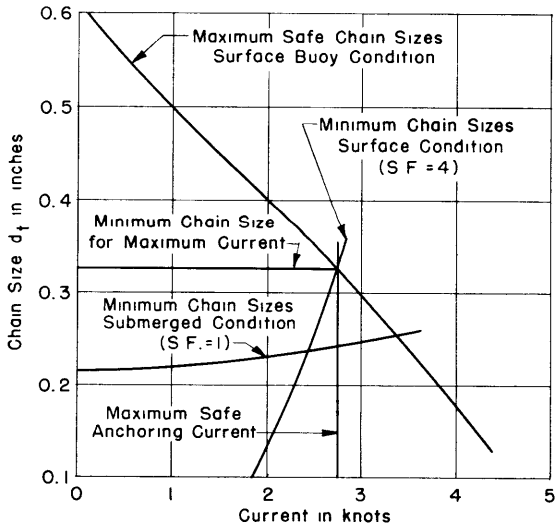

Figure 34c - Proof-Coil Chain

Figure 34 - Determination of Maximum Safe Anchoring Current for All-Chain Mooring Line

The anchoring depth is 600 feet and the chain length is 1200 feet.

developed in the submerged condition. The curve of minimum sizes for the submerged condition is derived as was discussed in the section "Graphical Determination of Mooring-Line Sizes." With this chain, then, the maximum current is 3.95 knots with a chain-bar size of 0.184 inch. The closest commercial size is a bar 7/32 inch in diameter (3/16-inch "trade" size)* which limits the maximum current to 3.68 knots.

For proof-coil chain, the size at maximum current is controlled by the surface condition if the safety factor is to be maintained. In this case, the maximum current is 2.75 knots with a chain-bar size of 0.325 inch. The recommended commercial size is a bar 11/32 inch in diameter (5/16-inch "trade" size) which limits the maximum current to 2.65 knots.

The sizes selected from these curves must be in the region below the maximum limit and above both lower limits.

PROBLEM 2b: MAXIMUM SAFE CURRENT FOR ANCHORING IN 600 FEET OF WATER WITH CHAIN AND CABLE IN COMBINATION

From Equation [23], the mean value of Rs is determined for a combination anchor line in which the chain and cable lengths are equal. This ratio of $k = 1$ was selected since the entire bottom half of the line, i.e., the entire length of chain, will be on the sea floor in a dead calm.

From Equations [11a] and [11f] for plow-steel cable and high-test chain, Equation [22] becomes

$$d_L = d_C \sqrt{\frac{18250}{2250}} = 2.85\, d_C \qquad [22a]$$

for maximum utilization of strength. For this combination, then, Equation [23] becomes

$$\overline{RS} = 600\, q d_C (0.91 \times 1 \times 2.85 + 1.5) = 2455\, q d_C \qquad [23a]$$

where d_C is in feet. For salt water with d_C in inches and the current V in knots,

$$\overline{RS} = 580\, V^2 d_C \qquad [23b]$$

By use of this value of $\overline{RS}$, Figures 35a and 35b are derived from Figure 30 in terms of the cable diameter.

In Figure 35a, a single curve of maximum line loads was again used because of the small variation at these speeds. The maximum current with the combination anchor line is 4.5 knots with a cable diameter of 0.241 inch and a chain-bar size of 0.184 inch. Recommended commercial sizes are 1/4-inch diameter for the plow-steel cable and 7/32 inch (3/16-inch "trade" size) for

---

* "Trade" sizes are listed as 1/32 inch smaller than the actual size.

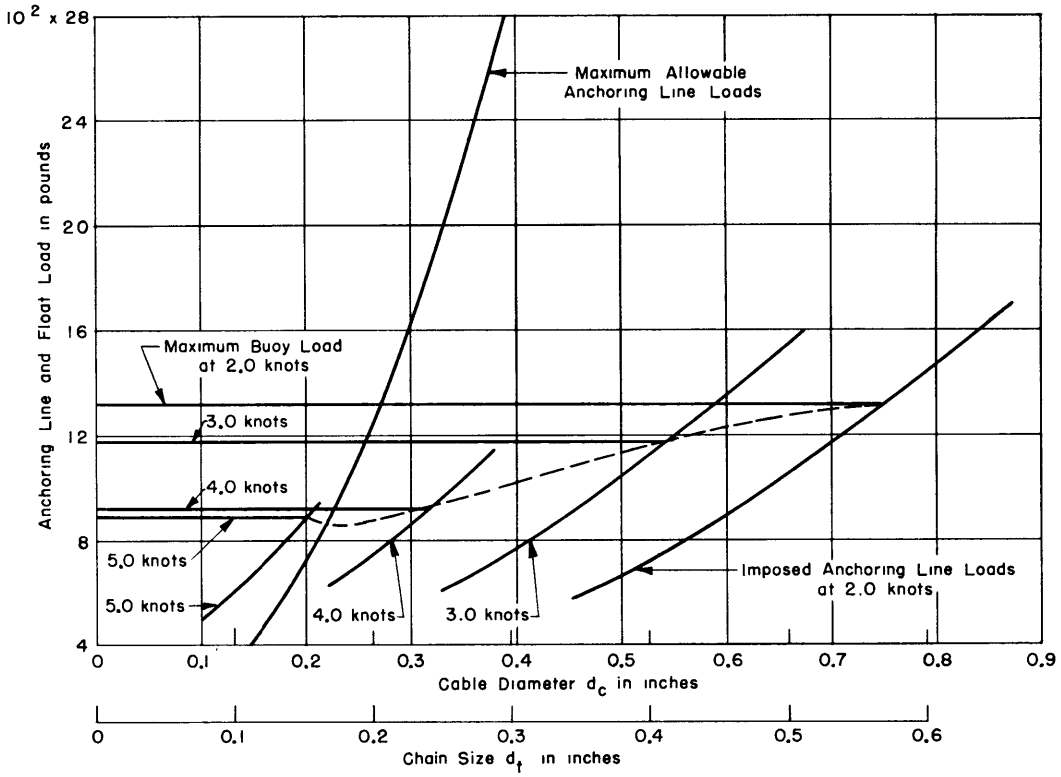

Figure 35a

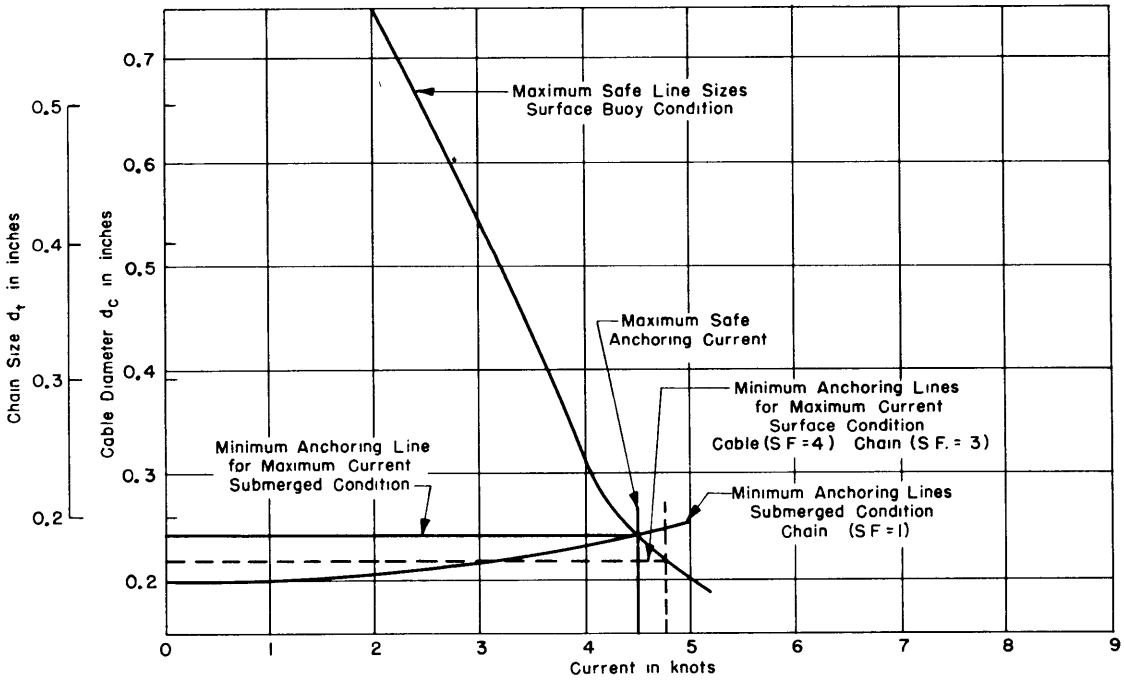

Figure 35b

Figure 35 - Determination of Maximum Safe Anchoring Current for Plow-Steel Cable plus High-Carbon High-Test Chain

The anchoring depth is 600 feet and length of cable and chain is 1200 feet.

the high-test chain. The maximum allowable current with the commercial sizes is 4.28 knots.

For proof-coil chain used in combination with plow-steel cable,

$$\bar{R}S = 820\, V^2 d_C \qquad [23c]$$

The derivation of the maximum allowable current is shown in Figure 36. The maximum allowable current is 4.05 knots with a cable 0.215 inch in diameter and a chain-bar size of 0.270 inch. The best commercial sizes are cable of 1/4-inch diameter with 9/32-inch (1/4-inch "trade" size) chain. The maximum allowable current with the commercial sizes is 3.94 knots.

PROBLEM 3: MAXIMUM SAFE CURRENT FOR ANCHORING IN 100 FEET OF WATER USING CHAIN ONLY

Figures 37 and 38 are derived from Figures 31 and 32 as for Problem 2a, but with a length of 200 feet of chain. For this case, the speed range is higher than for greater depths, and it is necessary to plot the curves of limiting chain loads for each speed above 4 knots (Figures 37a and 38a).

For the high-test chain, Figure 37, the allowable speed range extends beyond 9.0 knots. Since currents above 8.0 knots are unusual, no data were taken above this speed, and it is not possible, with the data on hand, to determine the absolute limit for this condition. However, a commercial size of chain, 11/32-inch (5/16-inch "trade" size), bar size, will permit operation in currents exceeding 9.0 knots.

With proof-coil chain, Figure 38, the limiting current is 7.55 knots with a chain-bar size of 0.432 inch. Using a commercial size with a bar diameter 13/32 inch (3/8-inch "trade" size), the limiting current is 7.30 knots.

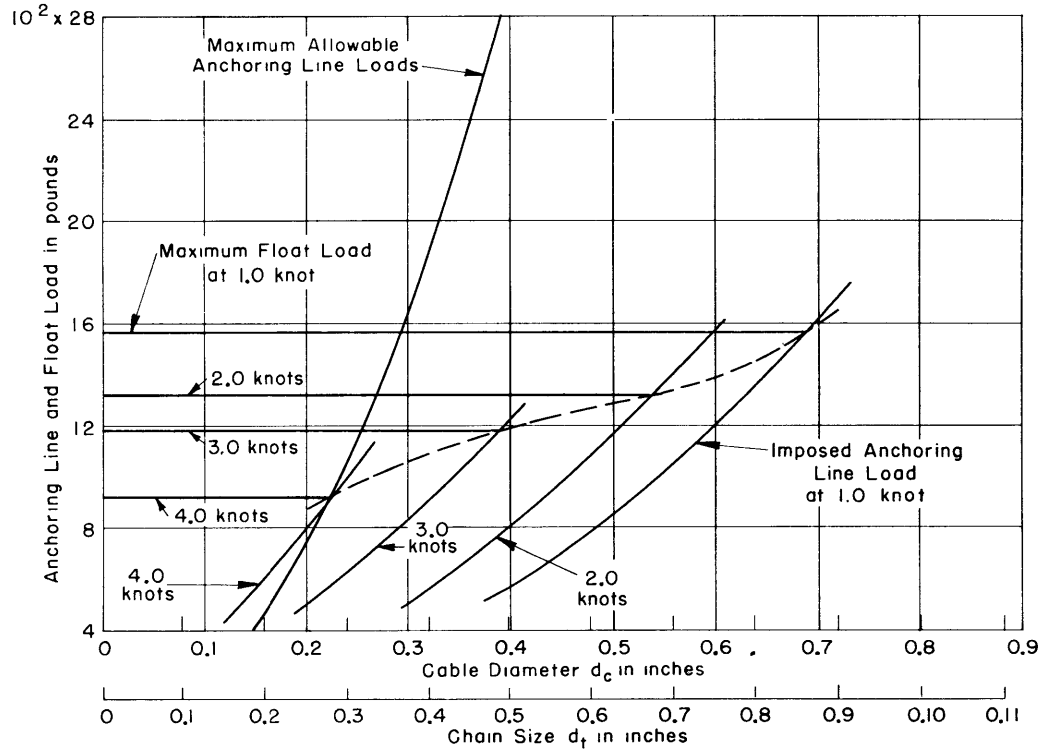

Figure 36a

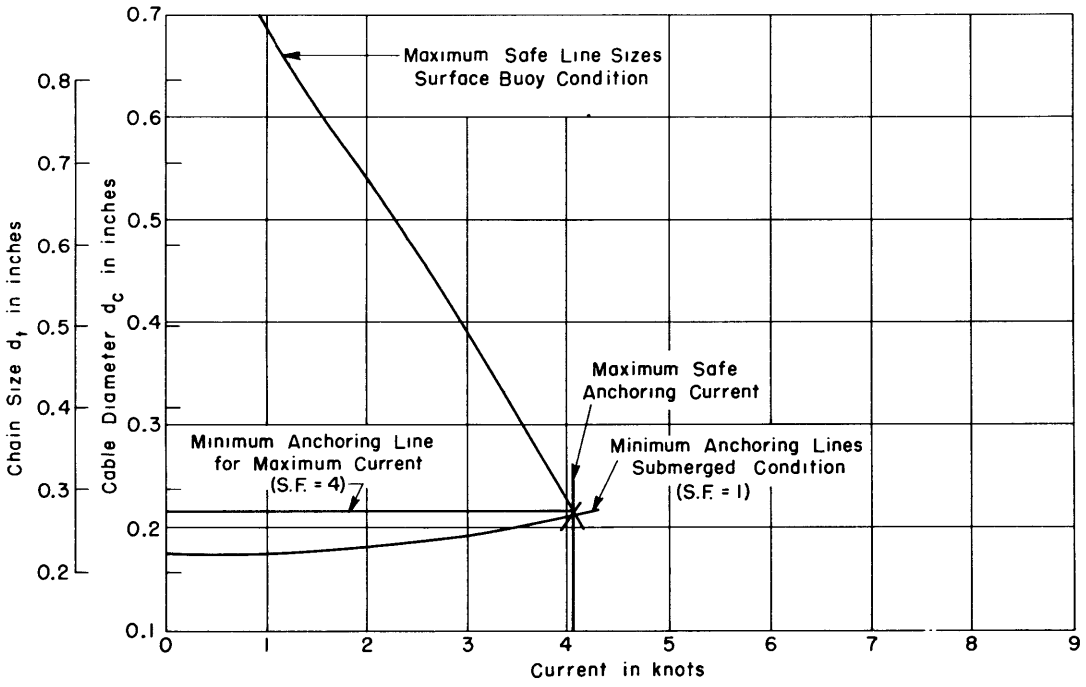

Figure 36b

Figure 36 - Determination of Maximum Safe Anchoring Current for Plow-Steel Cable plus Proof-Coil Chain

The anchoring depth is 600 feet and length of cable and chain is 1200 feet.

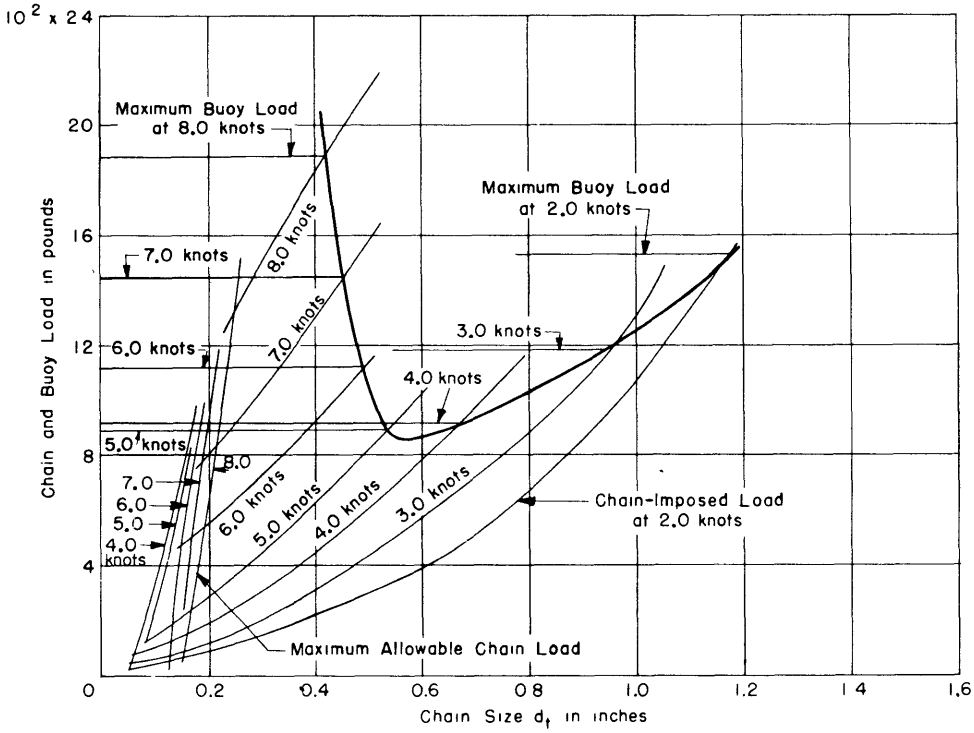

Figure 37a

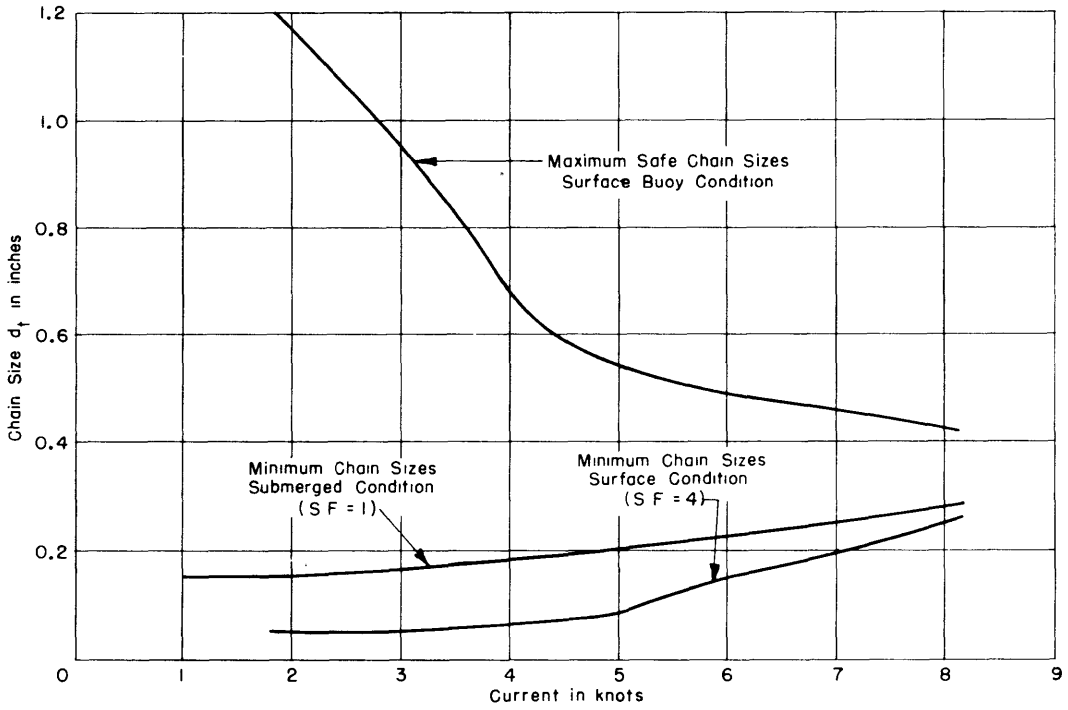

Figure 37b

Figure 37 - Determination of Maximum Safe Anchoring Current for High-Carbon High-Test Chain

The anchoring depth is 100 feet and length of chain is 200 feet.

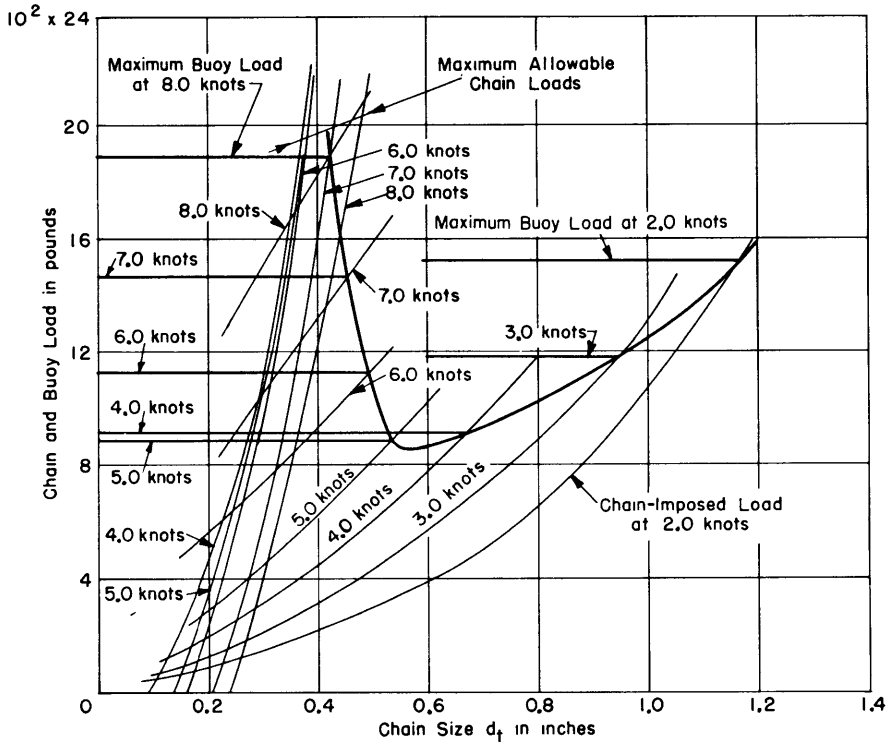

Figure 38a

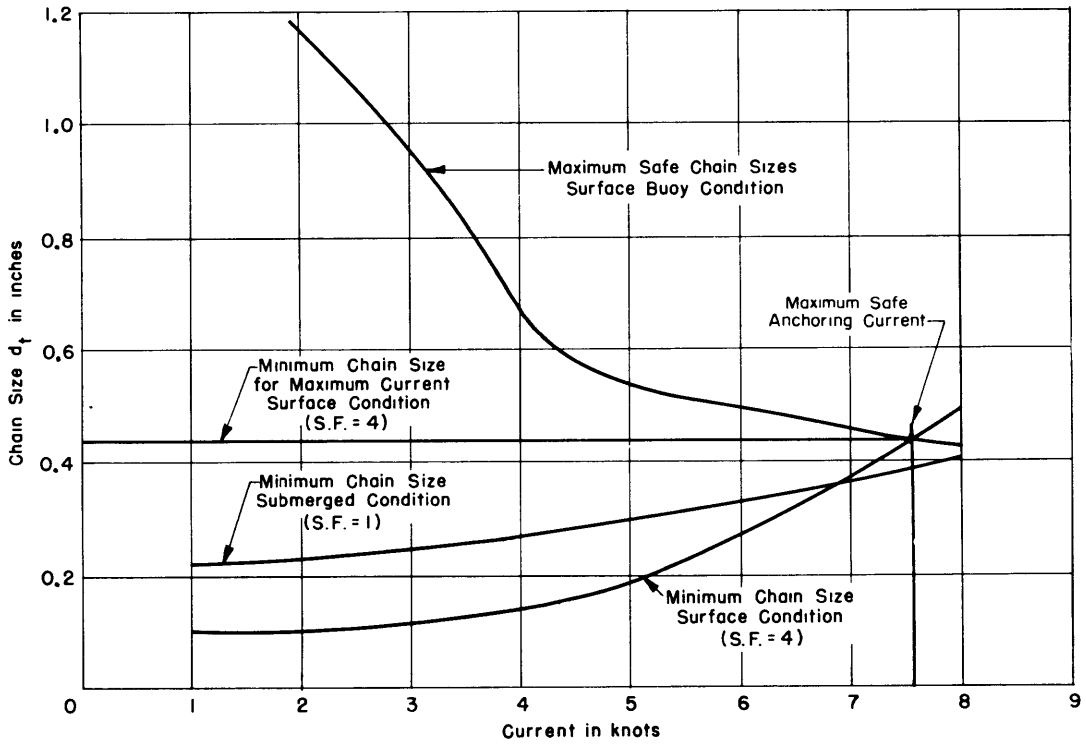

Figure 38b

Figure 38 - Determination of Maximum Safe Anchoring Current for Proof-Coil Chain

The anchoring depth is 100 feet and length of chain is 200 feet.

APPENDIX 4

DETERMINATION OF ANCHOR-LINE SIZES FOR BUOY B

POLAR DIAGRAM OF BUOY CHARACTERISTICS

The polar diagram of the buoy surface characteristics is shown in Figures 39, 40, and 41. The diagrams are derived in the same manner as those for Buoy A. In plotting the values of $L - W$, a margin of safety of 60 pounds was considered sufficient for Buoy B since the capacity of this buoy is considerably greater than that of Buoy A, and the weight of the equipment is already higher than that contemplated for Buoy A.

The Rs curves and the curves of chain and cable strength are the same as those of Figures 30, 31, and 32. The method of deriving chain and cable sizes when used in combination employs the Rs values derived in Appendix 3.

PROBLEM 1: CABLE SIZES FOR ANCHORING IN 1200 FEET OF WATER AT A MAXIMUM CURRENT OF 4 KNOTS

The range of permissible cable sizes for this condition is shown on Figure 42. For the surface condition, the permissible diameters, using 2400

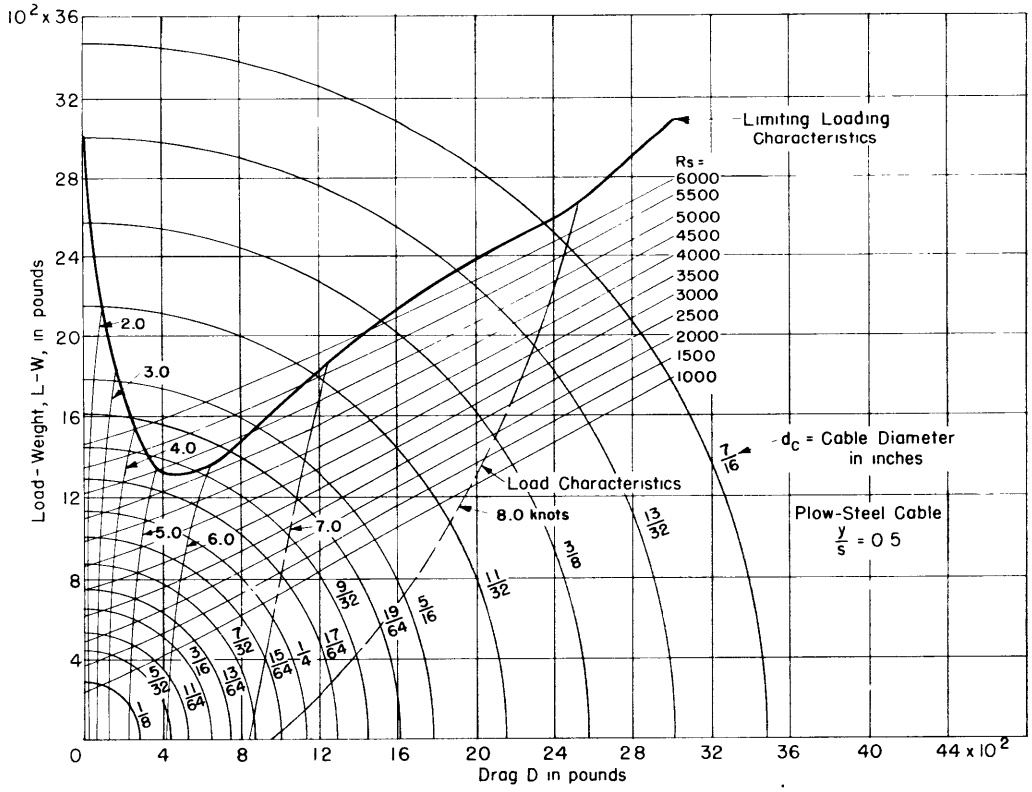

Figure 39 - Determination of Cable Size for Buoy B

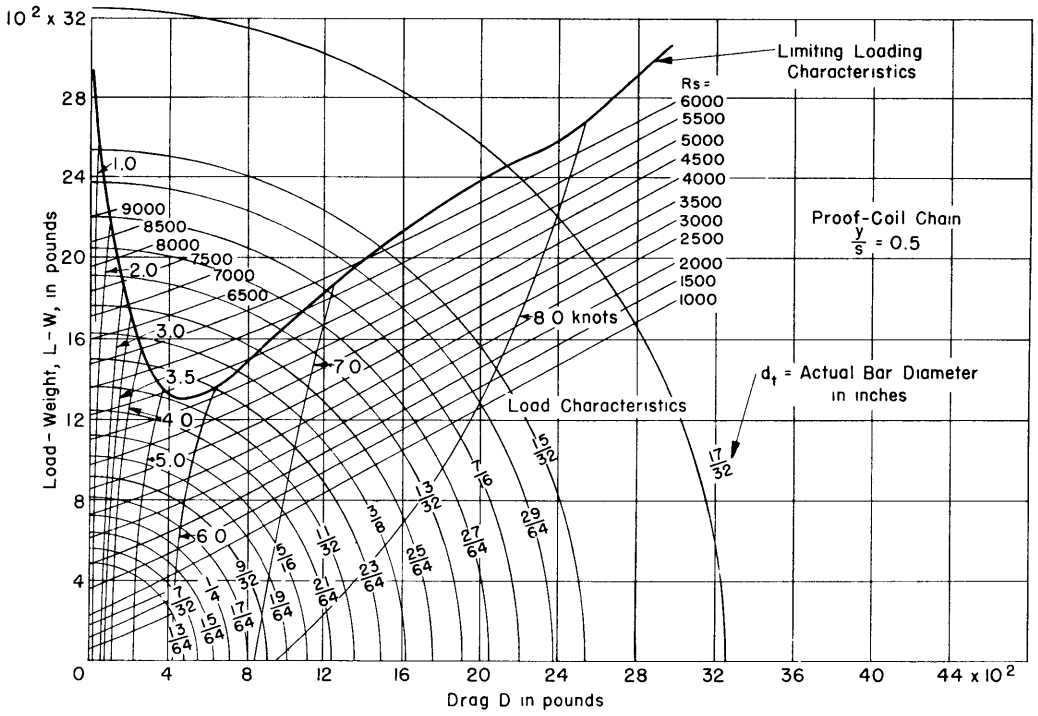

Figure 40 - Determination of Sizes of Proof-Coil Chain for Buoy B

feet of cable, vary from 0.222 inch to 0.368 inch. The minimum size is 0.226 inch on the basis of the submerged condition. A commercial size of 1/4-inch diameter is practicable in the range and will allow operation up to a current of 4.25 knots.

PROBLEM 2a: MAXIMUM SAFE CURRENT FOR ANCHORING IN 600 FEET OF WATER WITH CHAIN ONLY

The permissible range of sizes and the size at maximum speed for this condition are shown in Figure 43.

Using high-carbon high-test chain, the maximum anchoring current is 4.62 knots with a chain bar diameter of 0.212 inch. The best commercial size is chain of 7/32-inch (3/16-inch "trade" size) bar diameter which limits the maximum current to 4.55 knots.

For proof-coil chain, the size at the maximum current of 3.06 knots is 0.397-inch bar diameter. With a commercial size 13/32-inch (3/8-inch "trade" size) bar diameter, the maximum allowable current is 3.0 knots.

PROBLEM 2b: MAXIMUM SAFE CURRENT FOR ANCHORING IN 600 FEET OF WATER WITH CHAIN AND CABLE IN COMBINATION

Using the values of $\overline{RS}$ as defined by Equation [23b] and [23c], Appendix 3, the permissible sizes are determined as shown in Figures 44 and 45.

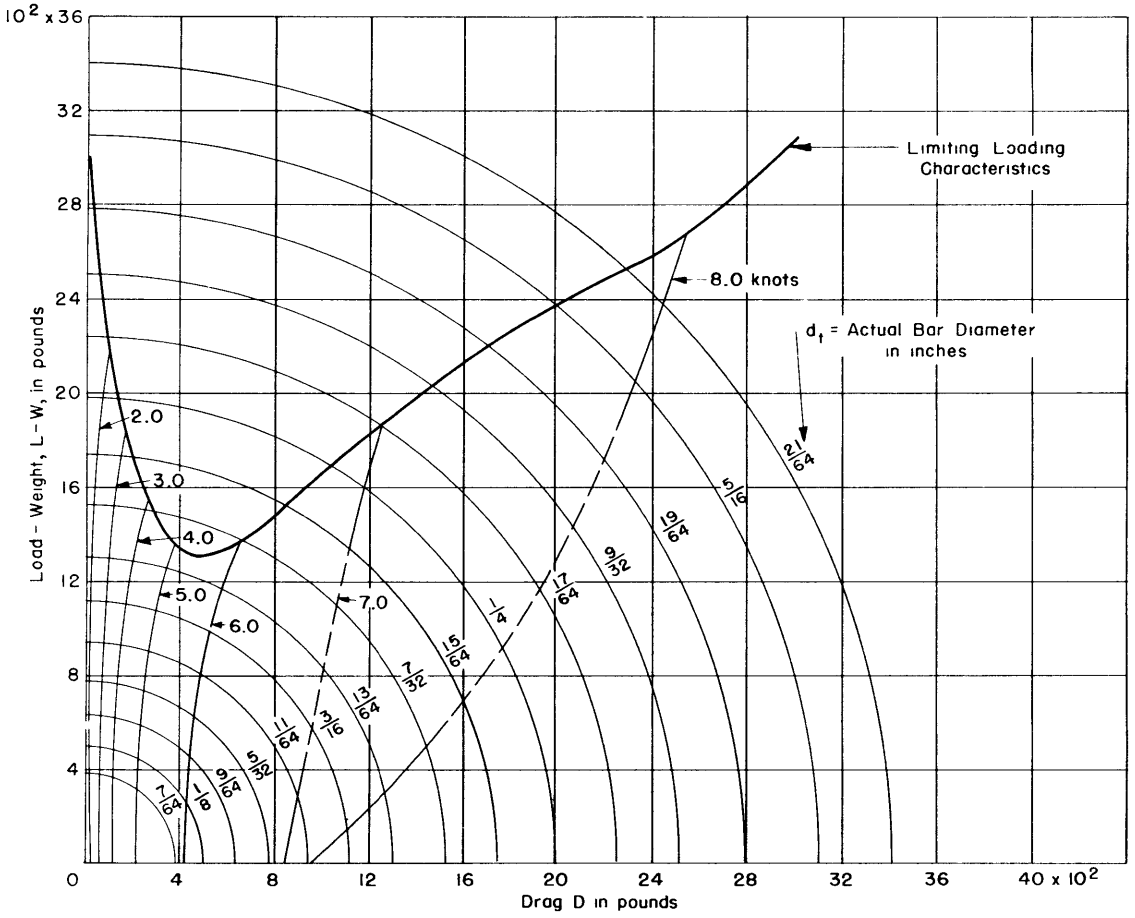

Figure 41 - Determination of Sizes of High-Carbon High-Test Chain for Buoy B

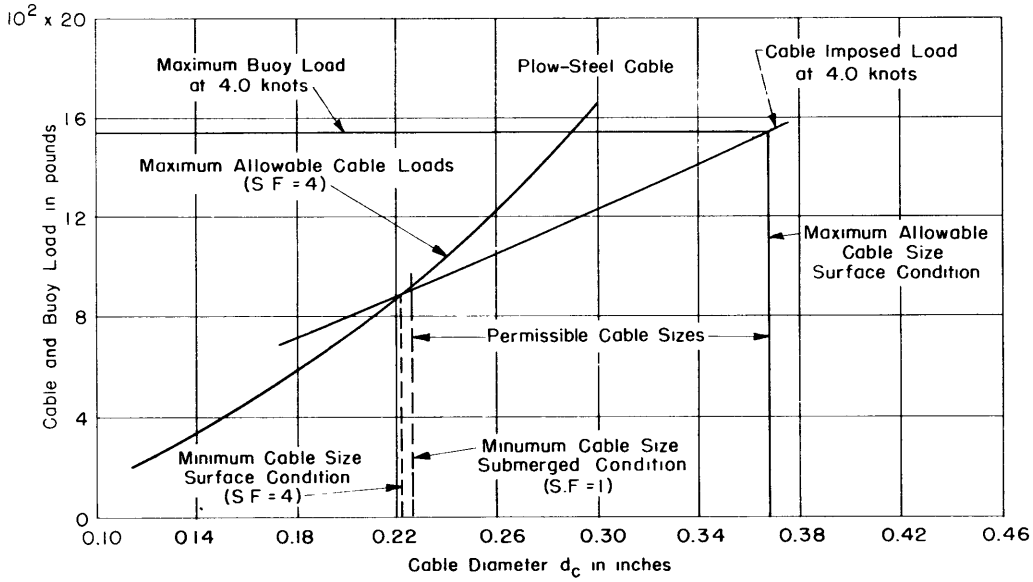

Figure 42 - Determination of Permissible Cable Sizes

The anchoring depth is 1200 feet, cable length is 2400 feet, and current speed is 4 knots.

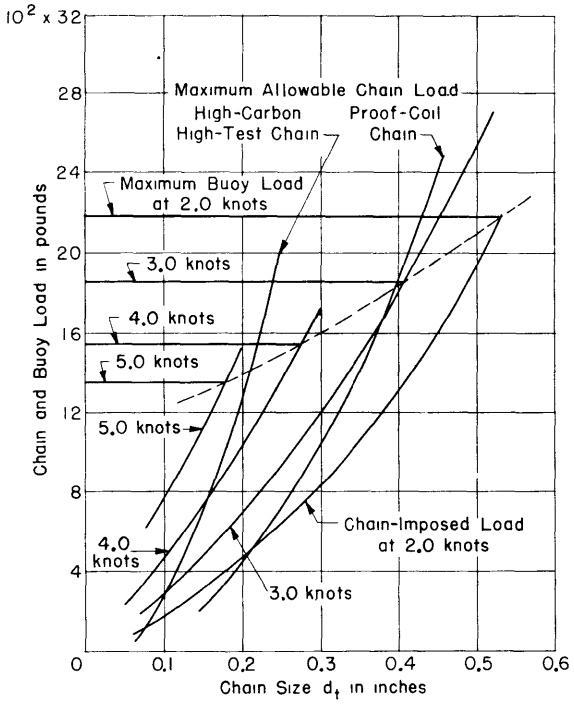

Figure 43a

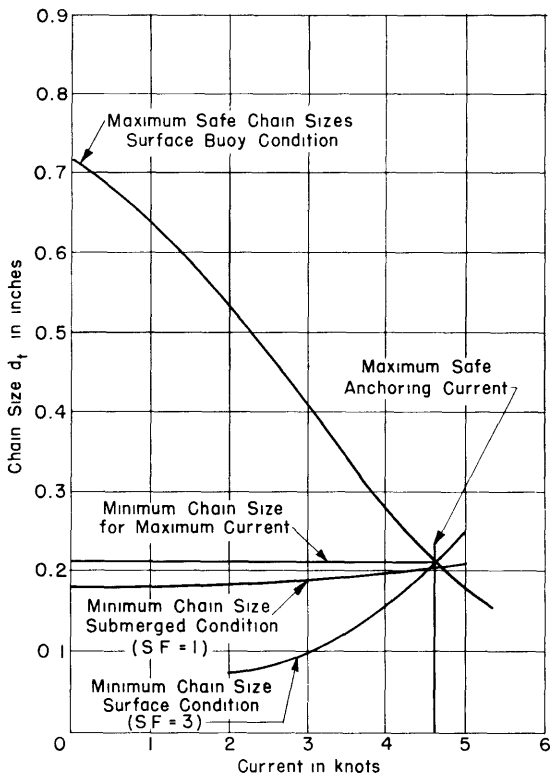

Figure 43b - High-Carbon High-Test Chain

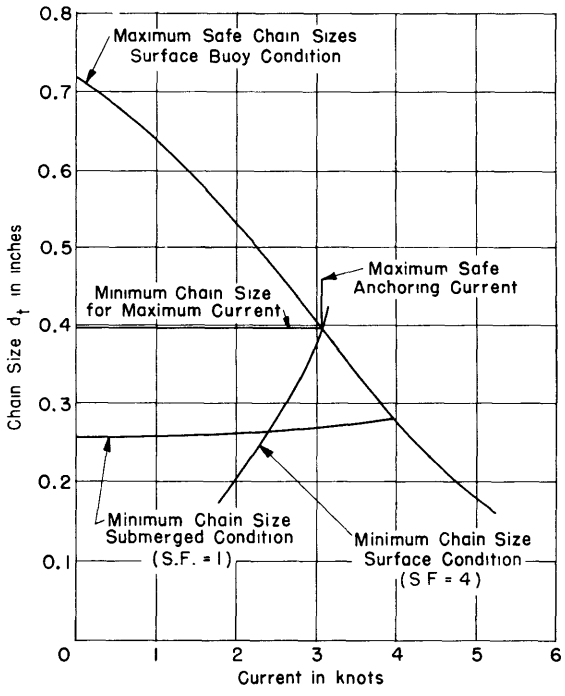

Figure 43c - Proof-Coil Chain

Figure 43 - Determination of Maximum Anchoring Current for All-Chain Mooring Line

The anchoring depth is 600 feet and the chain length is 1200 feet.

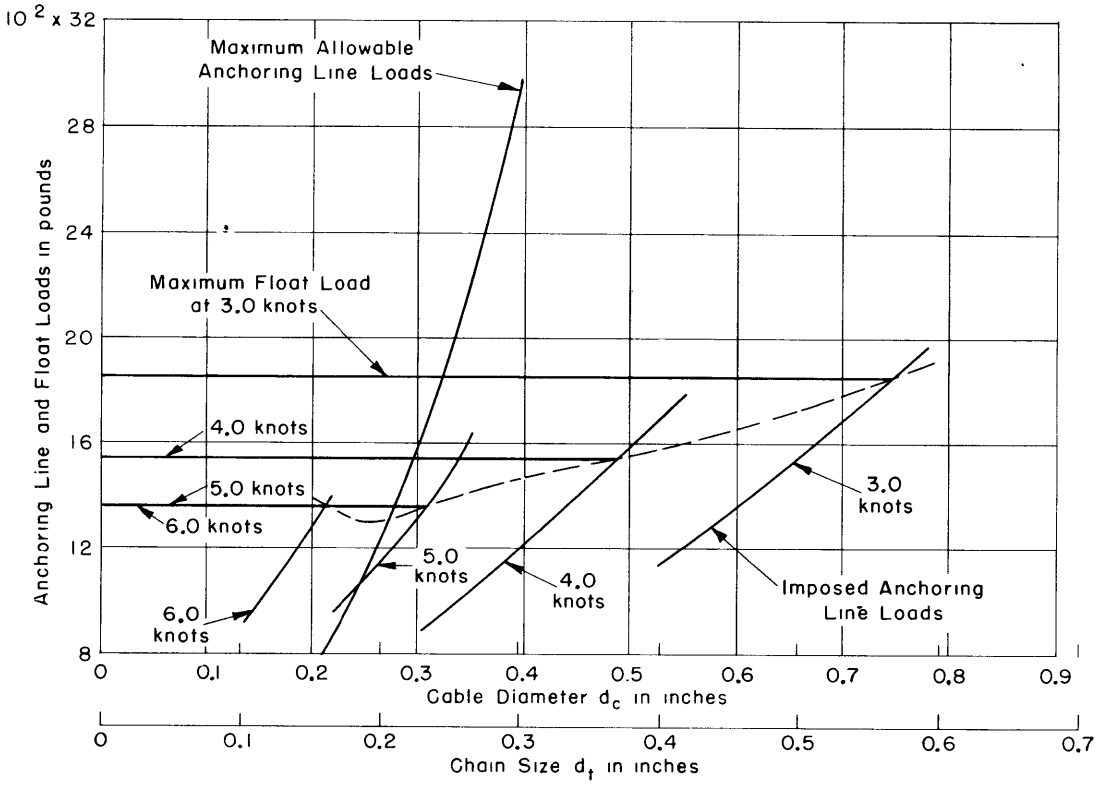

Figure 44a

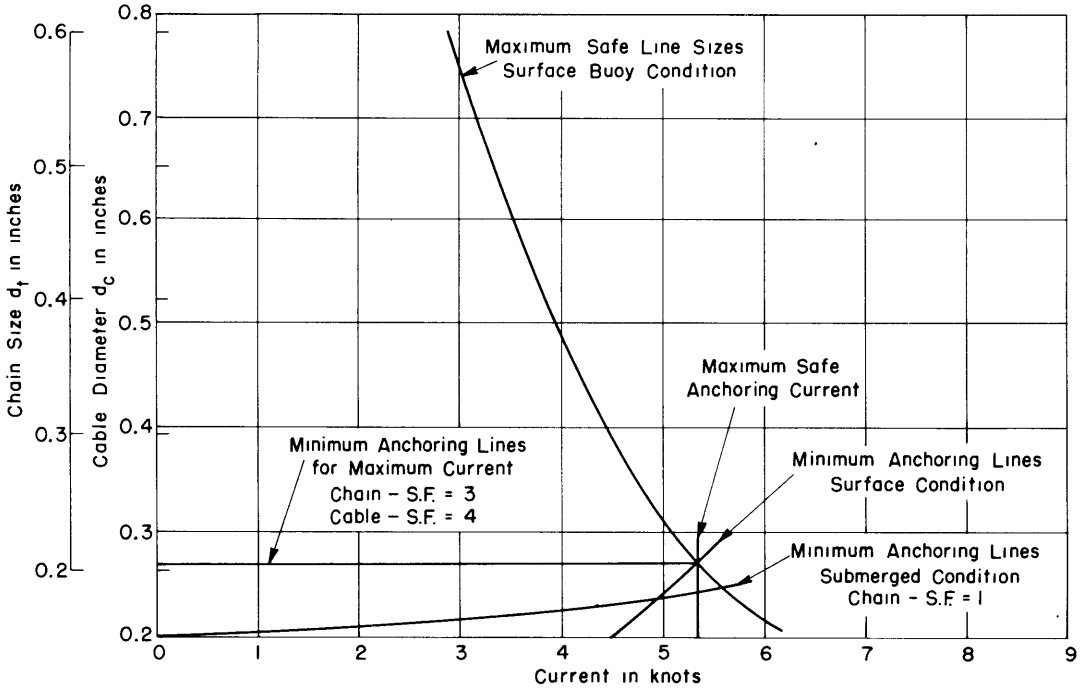

Figure 44b

Figure 44 - Determination of Maximum Safe Anchoring Current for Plow-Steel Cable plus High-Carbon High-Test Chain

The anchoring depth is 600 feet and length of cable and chain is 1200 feet.

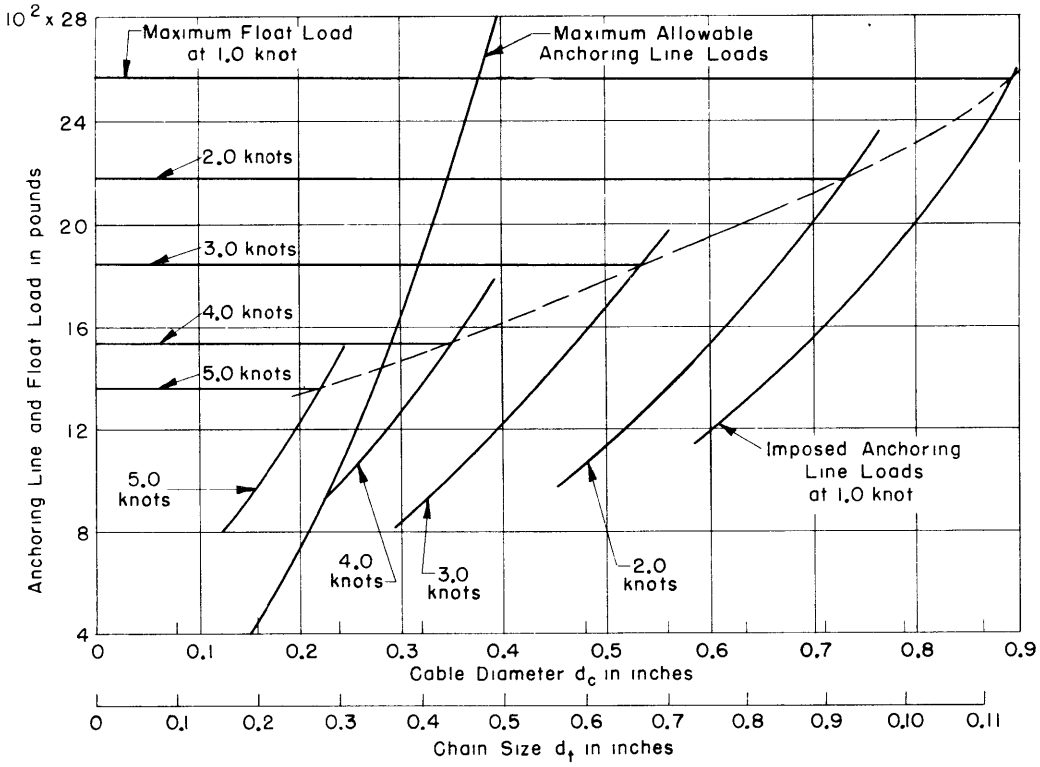

Figure 45a

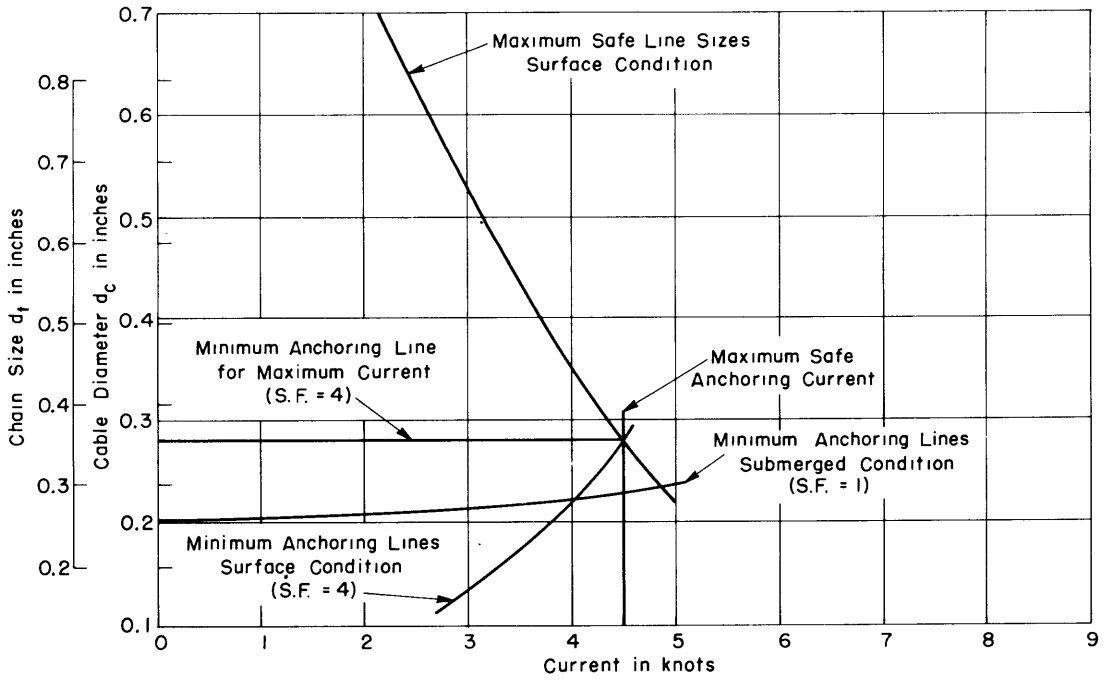

Figure 45b

Figure 45 - Determination of Maximum Safe Anchoring Current for Plow-Steel Cable plus Proof-Coil Chain

The anchoring depth is 600 feet and length of cable and chain is 1200 feet.

For high-test chain used in combination with plow-steel cable, the maximum current is 5.33 knots with a cable diameter of 0.271 inch and a chain-bar diameter of 0.205 inch. The best commercial sizes are cable of 1/4-inch diameter and chain of 7/32-inch (3/16-inch "trade" size) bar diameter with a resultant maximum allowable current of 5.12 knots.

With a proof-coil chain and plow-steel cable anchoring line, the maximum allowable current is 4.48 knots using cable of 0.281-inch diameter and chain of 0.352-inch bar diameter. The best commercial sizes are cable of 5/16-inch diameter and chain of 11/32-inch (5/16-inch "trade" size) bar diameter which lowers the allowable current to 4.35 knots.

PROBLEM 3: MAXIMUM SAFE CURRENT FOR ANCHORING IN 100 FEET OF WATER WITH CHAIN ONLY

The results of the analysis for this condition are shown in Figures 46 and 47. With high-test chain the maximum allowable current is well beyond 8.0 knots. Using a chain of 15/32-inch (7/16-inch "trade" size) bar diameter, anchoring in currents up to about 10 knots is probably safe.

With proof-coil chain, Figure 47, the maximum allowable-current is 8.18 knots with a chain-bar diameter of 0.582 inch. Using a commercial size of 17/32-inch (1/2-inch "trade" size) bar diameter, the maximum allowable anchoring current is 7.90 knots.

SELECTION OF STANDARD CHAIN AND CABLE SIZES

For purposes of uniformity in the field installations with Buoy B, several chain and cable sizes were investigated for suitability throughout the entire range of anchoring possibilities. The curves of maximum allowable anchoring current at various depths of water for the types considered, determined as discussed on page 38, are shown in Figure 48. These curves are determined only for plow-steel cable and high-test chain and combinations of these types.

The sharp break in the curves for 1/4-inch diameter and 9/32-inch chain is a result of the limit imposed by the submerged conditions for the buoy. The inflection points in the curves determine the limit beyond which the sizes are controlled by the strength of the line, and above which the line sizes are controlled by buoy overload.

From Figure 48, a chain of 9/32-inch (1/4-inch "trade" size) bar diameter and a cable of 3/8-inch diameter were selected as allowing the widest range of operation under the anchoring conditions likely to be encountered. The various combinations in which these two sizes should be used are shown in Table 4 on page 45.

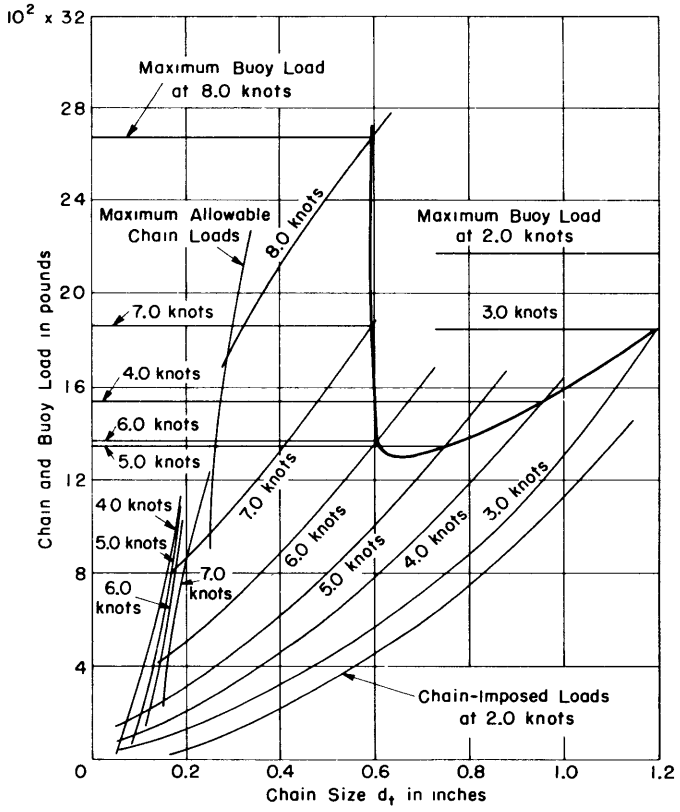

Figure 46a

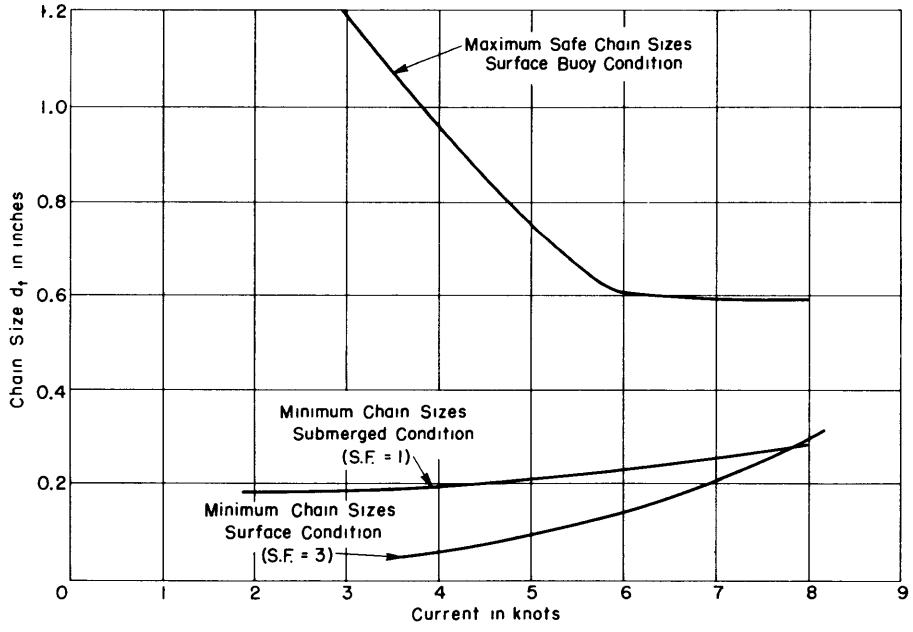

Figure 46b

Figure 46 - Determination of Maximum Safe Anchoring Current for High-Carbon High-Test Chain

The anchoring depth is 100 feet and length of chain is 200 feet.

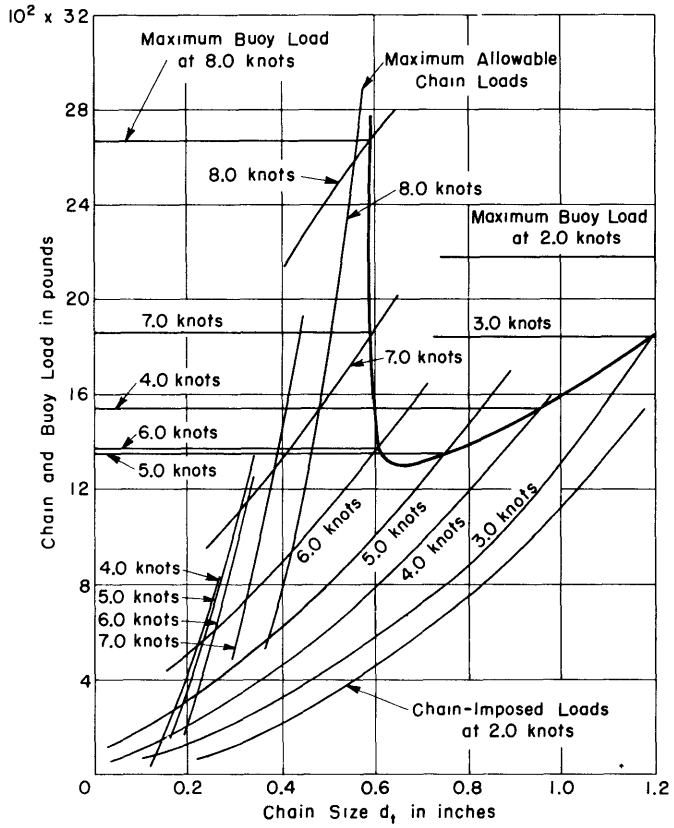

Figure 47a

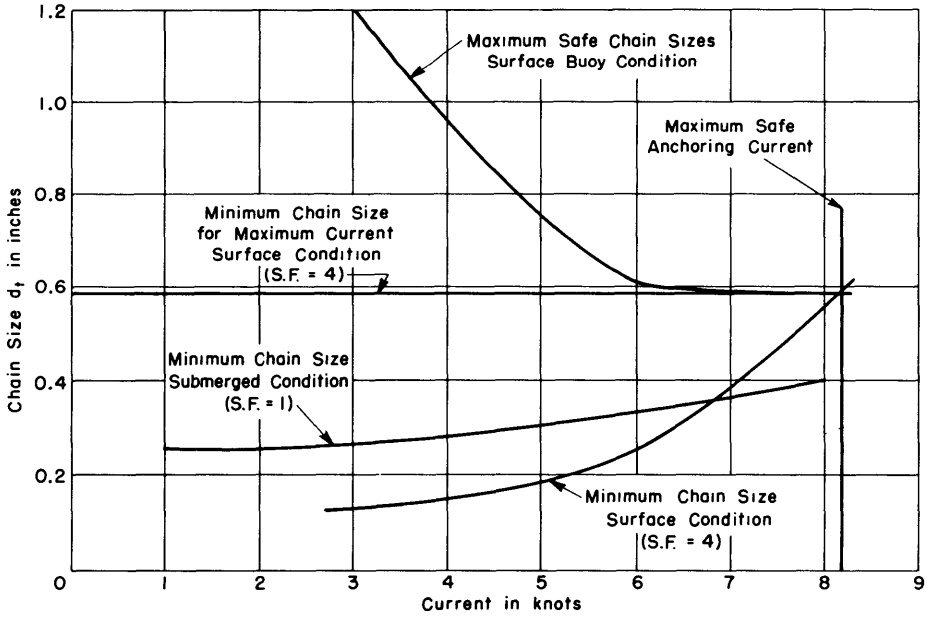

Figure 47b

Figure 47 - Determination of Maximum Safe Anchoring Current for Proof-Coil Chain

The anchoring depth is 100 feet and length of chain is 200 feet.

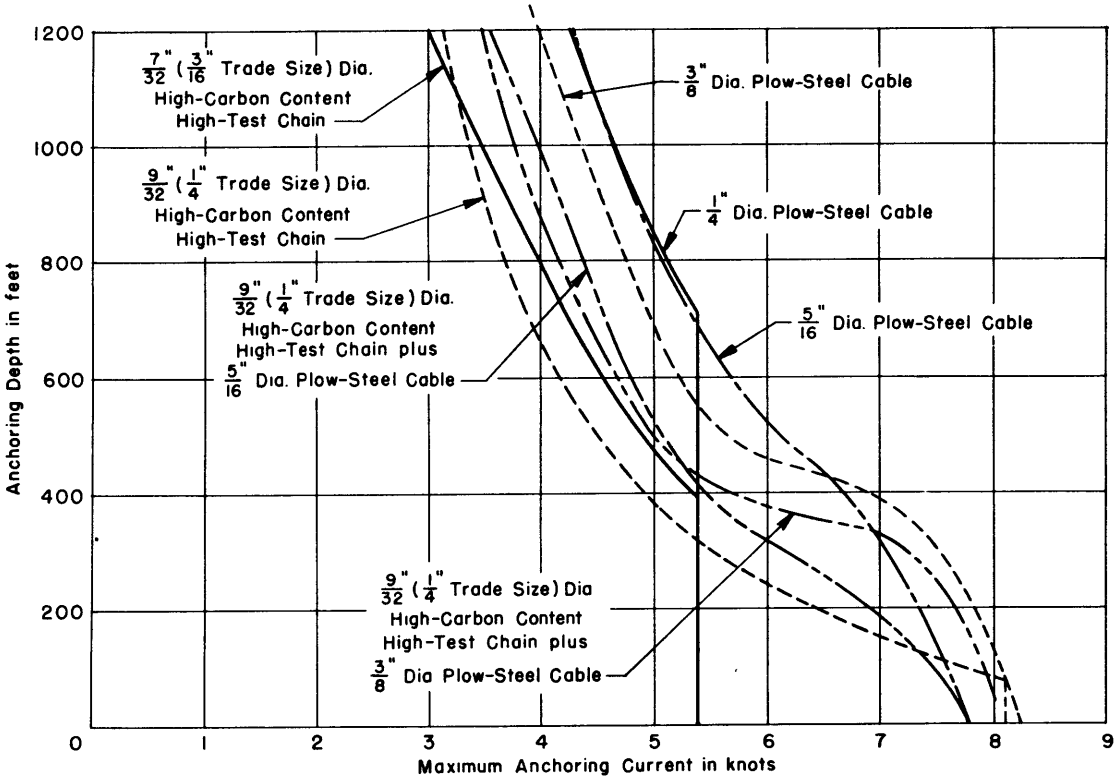

Figure 48 - Anchoring Depth Plotted Against Maximum Speed for Various Anchor-Line Sizes

USE OF CHARTS FOR TYPES OF CHAIN AND CABLE OF HIGHER STRENGTH

In the event that it is desired to use chain or cable of greater strength than the types considered in this report, the charts for the various specifications may be used with slight modifications.

Since the upper limit of line sizes has been established on the basis of buoy overload, these will be unaltered and it is only necessary to adjust the position of the curves of maximum allowable line load established on the basis of strength. The adjustment is first made on Figures 42, 43a, 44a, 45a, 46a, and 47a for the various conditions of anchoring. If a cable or chain of higher strength is used, the curves of maximum allowable line loads are adjusted upward at each speed and each size in the ratio of the strength of the new line to the strength of the chain or cable considered in the above figures. The intersections of the new curves of maximum allowable line load with the curves of imposed load define the lower limit of line sizes with the new line. The sizes must again be checked for strength on the basis of submerged buoy conditions.